ADAPTIVE DEEP BRAIN STIMULATION FOR PARKINSON'S DISEASE

Dr Simon J Little

Doctoral thesis

Nuffield Department of Clinical Neuroscience

Oxford University & Balliol College

November 2013

i) Declaration

I, Simon Little, confirm that the work presented in this thesis is my own. Where information has been derived from other sources, I confirm that this has been indicated in the thesis.

Signed: 

Date: 14 th October 2013

ii) Abstract

Our understanding of the pathophysiology Parkinson's disease has transformed over the last decade as we have come to appreciate the importance of changes in neuronal firing pattern that occur within the motor network in the dopamine deficient state. These changes in firing pattern, particularly increased synchrony result in oscillations that can be recorded as local field potentials. This thesis concerns itself with the study of beta oscillations which are characteristic of Parkinson's disease. Firstly, I investigate whether beta oscillations play a pathophysiological role in Parkinson's disease or whether they are purely epiphenomenal by augmenting beta with low frequency deep brain stimulation. In this study I show that rigidity is increased by ~25% with low frequency stimulation providing significant further evidence for a patho-physiological role of beta in Parkinson's disease. Next I investigate whether beta oscillations correlate with Parkinsonian severity at rest and could therefore potentially be used as a biomarker of clinical state. I demonstrate that the variability of beta amplitude recorded from the subthalamic nucleus strongly correlates with symptom severity at rest and also in response to levodopa administration. I then use beta amplitude as a biomarker for a trial of adaptive deep brain stimulation in Parkinson's disease. I show that by using beta amplitude to control stimulation, time on stimulation is reduced by >50% but despite this, clinical outcome is improved by 25% relative to conventional continuous high frequency stimulation. Finally, I investigate the bilateral subcortical beta network and its response to levodopa. I report statistically significant bilateral functional connectivity in the beta range which is driven by phase locking and modulated by levodopa in the low beta range with implications for bilateral adaptive deep brain stimulation. These findings further our understanding of the pathophysiological role of beta oscillations in Parkinson's disease and provide new avenues for treatment development.

iii) Contents

iv) List of Figures

v) List of Tables

vi) List of Equations

vi) Acknowledgements

I am enormously grateful for the supervision of Peter Brown whose support and guidance have steered me through my DPhil and given me the science bug. I hope to continue in research and that is largely down to his gentle, patient and insightful supervision thus far. His emails have also often made me chuckle.

I would like to thank all the patients who have given their time and energy during a personally stressful period to take part in the research and I have greatly enjoyed being able chat with them at length on everything from Turkish pottery to the fundamental nature of time and being.

I am also very grateful to members of the neurosurgical teams in London and Oxford who have supported the research and particularly to Tom Foltynie who locally supervised me regarding the UCLH experiments. The Brown lab has been a joy to be part of and I've greatly enjoyed getting to know and becoming friends with Anam, Andre, Alek, Arpan, Ash[2], Christiana, Huiling, Hayriye, John-Stuart, Ned, Raed, Spencer and Zar.

Lastly I would like to thank the Wellcome Trust for my clinical research training fellowship, the Rosetree foundation for ongoing financial support, my friends and family, and the lost property team of Southwest Railways.

v) Abbreviations

A/D	Analogue to digital
aDBS	Adaptive deep brain stimulation
ANOVA	Analysis of variance
BCI	Brain computer interface
BNC	Bayonet Neill–Concelman cable connector
cDBS	Conventional deep brain stimulation
CI	Confidence Interval
CNS	Central nervous system
COMT	Catechol-O- methyl transferase
CSF	Cerebrospinal fluid
CV	Coefficient of Variation
CT	Computerised Tomography
D/A	Digital to Analogue
DBS	Deep brain stimulation
DC	Direct current
EEG	Electroencephalogram
EMG	Electromyogram
EPSPs	Excitatory post-synaptic potentials
FDR	False discovery rate
GABA	Gamma-Aminobutyric acid
GPi	Globus pallidus interna
GPe	Globus pallidus externa
LFP	Local field potential
LRRK2	Leucine-rich repeat kinase 2
NICE	National Institute for Health and Care Excellence

MAO-I	Monoamine oxidase inhibitor
MCP	Meta-carpo-phalangeal
MEG	Magnetoencephalogram
MHRA	Medicines and Healthcare products Regulatory Agency
MOSFET	Metal–oxide–semiconductor field-effect transistor
MPP+	1-methyl-4-phenylpyridinium
MPTP	1-methyl-4-phenyl-1,2,3,6-tetrahydropyridine
MRI	Magnetic resonance imaging
NICE	National institute for clinical excellence
NMDA	N-methyl-D-aspartate
PD	Parkinson's Disease
PDQ-39	Parkinson's disease questionnaire
PET	Positron emission tomography
PIC	Peripheral interface controller
PLV	Phase locking value
PPN	Peduculopontine nucleus
PRKN	Parkin
QALY	Quality adjusted life year
RC	Resistor – capacitor
REM	Rapid eye movement
SEM	Standard error of the mean
SPSS	Statistical analysis in social science
SNc	Substantia nigra pars compacta
SNr	Substantia nigra pars reticulata
STN	Subthalamic nucleus
UCLH	University College London Hospital
UKF	Unscented Kallman filter

UPDRS	Unified Parkinson's Disease Ratings Scale
VIM	Ventralis intermedius nucleus of thalamus
VTA	Ventral tegmental area

vi) Publications incorporated into this thesis

1. Little S, Brown P. What brain signals are suitable for feedback control of deep brain stimulation in Parkinson's disease? Annals of the New York Academy of Sciences. 2012; 1265(1):9–24.

2. Little S, Joundi R, Tan H, Pogosyan A, Forrow B, Joint C, et al. A torque-based method demonstrates increased rigidity in Parkinson's disease during low-frequency stimulation. Experimental Brain Research. 2012; 219(4):499–506.

3. Little S, Pogosyan A, Kuhn AA, Brown P. Beta band stability over time correlates with Parkinsonian rigidity and bradykinesia. Experimental Neurology. 2012; 236(2):383–8.

4. Little S, Pogosyan A, Neal S, Zavala B, Zrinzo L, Hariz M, et al. Adaptive deep brain stimulation in advanced Parkinson disease. Annals of Neurology. 2013; 74(3):449–57.

5. Little S, Tan H, Anzak A, Pogosyan A, Kuhn A, Brown P. Bilateral functional connectivity of the basal ganglia in patients with Parkinson's disease and its modulation by dopaminergic treatment. PLOS one. In press.

6. Little S, Brown P. The functional role of beta oscillations in Parkinson's disease. Parkinsonism and related disorders. 2013. In press.

1. Introduction

1.1 Clinical characterisation of Parkinson's disease

"The disease, respecting which the present inquiry is made, is of a nature highly afflictive…"

Dr James Parkinson captured many of the motor and non-motor symptoms of Parkinson's disease (PD) in his humble but brilliant description of six cases in 1817, in addition to the burden of suffering it caused to patients and the slow progression of the disease (Parkinson 1817). His optimism regarding research and remedies for PD has in part been vindicated by the range of medical and surgical treatments that have been developed. Unfortunately however, these treatments at present still remain symptomatic and the need for further research to improve current symptomatic therapies and develop new disease modifying treatments is as pressing as ever.

1.1.1 Epidemiology & Aetiology

PD is one of the most common neurological disorders with a general population prevalence of 0.3% in industrialised countries (Lau & Breteler 2006). Prevalence rises sharply with age to approximately 1% in those in their 60s and up to 3% among persons 80 years or older (Tanner 1992). Standardised incidence rates are reported as 8-18 per 100,000 person-years (Twelves et al. 2003). Worldwide epidemiological data indicate that males have a slightly higher incidence of PD than females (x 1.5) (Wooten 2004). Incidence and prevalence rates have remained stable for the past 40 years although there are considerable (x4 fold) regional and ethnic differences in incidence with lowest levels found in Asia and Africa and highest levels found in western Caucasians (Zhang & Román 1993). The degree to which ethnic, environmental and methodological factors differentially contribute to these differences is

still being explored. There is a considerable literature investigating possible environmental and lifestyle risk factors contributing to PD and yet consistent associations are still few. The evidence for a protective effect of coffee and smoking is relatively strong with a weaker positive protective association related to Uric acid (Wirdefeldt et al. 2011). Conversely, PD risk is increased by exposure to pesticides (of any sort), herbicides and solvents and this is reflected in an association with farming and rural living (Pezzoli & Cereda 2013). A more dramatic demonstration of environmentally induced PD occurred in six people in California in 1982, who all became profoundly Parkinsonian after exposure to 1-methyl-4-phenyl-1,2,3,6-tetrahydropyridine MPTP (Ballard et al. 1985). MPTP is oxidised to 1-methyl-4-phenylpyridinium (MPP+) after it crosses the blood brain barrier whereby it binds to and interferes with complex 1 of the respiratory chain of mitochondria. This has lent support to the environmental exposure hypothesis of PD and led some to speculate that chronic exposure to low level amounts of an environmental toxin similar to MPTP may be the cause of PD, particularly in genetically susceptible individuals.

1.1.2 Genetics of Parkinson's disease

Our genetic understanding of PD has changed markedly over the last 15 years. Initially thought of as a non- genetic disease, twin studies have revealed that genetics appears to play a particularly strong role in young onset (<50 years) PD, although this effect lessens in disease that starts later (Tanner et al. 1999). Subsequent investigation has delineated a number of single gene disorders which account for 5-10% of patients with PD (Lesage & Brice 2009). In addition, success has been made in the mapping of common variants which confer additional risk (Singleton et al. 2013). To date there are 6 confirmed causes of familial Parkinsonism with LRRK2 (autosomal dominant) and PRKN (autosomal recessive) being the most common. It seems likely that a simple dichotomy between environmental and genetic

causes of PD will continue to break down and that it is possible that all patients with PD have a genetic component. As well as guiding diagnosis, these genetic and etiological findings help inform on possible pathophysiological mechanisms.

1.1.3 Motor symptoms of Parkinson's disease

The diagnosis of idiopathic PD is made clinically and is defined by the presence of bradykinesia in addition to one of the following: muscular rigidity, tremor or postural instability (Hughes et al. 1992). Idiopathic Parkinsonism can be mimicked by a number of other conditions such as Progressive Supranuclear Palsy and Multiple Systems Atrophy and therefore diagnosis also depends on the absence of certain findings (e.g. supranuclear gaze palsy, cerebellar signs) and is further strengthened by the presence of others (e.g. excellent levodopa response). Onset is insidious, usually unilateral and may not conform to the diagnostic criteria outlined above in the early stages. As such, symptoms invariably significantly predate diagnosis and may manifest with subtleties such as a fixed flexed stiff elbow plus change in arm swing and a reduced level of facial expression, the poker face or hypomimia (Lees 2009). Clinical Parkinsonism is manifest by the inevitable emergence of bradykinesia defined as the progressive decrement in amplitude and speed of movement. Rigidity, another cardinal sign, clinically expressed as an increased resistance to passive movement, can be reinforced by voluntary movement of the contralateral limb and may be associated with pain, often initially misdiagnosed as joint dysfunction (Jankovic 2008). A proportion of patients will also develop a coarse "pill rolling" rest tremor of the upper limb (4-6Hz) which is not prominent during action but re-emerges after placing the arms in a fixed outward posture and is associated with a slower and more benign progression of disease (Zetusky et al. 1985). For other patients, symptoms will be more dominated by postural instability and a gait disorder. Postural instability is mainly due to a loss of postural reflexes and can be

demonstrated clinically by the sign of retropulsion. Postural instability combined with motor freezing (sudden and transient inability to move) and freezing of gait can be particularly debilitating as it predisposes patients to falls. The latter are only partially amenable to therapy. The classic clinical motor signs described may be accompanied by less common, but equally problematic, bulbar motor symptoms of speech and swallowing dysfunction highlighting the widespread and highly heterogeneous presentations which PD can take.

1.1.4 Non – motor symptoms and disease progression

PD is slowly progressive and during the course of the disease the primary motor symptoms will, after a number of years, be joined by motor complications including dyskinesias and on – off fluctuations in the majority of cases (Schrag 2000). Although motor symptoms are often the most prominent manifestation of PD and have historically drawn the most attention from physicians, non-motor symptoms have increasingly been recognised to contribute significantly to quality of life for patients (Martinez-Martin et al. 2011). These include gastro-intestinal (e.g. constipation, nausea and swallowing difficulties), genito-urinary (e.g. urinary urgency, erectile dysfunction), neurological (e.g. falls, restless legs, excessive sweating / drooling,) and neuro–psychiatric (e.g. memory loss, somnolence, hallucinations, depression / anxiety, rapid eye movement (REM) behaviour sleep disorder), (Chaudhuri et al. 2006). Although there is now evidence that some of these symptoms may even predate the onset of motor dysfunction they generally become a more prominent and troubling feature of late disease, when they may overshadow the motor symptoms and necessitate a reduction in dopaminergic therapy (Chaudhuri et al. 2006).

1.2 Pathophysiology

1.2.1 Cellular pathology

Idiopathic PD is characterised by severe loss of dopaminergic neurons in the substantia nigra pars compacta and the accumulation of intracellular cytoplasmic inclusion Lewy bodies (Hassler 1938; Gibb & Poewe 1986). Disease progression is associated with a spread of Lewy body pathology rostrally up the brainstem to the mesocortex and finally neocortex with the development of associated clinical signs (Braak et al. 2003). Lewy bodies have a complex ultrastructural makeup comprising a strongly staining ubiquitin core, a high concentration of alpha-synuclein in the periphery and up to 70 other different molecules (Wakabayashi et al. 2007). The discovery of the first monogenic gene for PD in 1996 for alpha-synuclein converged the long standing pathological research with newer genetic understandings and as such further implicates alpha-synuclein in the pathophysiology of PD (Polymeropoulos et al. 1997). The role of alpha-synuclein is still however strongly debated. It may be that aggregation of alpha-synuclein is itself toxic to neurons or conversely it could represents a failed attempt to protect the damaged neuron (Lees 2009). It is clear that the molecular biochemistry underpinning PD is highly complex, involving many different molecular pathways including protein folding and clearance, mitochondrial function and oxidative stress, and the ubiquitin-proteasome system (Moore et al. 2005). These cellular level changes result in severe reductions in dopamine and consequent motor dysfunction. To understand how comparatively focal neuro-degeneration in the substantia nigra pars reticulata (SNr) gives rise to such a severe and pervasive motor disorder we must consider the system in which it is embedded and the pathophysiology of the system as a whole. Additionally, in addition to dopamine, it is now appreciated that other neurotransmitter systems are also involved and may be more related to non-motor symptomatology. The cholinergic, serotonergic,

adrenergic, glutamatergic, gamma-aminobutyric acid (GABAergic) and adenosine-mediated systems have all been found to be affected and addressing the dysfunction in these other systems may provide new therapeutic avenues for PD (Barone 2010).

1.2.1 Network pathophysiology

The SNr is integral to and integrated within the basal ganglia and its normal functioning. The basal ganglia have been implicated in movement control for more than a century since David Ferrier identified the corpus striatum as "the centres of automatic or sub-voluntary integration". Although disruption of the basal ganglia clearly causes a range of diseases, often characterised by movement abnormalities, its role in the normally functioning brain is still debated (Nambu 2008). The basal ganglia are a group of anatomically distinct, functionally unified, bilaterally symmetrical subcortical nuclei. Analysis of the anatomy of the basal ganglia advances us towards an understanding of its possible functional role. Early work on the basal ganglia, reflecting on the diverse and rich inputs from the entire neocortex to the striatum, suggested that the basal ganglia serve to integrate diverse inputs from widespread cortex and to "funnel" them to the motor cortex via the thalamus (Kemp & Powell 1971). This was challenged by a seminal paper that delineated multiple, parallel, segregated, closed loops from cortex through the basal ganglia and back to input cortices suggesting that the basal ganglia, like the cortex, demonstrated organisation in keeping with a degree of functional specificity (Fig. 1.1), (Alexander et al. 1986)

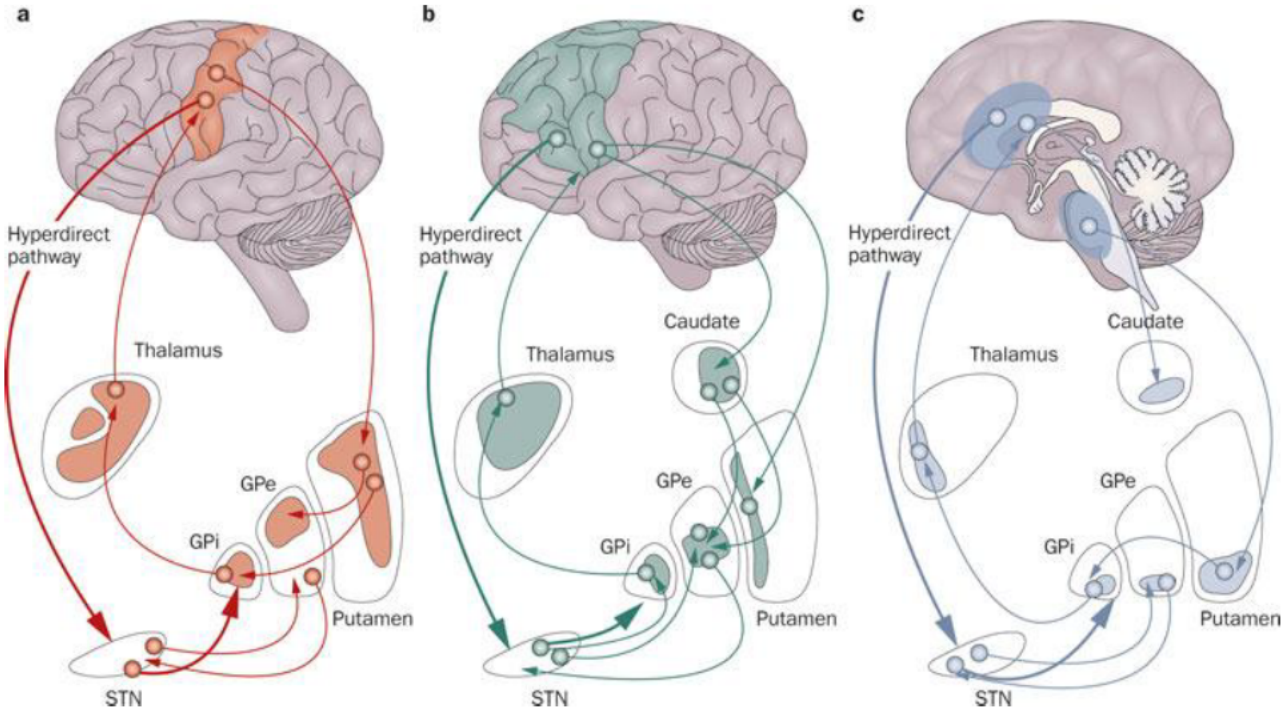

Figure 1.1. A schematic of the basal ganglia showing distinct, functionally segregated, loops. A The motor circuit involves the motor and supplementary motor cortices, the posterolateral part of the putamen, the posterolateral GPe and GPi, the dorsolateral STN, and the ventrolateral thalamus. **B** The associative loop and **C** the limbic loop connect the prefrontal and cingulate cortices with distinct regions within the basal ganglia and thalamus. In the STN, a functional gradient is found, with a motor representation in the dorsolateral aspect of the nucleus, cognitive–associative functions in the intermediate zone, and limbic functions in the ventromedial region. Via a 'hyperdirect' pathway, the STN receives direct projections from the motor, prefrontal and anterior cingulate cortices. Abbreviations: GPi, globus pallidus interna; GPe, globus pallidus externa; STN, subthalamic nucleus. Reprinted with permission (Volkmann et al. 2010)

The main input nucleus of the basal ganglia is the striatum which receives excitatory glutamatergic projections from the entire neocortex. The output of the striatum is comprised of inhibitory GABA-ergic medium spiny projection neurons which account for 90% of the striatal neuronal population in conjunction with some 10% inhibitory interneurons (Kawaguchi 1997). Medium spiny neurons fire rarely and only in the presence of synchronised activity within the multiple cortico-striatal afferents, effectively filtering out uncorrelated cortical inputs before passing on filtered patterns through the loop (Hammond et al. 2007). The most studied of the circuits is the motor circuit which provides a template for the other loops (Albin et al. 1989). The early conceptualisation of this model involved

two opposing streams: the direct and the indirect pathways (Fig. 1.2a). The direct circuit consisted of an inhibitory GABA-ergic pathway from the striatum to the GPi with a second inhibitory stream which acted to disinhibit the thalamus (i.e. excitatory). This was countered by a second circuit, the indirect pathway which incorporated an extra nucleus, the STN that provided an excitatory input to the GPi and in conjunction with the GABA-ergic output of the GPi acted to inhibit the thalamus. The equilibrium between these two pathways, and subsequently the balance between movement and inaction was controlled by dopamine, with its action on the two pathways being via D1 (direct pathway; excitatory) and D2 receptors (indirect pathway; inhibitory). This relatively simple model, which is predicated on a pure rate coding scheme, was remarkably successful in explaining numerous experimental results relating to the basal ganglia in addition to a number of clinical disorders such as PD. Thus PD can be understood as an imbalance between the direct and indirect pathways with excessive inhibitory activity in the latter causing akinesia in the absence of dopamine. Although a great step forward, it is now generally recognised as an oversimplification (Nambu 2008). The anatomy of the basal ganglia has revealed itself to be significantly more complex than initially conceived (Fig. 1.2b) with one substantial advance being the recognition of the STN as a major input nucleus to the basal ganglia via the hyper-direct pathway from the cortex (Nambu et al. 2002). This knowledge, in addition to the appreciation of new inter-connections between basal ganglia nuclei and between these and the thalamus, and the incomplete segregation of outputs within the direct and indirect pathways makes the previously accepted simple anatomical dichotomy between the two streams less plausible. Paradoxically, the successful neurosurgical treatment of movement disorders with lesioning or DBS of the globus pallidus and the thalamus have further cast doubt on the firing rate scheme given their demonstrable improvement of akinesia which is not predicted under the earlier model (Marsden & Obeso 1994).

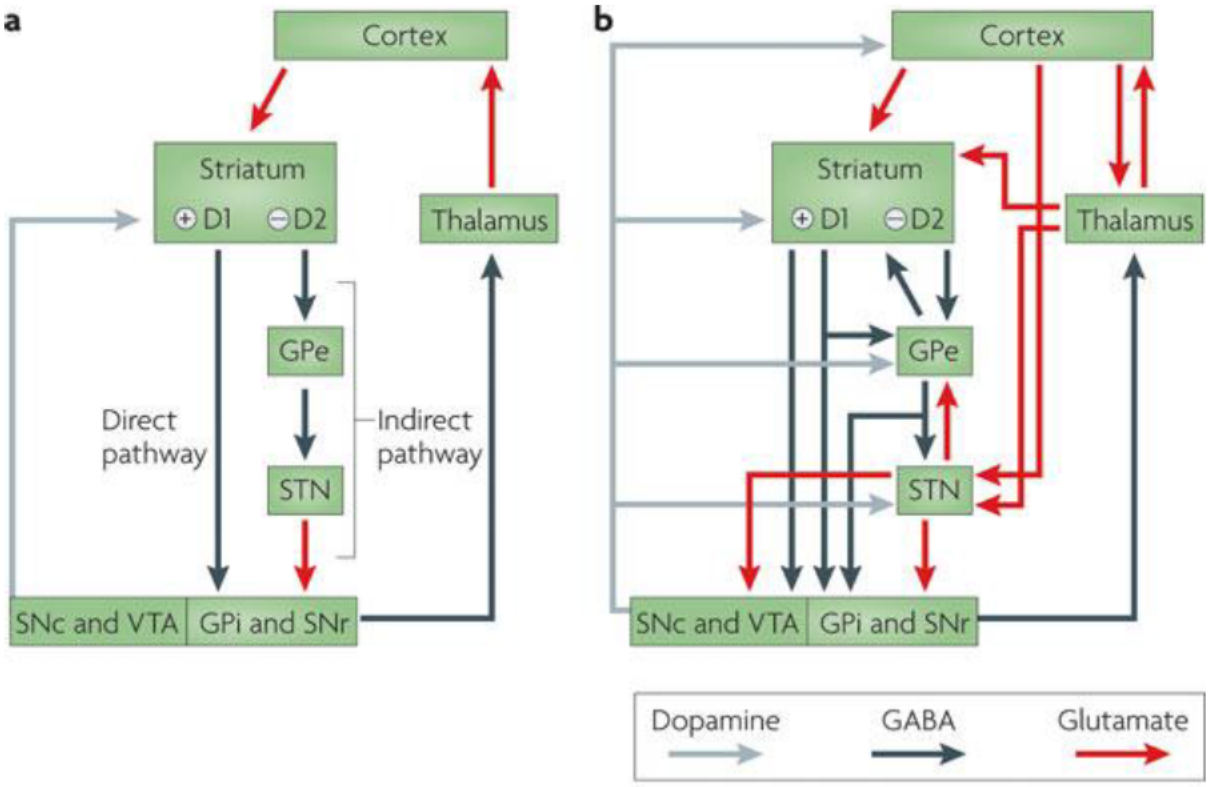

Figure 1.2. Schematic of the basal ganglia as proposed by Albin and Delong with the more recent version with new anatomical pathways indicated. a) Model based on the influential proposal by Albin and colleagues (Albin et al. 1989), according to which the output of the basal ganglia is determined by the balance between the direct pathway — which involves direct striatonigral inhibitory connections that promote behaviour — and the indirect pathway — which involves relays in the GPe and STN and suppresses behaviour. The balance between these two projections was thought to be regulated by afferent dopaminergic signals from the SNc and the VTA acting on differentially distributed D1 and D2 dopamine receptors. b) Recent anatomical investigations have revealed a rather more complex organization in which the transformations that are applied to the inputs to generate outputs are less easy to predict. Modified from Ref. (Redgrave 2007).

Objections to the rate firing model did not only emerge from the new anatomical insights described. Physiological studies also started to paint a more complex and curious picture of basal ganglia function. Recordings in MPTP treated primates demonstrated a change in the basal ganglia firing patterns as well as the firing rate in the absence of dopamine with neuronal firing demonstrating oscillations and bursting (Bergman et al. 1994). These findings in the primate model were subsequently corroborated

by micro-electrode recordings in PD patients during DBS electrode insertion again confirming oscillatory activity of neuronal firing in the absence of dopamine (Levy et al. 2000).

This increased bursting pattern of individual neurons can also be seen at the population level as recorded through the local field potential (LFP) (Fig. 1.3). The LFP measures the sum of pre-synaptic potentials within the vicinity of the recording electrode and therefore represents the population level synchronised activity within different frequency bands (Buzsáki et al. 2012). In patients with PD there is marked synchronisation in the absence of levodopa in the beta range (12 -33 Hz). As such it appears that firing pattern, in addition to firing rate, is important in the normal functioning of the basal ganglia.

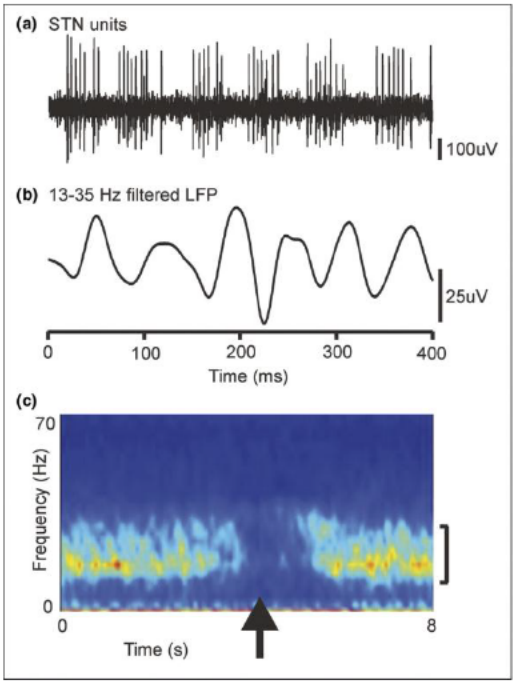

Figure 1.3. Intraoperative recordings of neuronal and LFP activity in the STN of a patient with Parkinson's disease withdrawn from their medication. (a) Neuronal discharges. (b) Simultaneously recorded LFP. Note oscillations at about 15 Hz coincide with bursts of discharges. (c) Colour plot of time-evolving Unit-LFP coherence averaged around 20 self- paced contralateral hand movements (movement onset is arrowed). Note suppression of beta activity (see vertical bar) before and during movement (Brown 2007)

1.4 Treatment for Parkinson's disease

1.4.1 Medical treatment

PD involves, amongst other changes, a loss of dopaminergic cells in the SNr and the mainstay of treatment is the replacement of dopaminergic drive through medication. This was dramatically discovered in the 1960s with administration of firstly intravenous and later chronic oral levodopa with near miraculous initial results (Cotzias et al. 1967; Hornykiewicz 2010). However, even in the early studies, side effects of high dose oral therapy were noted – motor fluctuations, dyskinesias and cognitive problems. Levodopa is able to cross the blood brain barrier and is broken down to active dopamine by central decarboxylation. Therefore a further advance in the 1970s was that of combining levodopa administration with a peripheral dopa-decarboxylase inhibitor (Carbidopa / Benserazide) in order to block peripheral conversion to dopamine and thereby increase delivery to the CNS and reduce side effects of peripheral dopamine. This was highly effective in reducing nausea associated with stimulation of brainstem chemoreceptors outside the blood brain barrier in addition to enabling much more rapid titration of levodopa dosage into the therapeutic range and remains the mainstay of treatment today (Tolosa et al. 1998). However, a growing awareness of the side effects of long term high dose levodopa prompted a search for alternatives. The pathophysiology of levodopa induced motor complications is still only partially understood. It is well established however, that disease severity, duration of therapy and the half-life of the dopaminergic agent employed are all important factors for their development (Obeso et al. 1989). This gave rise to the pulsatile dopamine hypothesis in which denervated striatal dopamine receptors are subject to non-physiological pulsatile dopamine in the form of oral levodopa leading to molecular, genetic and physiological alterations in neuronal function. Studies are now starting to delineate the genetic mechanisms involved and evidence is

pointing towards striatal NMDA dysfunction as playing a critical role, particularly in the case of dykinesias (Ahmed et al. 2011). These findings may well pave the way for the rational development of new drug targets in Parkinson's disease. However, to date, the prevention and treatment of motor complications has centred on attempting to prevent severely non - physiological pulsatile dopamine administration.

Dopamine agonists are structurally similar to dopamine and thus similarly stimulate postsynaptic dopaminergic receptors, but have different pharmacokinetics to levodopa. Apomorphine, was the first dopamine agonist to be shown to be effective but was unfortunately limited by side effects in both the intravenous and oral forms (Tolosa et al. 1998). This was soon followed by the introduction of ergot derived agonists, with Bromocriptine being introduced in the 1970s. The longer half-lives and higher receptor specificity of dopamine agonists suggests that they may be better suited than levodopa for avoiding pulsatility and thus motor complications. Early, ergot-derived, agonists have now been mainly replaced by non – ergot derived agonists including Ropinirole, Pramipexole and Rotigotine which don't cause side effect of vasospasm, erythromelalgia, retroperitoneal fibrosis and cardiac valvular disease. Subsequently, treatment with dopaminergic agonists was indeed shown to cause less dyskinesias than with levodopa treatment alone (Rascol et al. 2000). Monotherapy with a dopamine agonist in early stage PD to limit exposure to levodopa and prevent dyskinesias has become common practice. However, there are now voices of dissent against the demonising of levodopa and a reappraisal of the evidence on which this is based. Specifically, it has been noted that the doses of levodopa and agonists were not equipotent in the initial trials and thus the reductions in dyskinesias may have come at the cost of worse symptomatic control and agonist related side effects such as impulse control disorders (Vlaar et al. 2011). Although good symptomatic control is obtainable in most patients with

combination dopaminergic replacement, these drugs give only symptomatic benefit and at present there are no medications which have been shown to be definitively disease modifying.

A different class of drugs, the MAO-Is, increase dopamine levels by inhibiting its breakdown by monoamine oxidase. The most commonly used now is Rasagaline which has mild symptomatic benefit and at a medium dose (1 mg) showed a possible effect suggestive of slowing of disease progression. This however, was not found at higher dosages leading to any suggestions of disease modification being interpreted with caution (Siderowf & Stern 2002; Olanow et al. 2009). As such, MAO-Is are used in some patients with very early mild disease to delay levodopa initiation or in combination with levodopa and dopamine agonists to manage motor fluctuations. Likewise anti-cholinergic medications such as Trihexyphenidyl or Procylidine can be used in young, cognitively robust individuals with tremor dominant disease to delay the initiation of levodopa. The COMT enzyme is responsible for the breaking down of catecholamines peripherally, including dopamine, and therefore COMT inhibition, like the dopa decarboxylase inhibitors, increases the central bioavailability of levodopa, thus prolonging its action. Entacapone and Tolcapone thus provide another option for the management of motor fluctuations. Amantadine, a weak NMDA antagonist reduces dyskinesias but its effect is short lived (< 8 months). Over time as the disease progresses, in practice, the majority of patients end up on a combination drugs including levodopa and dopamine agonists with a balance being struck between motor control versus side effects in each individual patient (Lees 2010). In addition to medical therapy, a holistic approach should also be maintained that supports patients' general physical and mental wellbeing. This can partly be facilitated through the support available through organisations such as Parkinson's UK as well as maintenance of physical condition through exercise and PD specific physical therapy (Suchowersky et al. 2006).

1.4.2 Advanced treatments

Whereas the management of early Parkinson's is relatively straightforward with patients generally responding well to intermittent dopaminergic replacement, as the disease progress, the majority of patients develop complications (Schrag 2000). Drug adjustment, addition of agonists, MAO-Is, COMT inhibitors or amantadine can help in some cases (NICE 2005). However, for some patients, despite these changes, they remain significantly disabled by poor motor function and should be considered for the advanced therapies. The advanced therapies at present comprise Apomorphine injection/infusion, Duodopa infusion and deep brain stimulation (DBS) and all have their advantages and disadvantages but all are invasive to a degree and their initiation marks the transition to complex disease management (Worth 2013).

Apomorphine, is a potent D1 and D2 dopaminergic agonist which has been available since the 1960s but was initially surpassed by more effective oral levodopa. It has since been rediscovered for use in patients with advanced PD as its injectable format allows precise and rapid control of dopaminergic drive. It is now available as an intermittent rescue formulation or as a subcutaneous infusion and increases daily ON time and reduces dyskinesias by allowing the down titration of concomitant oral dopaminergic drugs (Stibe et al. 1988). However, there are no quality randomised controlled studies of continuous subcutaneous Apomorphine infusion (its most common use) and the reported benefits in open label trials have been variable; 38-80% reductions in OFF time (Worth 2013). Additionally, being a dopamine agonist, it is subject to the standard side effects of this class of drugs, including; sedation, nausea, psychosis, hallucinations, dopa dysregulation in addition to infusion specific side effects of subcutaneous nodule formation.

An alternative and advanced dopaminergic delivery method that aims to deliver a constant dopaminergic drive is found in the form of Duodopa which involves the infusion of levodopa / Carbidopa suspension gel directly into the jejunum, thereby bypassing the variable passage and absorption of the stomach. This treatment has the advantage of being slightly less restrictive in its inclusion criteria than DBS, with some patients who are >70 years old with mild dementia or gait disorders still being considered. It has been shown to increase daily ON time (4 hours) and improve quality of life on the PDQ-39 (Nyholm 2012). However, the treatment is invasive and associated with intermittent device malfunctions, axonal neuropathy and at >£30,000 per annum with a relatively limited evidence base, is still only considered in very occasional cases.

1.4.3 Deep Brain Stimulation

The most well-established of the advanced therapies, with the strongest evidence base for motor and quality of life improvement in both the acute and chronic setting is DBS (Deuschl et al. 2006; Weaver et al. 2009; Williams et al. 2010). Surgical therapies for PD appeared in the first half of the 19th century following observations that vascular lesions could ameliorate symptoms in some patients (Meyers 1940; Cooper 1953). The introduction of the stereotactic frame in the 1950s improved safety and side effects and it was even noted at this early stage that electrical stimulation of basal ganglia could reversibly ameliorate symptoms (Speigel 1952; Hassler et al. 1960). Despite some early successes, surgical intervention for PD was surpassed by the arrival of levodopa and it wasn't until the 1970s and 1980s, when a new appreciation of the side effects associated with levodopa use developed that lesioning of the GPi re-emerged as a treatment of late stage medical complications (Worth 2013). Subsequently, it was the remarkable demonstration that reversible interventions within the basal ganglia using electrical stimulation could reverse symptoms of PD which brought surgical therapies for

PD truly back to the fore (Benabid et al. 1987; Limousin et al. 1995). The operation involves permanently implanting multicontact electrodes bilaterally within the basal ganglia which are connected subcutaneously to a battery and stimulator pack residing in the subclavicular fossa for the chronic delivery of pulses of electrical stimulation (Foltynie & Hariz 2010). Initially considered as a 'virtual' lesion in line with the earlier permanent lesion studies, multiple sites were investigated for efficacy in PD. Three key nuclei have emerged as being effective in PD, the STN, the globus pallidus interna (GPi) and thalamus, specifically the ventralis intermedius area (VIM) with different indications for each implantation site. The STN was initially favoured as the preferred target for PD as it appeared to result in greater motor improvement and more marked reductions in dopaminergic medications (Krack et al. 1998; DBS PD Study Group 2001). However, more recent research studies have suggested that the GPi may be equally effective in terms of motor efficacy for PD with the possibility of being associated with slower cognitive decline over time (Follett et al. 2010; Weaver et al. 2012). The decision of which nucleus to target is complex and further research is required to definitely answer which is superior. However, evidence is accruing that both STN and GPi DBS have different strengths and weaknesses and as such, nucleus selection should be tailored on an individual basis. Alternatively, thalamic (VIM) implantation is mainly reserved for PD subjects with severe disabling tremor with minimal bradykinesia / rigidity, who may not be able to tolerate STN or GPi implantation (Limousin et al. 1999). Pedunculopontine nucleus implantation is also used in some highly selected PD cases whose dominant problem is gait freezing (Stefani et al. 2007).

DBS of STN and GPi is currently implemented in advanced medically resistant PD to increase overall ON time and to reduce dyskinesia and medication requirements. That DBS is effective for improving the cardinal symptoms of PD in the absence of levodopa is now well established (Pollak et al. 1993; Siegfried & Lippitz 1994; Kumar et al. 1998; Limousin et al. 1998; Burchiel et al. 1999; Okun et al.

2009). Motor improvement measured by Unified Parkinson's Disease Ratings Scale (UPDRS) with DBS off medication was initially found to be as high as 40-60%. This is complemented by the finding that DBS also improves other symptoms associated with late stage disease such as motor fluctuations, dyskinesias and off period dystonia (Krack et al. 2003). However, to justify its role in advanced PD, the clinically relevant question is whether it is superior to medical management alone and a number of recent trials have addressed this issue (Deuschl et al. 2006; Weaver et al. 2009; Williams et al. 2010; Weaver et al. 2012; Schuepbach et al. 2013). Motor function on medication improved from a UPDRS score of 18.9 to 14.6 in the ON medication ON DBS group, with no improvement in the group on best medical management alone (Deuschl et al. 2006). There was also a 9.5 point (25%) improvement in quality of life as measured by the PDQ-39. Total daily ON time was also greater in the DBS group, increased by 4.6 hours a day and improvements in motor function were stable at 36 months duration (Weaver et al. 2009; Weaver et al. 2012). This has since been corroborated by trials showing PDQ-39 improvements of 5 points and 8 points in the DBS group compared with the medical management alone group (Table 1.1) (Williams et al. 2010; Schuepbach et al. 2013).

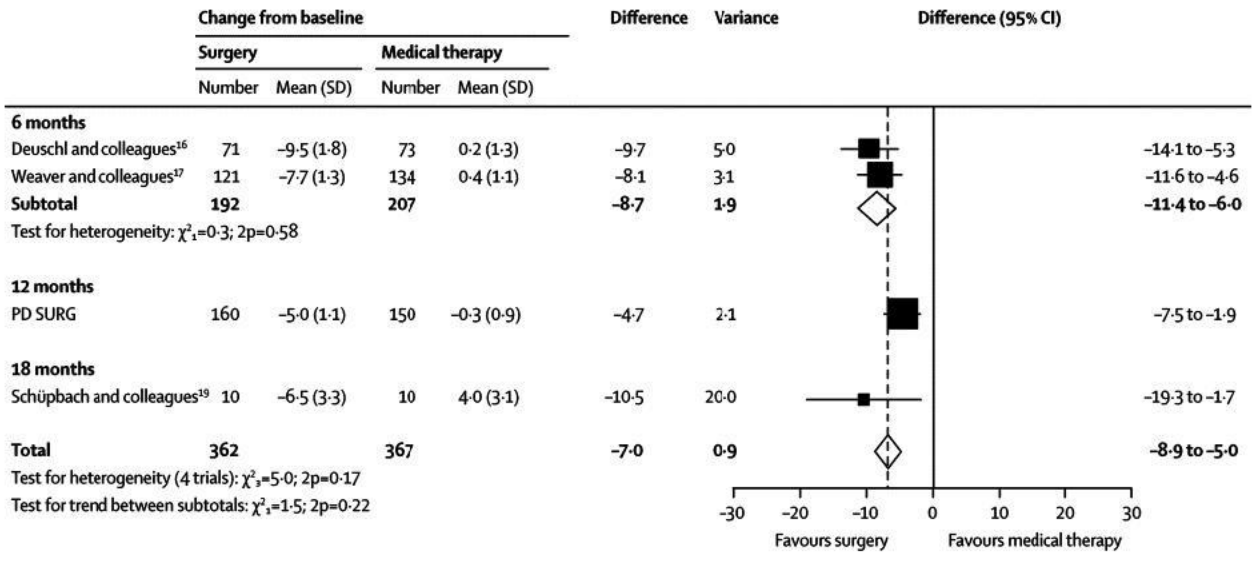

Table 1.1 Meta-analysis of 39-item Parkinson's disease questionnaire summary index score in trials of deep brain stimulation versus medical therapy. Reprinted with permission. (Williams et al. 2010)

Importantly, motor improvements are maintained and have been documented over the longer term in a range of studies of STN and GPi DBS at 5 and even 10 years, although the late stage disease phenotype disease is typically dominated by features which are neither medication or DBS responsive, namely speech, gait and neuropsychiatric symptoms (Rodriguez-Oroz et al 2012). As such, it appears that DBS treatment offers improvements in motor scores and quality of life compared with best medical management and therefore the question of when to intervene has become pertinent. Traditionally, DBS was reserved for severe advanced, medical refractory PD when quality of life and psychosocial competence are already significantly impaired. The mean disease duration at DBS implantation is 11- 13 years (Deuschl et al. 2006; Williams et al. 2010; Follett et al. 2010). Given the motor efficacy thus far demonstrated, there is an argument for earlier intervention to maximise these gains prior to the emergence of dopa-unresponsive symptoms. One study has investigated this issue and found DBS to be effective in milder, early disease with a mean duration of 7.5 years, raising the possibility that further improvements in outcome could be achieved with earlier treatment (Schuepbach et al. 2013). Although, this study gives grounds for optimism, it did involve a highly selected group of younger patients (all < 60 years of age) and whether these results will extend to older patients with PD remains to be determined.

1.4.4 Disease modification & Deep Brain Stimulation

DBS is currently advocated only as a symptomatic treatment in PD. There is though both theoretical and limited clinical evidence that it may have a disease modifying effect in slowing progression. Studies in rodent and primate models of PD have demonstrated reduced dopaminergic cell loss in those

animals treated with DBS (Wallace et al. 2007; Spieles-Engemann et al. 2010). There have also been some hints from clinical studies, although these remain inconclusive. One study found no significant deterioration in UPDRS score off DBS and levodopa from pre-surgical baseline 4 years after implantation, although this was not one of the primary end points (Visser-Vandewalle et al. 2005). Other studies have however shown deterioration both clinically and at the dopaminergic receptor level as measured by 18F-fluorodopa PET quantification (Krack et al. 2003; Hilker et al. 2005). Consequently, a study is currently underway to investigate directly the potential for disease modification by DBS (Kahn et al. 2012).

1.5 Side effects and limitations of Deep Brain Stimulation

1.5.1 Surgical

The documented, positive clinical effects of DBS must be considered against its risk of side effects and adverse events. The surgical procedure involves placement of hardware deep within the brain and therefore comes with attendant risks. Reported risk of death is 0.6% and permanent neurologic sequelae 2.8 % (Pahwa et al. 2006). In addition, to the serious long term side effects stated, there are documented risks which cause only transient symptoms including infection (5.6 %), haemorrhage (3.1 %), confusion (2.8 %), seizures (1.1 %), pulmonary embolism (0.6 %), CSF leak (0.6 %), peripheral nerve injury (0.6 %) and venous infarction (0.3 %) (Pahwa et al. 2006). The rates of risk reported by different groups varies significantly and this may be in part due to the different choice of operative technique between groups. A recent retrospective review of 76 consecutive patients by one group that uses an MR guided technique and doesn't perform micro-electrode recordings intra-operatively

revealed no haemorrhagic complications with a mean 52% reduction in motor UPDRS scores (Foltynie et al. 2011).

Complications related to the hardware itself are also not uncommon and include electrode / wire malfunction (4.4 %), device dysfunction (3.0 %), device infection (1.9 %) and device migration (1.5 %) (Kleiner-Fisman et al. 2006).

1.5.2 Stimulation induced side effects

There exist also a number of complications related to stimulation itself, which may be voltage dependent and reversible on cessation or adjustment of stimulation. These include dysarthria (9.3 %), weight gain (8.4 %), depression (6.8%) and eyelid opening apraxia (3.6 %) (Kleiner-Fisman et al. 2006). At higher voltages during parameter exploration whilst programming the stimulator, paraesthesia and facial contractions are not uncommon. The most disturbing of the stimulation induced side effects relates to its neuro-psychiatric sequelae affecting cognition and behaviour and although these have been clearly documented, the rates of these different symptoms is conflicting through the literature. The majority of studies report only mild or absent cognitive or behavioural side effects once treatment is established, although it is more common in the immediate postoperative period (Ardouin et al. 1999; Woods et al. 2002; Daniele et al. 2003; Morrison et al. 2004; Funkiewiez et al. 2004; Parsons et al. 2006; Witt et al. 2008). Other studies have shown significant adverse psychiatric, behavioural, verbal and cognitive side effects particularly in older subjects (>70 yrs.) even in the presence of motor benefit (Saint-Cyr et al. 2000; Schüpbach et al. 2006; Smeding et al. 2006). The issue is further complicated when basal ganglia nuclei are examined separately and again the evidence is conflicting. A number of studies have reported that cognitive and executive dysfunction are more common following STN implantation than with GPi (Anderson et al. 2005; Rodriguez-Oroz et

al. 2005). However, this was not backed up by another recent larger multi-centre study which found equivalent rates of adverse effects between the two nuclei (Odekerken et al. 2013). As such, although it is clear that some patients do experience a deterioration in their cognitive or verbal skills, further research is required to further delineate the risk factors for this, although age already appears to be one such factor (Saint-Cyr et al. 2000). A further concerning side effect, particularly of the STN, relates to increased rates of suicide seen following implantation. A very large, multi-centre retrospective study that examined the results from 5311 patients who had received DBS found a suicide rate of 0.26% per year which was 13 times higher than that seen in the age, gender, country matched controls (Voon et al. 2008). They identified independent risk factors for suicide including post-operative depression, single marital status and a previous history of impulse control disorders or compulsive medication use accounting for 51% of the variance in suicide risk. These factors must be looked for during patient selection for DBS procedures and such patients should be closely followed up post operatively looking for depression.

1.5.3 Cost of Deep Brain Stimulation

Limitations to DBS are not limited only to side effects, but being an advanced complex therapy, there are financial constraints as well. The National Institute of Clinical Excellence (NICE) have reported model derived costs of £42,100 for DBS over 5 years compared with £28,100 for medical therapy alone (NICE 2006). Studies reporting on cost effectiveness have been variable although a number of different groups have reported cost per QALY at around €35,000 making DBS cost effective if a quality of life improvement of at least 18% is achieved (Tomaszewski & Holloway 2001; Dams et al. 2013). Other groups have even reported savings with DBS compared to medical management alone highlighting the complexity and also healthcare system specific costs of these types of analyses

(Meissner et al. 2005). DBS is an expensive treatment and much of the long term cost relates to replacement of batteries and stimulator apparatus approximately every 4 years (Bin-Mahfoodh et al. 2003). Rechargeable stimulators have been introduced in the last few years which have the potential to reduce these replacement costs, although these devices are not appropriate in all patients (Timmermann et al. 2013).

1.6 Closed Loop Deep Brain Stimulation

1.6.1 Why close the loop?

Therefore, the cost of DBS, its partial efficacy and its side-effects mean that there is still a pressing need for improvement. With DBS as currently used, stimulation is always on, relentlessly interfering with neural circuits regardless of the level of pathological activity. With a closed loop approach, stimulation is delivered according to clinical state so that networks are stimulated only when necessary, saving on battery power, limiting habituation and improving patient outcome. Closed loop stimulation has already proved very effective in the treatment of cardiac arrhythmias and is being trialled in epilepsy (Morrell 2011; Fisher et al. 2010; Jobst et al. 2010; Sutton et al. 2007).

The underlying assumption in closed loop therapy is that there are gains to be had from varying stimulation intensity over time, -including, when appropriate, turning stimulation off. The advantages with respect to therapy in diseases like PD are complex. One advantage is more economical power consumption, provided power savings are not offset by the additional power demands of the closed loop circuit. But the introduction of rechargeable batteries and their future refinement has somewhat lessened the significance of power savings over time, although not all patients are suitable for such devices (Timmermann et al. 2013). Another possible advantage is that discontinuous stimulation might limit accommodation and loss of therapeutic efficiency over time. However, with the exception

of some patients undergoing thalamic DBS for tremor, accommodation has not been a significant phenomenon in clinical practice. Potentially more important is the reduction in side-effects if stimulation can be limited or discontinued during periods when it is not needed. Some of these side-effects are obvious, such as the reduced intelligibility of speech present in some parkinsonian subjects undergoing DBS of the subthalamic nucleus, but others are more subtle and only exposed when performance would otherwise have been good at that particular moment in time. An example of the latter is the paradoxical worsening of manual tapping during DBS in those PD patients that can manage high tapping speeds on the morning of study (Chen, Brücke, et al. 2006). Response inhibition can also be worsened by DBS in previously good performers with a slowing of reaction times in stop stimulus reaction time tasks (Ray et al. 2009). These effects have also been shown in dystonia, where DBS can worsen bradykinesia in the non-dystonic limb and induce hypokinesia and freezing of gait (Berman et al. 2009; Schrader et al. 2011).

Such deterioration may reflect the disruption of physiological as well as pathological functioning by standard high frequency DBS regimens. As such, it is hoped that paradoxically, by stimulating less, motor function may be improved as the balance between suppression of pathological and physiological motor physiology is optimised. Finally, the closed loop mode opens up the possibility of alternative stimulation regimens which deliver stimuli specifically patterned according to the temporal structure of the brain signal used in feedback control. Here, it is assumed that the feedback biomarker is mechanistically involved in the disease process and stimulation is then designed to suppress the detected activity through specific spatio-temporal patterning of stimuli, such as in multi-site delayed reset or phase cancellation (Hauptmann et al. 2005). Such tailored stimulation regimens have the potential to be more effective and yet cause fewer side-effects as they should be more selective for underlying pathological activity.

Another way that DBS could be improved is to optimise the precise pattern of stimulation delivered, irrespective of whether this is under closed-loop control. Standard DBS for PD is usually delivered at 130 Hz with a power or 1-4 volts and pulse width of 60 microseconds. These parameters have been selected on empirical grounds but the available parameter space has not been fully searched and the possibility of strategically patterning stimulation according to the form and phase of pathological network activity has been barely explored. Yet patterned stimulation regimes that specifically target pathological activities may potentially be more efficient and have less effect on physiological processing, and thereby have less power consumption and fewer side-effects.

1.7 Biomarkers of Parkinson's disease

The above approaches to improving DBS require a detailed understanding of pathological brain signals. In closed loop DBS, where when to stimulate is determined by clinical state, there is no single kinematic measure that can comprehensively capture diverse impairments such as rigidity, slowness of movement or tremor and yet be miniaturised. Hence, the search is on for brain signals that faithfully reflect clinical state and can be measured with minimal extra intervention. Such a signal should be sensitive and specific to the clinical state and reliable over time and in different conditions. Yet it should also provide a more-or-less instantaneous measure of clinical state so that therapy does not lag impairment. Moreover, it should be calculable with the lowest possible computational requirement as this will impact on both battery consumption and time delays in the efferent limb of any control system. In the case of strategically patterned stimulation the requirements are even more stringent, for the brain signal must not merely correlate with clinical state but must also cause it in order to be a legitimate target. Unsurprisingly, there is as yet no single biomarker which fulfils all these criteria.

1.7.1 Cortical Signals

Parkinson's disease is classically defined as the triad of bradykinesia, tremor and rigidity. When considering feedback parameters for PD therefore, one must first establish whether the different aspects of the disease represent different manifestations of a single pathological system that could be potentially represented by a single biomarker or whether these different motor manifestations have different substrates and are therefore likely to be represented by separate biomarkers. There is now strong evidence for more than one system and specifically it appears that rigidity-bradykinesia is functionally discrete from tremor (Rivlin-Etzion et al. 2006). This dichotomy is further complicated when one considers other well recognised PD symptoms such as gait disorders and non – motor symptoms. Thus the dominant phenotype of the patient should direct the choice of biomarker or biomarkers for closed-loop DBS in an individual patient. Fortunately, growing evidence that disturbed temporal coding at the neuronal and population level may lie at the heart of parkinsonian impairment affords hope that different biomarkers may be organised in the frequency domain and available through recordings from the same site (Brown 2003).

Given the location of the DBS electrodes precisely at the site of interest, namely within the pathological basal ganglia circuit itself, it seems most rational to seek potential biomarkers within this region, and, preferably, to record these through the stimulating electrode itself. On the other hand, an advantage of recording relevant biomarkers away from the stimulation site would be avoidance of contamination via stimulation artefact, opening up the possibility of using biomarkers over a wider frequency band, as current approaches to recording from stimulation sites rely on low-pass filtering to recover biological signal (Rossi et al. 2007; Eusebio et al. 2011). In view of this it is worth first considering the possibility of deriving suitable biomarkers from the cerebral cortex. The

electroencephalogram (EEG) has been the predominant signal used for brain computer interfacing (BCI) previously, due to its non – invasive nature. It records the aggregate signal from a surface cortical population of an area of about 6 cms^2 and has successfully been used to control simple movements in healthy volunteers and in patients (Curran & Stokes 2003). EEG and MEG signals in patients even with early untreated PD have been shown to be distinguishable from age matched controls by both linear and non-linear analyses, but only at the group level (Müller et al. 2001; Pezard 2001; Pollok et al, 2013). So far only a handful of studies have demonstrated a correlation between EEG / MEG derived measures and motor impairment, and between treatment induced change in such measures and changes in motor impairment (Silberstein, Pogosyan, et al. 2005; Stoffers et al. 2008). These EEG / MEG based measures are based on inter-regional synchronisation and need extensive head coverage. Thus EEG and electrocorticography (ECoG) are currently impractical approaches to long-term closed loop control. MEG is non-portable and also inappropriate. Moreover, it remains to be shown that correlations with motor impairment can be made within subjects as state changes over time, and not just across subjects.

An alternative approach to deriving cortical signals is to record the activity of single or multiple units in the cortex. This affords remarkable spatial resolution but this is potentially at the cost of the loss of diffuse population coded information. The latter is often addressed by the use of multiple microelectrodes. However, there are considerable technical limitations to their application in the chronic setting which has thus far limited their widespread clinical use. It has been found that only approximately a half of implanted microwires deliver recordable units and this further deteriorates over time due to neuronal gliosis around the electrode tips and other hardware failures (Schwartz et al. 2006). Additionally, there is a significant computational cost involved in the online analysis of multiple discrete electrode signals of this sort.

1.7.2 Basal Ganglia signals

Most attention has been focussed on recording potential biomarkers directly from the basal ganglia in PD. Again, there are several approaches. One is to record single units and Weinberger et al showed not only that there was increased burst activity on recording from individual neurons in the off drug state but that there was also a significant correlation between the incidence of oscillatory neurons and the patient's benefit from dopaminergic medications, although this correlation did not extend to motor deficit at rest, off medications (Weinberger et al. 2006). A related approach is to record the background activity from the microelectrode. Individual neuronal spikes are selectively removed from the data and replaced with randomly selected surrogate spike-free data from the same trace. The data are then high pass filtered at 70 Hz to remove synaptic potentials. Signals processed in this way are thought to represent the highly localised aggregate activity of action potentials of the population of neurons very close to the microelectrode tip (Moran et al. 2008). This too has been shown to correlate with motor impairment but its utility in closed loop stimulation regimes may be limited by the need to reject from the signal both unit activity and stimulation artefact, which share a similar frequency content.

Intracranial micro-dialysis provides a very different approach and is already routinely used in the research setting in animal models of Parkinson's and in humans for other conditions such as post-traumatic head injury for real-time and continuous monitoring of cerebral metabolites (Kilpatrick et al. 2010). It is possible that dopamine or dopamine metabolites from the striatum may provide a useful biomarker of clinical state that could be used for closed loop stimulation. Some newer silicon electrodes have micro- dialysis tubules included within them and show that micro-dialysis can be integrated into stimulation electrodes (Schwartz et al. 2006). However, there may be significant technical barriers to implementing this type of approach including tube blockage and miniaturisation of the chemical

analysis hardware for implementation in an implantable device. Moreover, it seems unlikely that microdialysis will have the temporal resolution to avoid lags between clinical change and therapy titration. More suitable may be fast scan voltammetry, which is an electroanalytical technique that extracts information on a subsecond temporal scale regarding the chemical composition of the extracellular fluid by varying the potential at a microelectrode and measuring the evoked current. This has successfully been piloted in a large animal model to show that DBS elicits a time-locked release of dopamine which is both intensity and frequency dependent (Shon et al. 2010).

1.7.3 Local Field Potentials

Despite the above endeavours most research has concentrated on the use of the LFP that can be recorded from the contacts at the end of the very same electrode used for chronic stimulation and so requires no additional electrodes or hardware. Typically the LFP is picked up from the STN, where, although focal and localised, it still represents a population averaged signal. It is recorded at lower frequencies than single-unit recordings, which is believed to be beneficial since these lower frequencies are less affected by electrode interface or by local geometry (Schwartz et al. 2006). Reassuringly though, research has still shown that the LFP potentials are closely related to the activity of individual neurons with synchronised bursting of neurons occurring in phase with beta (13-30Hz) activity off medication (Weinberger et al. 2006; Kühn et al. 2005). In view of the averaged nature of LFP activity across a population of neurons it could be questioned whether these signals are appropriate for monitoring of complex state dynamics. However, it should be noted that within the basal ganglia and particularly the STN, there is great convergence of information processing from across the cortex into the localised area around the LFP recording site. Additionally, a population based metric may well be superior to that of single unit recordings, given that many states are represented diffusely across populations rather than

within single neurons and this is likely to be particularly the case when tracking general state changes in PD rather than the subtle and highly localised motor coding that is involved in precise voluntary movements. Indeed, in some situations LFPs are superior to single units for representing movements (Andersen et al. 2004). These considerations combined with the long term stability of DBS at the tissue-electrode interface make LFPs very attractive feedback control parameters for responsive DBS. But how informative are they about different clinical features?

1.7.4 Bradykinesia & Rigidity

Early recordings in PD patients with DBS electrodes revealed that when recorded in the off medication state power spectra showed high levels of synchronised activity between 13 and 30 Hz (beta frequency band) in both the STN & the Globus Pallidus Interna (GPi) and subsequent follow up studies have confirmed this in the majority of cases (Table 1.2). It has been shown that beta activity is suppressed with levodopa treatment and that the degree of suppression correlates with motor improvement measured by the UPDRS clinical rating scale, particularly in the range of <20Hz (Kühn, Kupsch, et al. 2006; Kühn et al. 2009; Ray et al. 2008). It has recently been demonstrated that DBS treatment also suppresses beta activity and STN–DBS driven improvement in rigidity and bradykinesia (but not tremor) correlates with suppression of synchronisation (Fig. 1.4) (Eusebio et al. 2011; Kühn et al. 2008; Bronte-Stewart et al. 2009; Foffani et al. 2006; Rossi et al. 2008; Wingeier et al. 2006; Whitmer et al. 2012). Reassuringly it also appears that the beta profile is stable within patients over time and following DBS treatment (Bronte-Stewart et al. 2009; Rosa et al. 2011; Foffani et al. 2006; Abosch et al. 2012).

GROUP	Year	No of Patients / (nuclei) recorded	Number with Beta peaks Patients or (nuclei)	%
(Brown et al. 2001)	2001	4	4	100
(Cassidy et al. 2002)	2002	6	6	100
(Levy 2002)	2002	14	9	64
(Silberstein et al. 2003)	2003	(17)	(17)	100
(Kühn et al. 2004)	2004	8	8	100
(Priori et al. 2004)	2004	(20)	(17) low beta	85
(Kühn et al. 2005)	2005	6 (8)	(8)	100
(Doyle et al. 2005)	2005	14	14	100
(Wingeier et al. 2006)	2006	4 (6)	(6)	100
(Foffani et al. 2006)	2006	(13)	(11) low beta	85
(Kühn, Kupsch, et al. 2006)	2006	9 (18)	(17)	94
(Kühn, Doyle, et al. 2006)	2006	8	8	100
(Alonso-Frech et al. 2006)	2006	(28)	(28)	100
(Weinberger et al. 2006)	2006	14	14	100
(Ray et al. 2008)	2008	(13)	(11)	85
(Bronte-Stewart et al. 2009)	2009	(22)	(22)	100
(Kühn et al. 2009)	2009	30 (57)	(52)	89
(De Solages et al. 2010)	2010	(28)	(28)	100
(Eusebio et al. 2011)	2011	16 (28)	(25)	89

Table 1.2. Table summarising studies that have recorded from the STN with the proportion of patients or nuclei (in brackets) that have demonstrated beta peaks in the off state at rest. The mean proportion of patients/nuclei showing beta peaks are 94 %. The whole beta band is considered, except where otherwise indicated. A number of studies have also reported beta activity but not explicitly stated the number of peaks detected (Priori et al. 2002; Williams et al. 2002; Williams et al. 2005; Marsden et al. 2001; Devos et al. 2006;

Fogelson et al. 2006; Marceglia et al. 2006; Androulidakis et al. 2008). Reprinted with permission (Little & Brown 2012)

However, several studies have failed to show a correlation between the Unified Parkinson's Disease rating scale (UPDRS) motor score and beta activity at rest across patients, leading some to downplay its significance (Kühn, Kupsch, et al. 2006; Weinberger et al. 2006; Ray et al. 2008; Kühn et al. 2009). Additionally, a minority, of patients fail to show a substantial beta peak off medication (Table 1.2). A number of reasons have been proposed to explain these conflicting results. Some have argued that this may be due to a "stun effect" from localised oedema post operatively which causes a transient improvement in symptoms even without medication or the stimulator being initiated (Chen, Pogosyan, et al. 2006; Rosa et al. 2010). Alternative considerations include variability in electrode targeting between patients, the weaknesses of the UPDRS clinical scale and issues related to signal normalisation. Although there is still debate surrounding beta in PD, in particular its causal role, it appears clear that in the majority of patients beta is present at rest in the off state (mean 95%, see Table 1.2) and may therefore be useful as a feedback signal for DBS. Encouragingly, it has been shown that despite the enormous differential in magnitude between recorded beta and DBS stimulation voltage one can successfully monitor beta during DBS (Rossi et al. 2007; Eusebio et al. 2011).

Thus far, we have examined LFP signals at rest and their relationship to rigidity and bradykinesia. A useful feedback parameter however must also reliably indicate state information during more complex situations including voluntary and cued movements. Prior to and during movement, synchronised beta oscillatory activity is reduced and this has been shown at the single-unit, LFP and cortical levels (Amirnovin et al. 2004; Cassidy et al. 2002; Levy 2002; Alegre et al. 2003; Androulidakis et al. 2008). Cassidy et al found not only was there increased beta activity off medication in the GPi and STN and that these were reduced with levodopa, but that coupling through coherence was also reduced between

these two nuclei during action. They also found that in the on state, LFP activity was dominated at higher frequencies in the gamma range (70-85Hz) and this was augmented with movement, displaying a double dissociation between off and on drug states and changes with action in the beta vs. gamma band. Foffani et al have shown that not only does beta amplitude change during movement but the frequency of the prominent peaks also changes slightly in response to movement and dopamine therapy (Foffani et al. 2005). This suggests that amplitude modulation and frequency modulation might both be important for coding motor state.

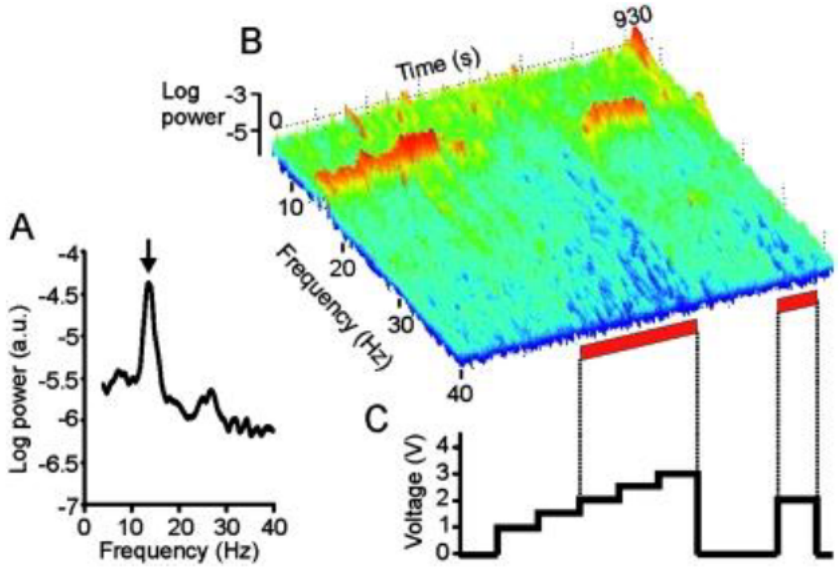

Figure 1.4. Effect of DBS of subthalamic nucleus on the LFP. (A) Power autospectrum of LFP recorded without stimulation. There is a large peak arrowed at 14 Hz. (B) Frequency–time log power spectrum of LFP. Power, as in (A), shown over the pass band of the amplifier (4–40 Hz). Red bars along the time axis denote periods of DBS at 2.0–3.0 V. Dyskinesias of the contralateral foot were noted at voltages of 2.0 V and above. Note suppression of spectral peak with stimulation ≥2.0 V, with evidence of a temporary increase in the power of the peak with stimulation at 1.5 V and a delayed return of the peak after stimulation at 3.0 V is terminated. (C) Timing and voltage of DBS. Adapted from Ref (Eusebio et al. 2011).

Physiological states other than movement also modulate LFP rhythms including beta. It has been shown for example that during slow wave sleep, beta activity is reduced whereas in rapid eye-movement sleep - beta is similar to, or possibly greater, than in the awake state (Urrestarazu et al. 2009). It has also

been found that motor control improves during sleep in those with PD (De Cock et al. 2007). Thus monitoring of beta might also signal non-REM sleep, affording the potential for DBS to be turned off, thereby saving on power consumption if implemented in a closed loop setup.

The changes in LFP signals prior, during and after movements and during sleep show the complex relationship between brain rhythms and physiological state in patients with PD. If beta in particular were to be used as a biomarker for feedback control, one concern given the pre-emptive suppression prior to movement would be that if stimulation were to be turned off at this critical period in response to beta reduction, then freezing of action or gait may be exacerbated. Consideration to the length of the beta averaging window may alleviate this problem.

Although beta appears to be a pathological signal in the PD off state with a relationship to bradykinesia-rigidity, other studies have suggested that this bradykinetic signal may be balanced by a prokinetic one, namely gamma (Brown et al. 2001), and that the relationship between the two is reciprocal (Fogelson, Pogosyan, et al. 2005). Gamma activity is related directly to movement and EEG studies have demonstrated that it is differentially involved in ballistic vs. negative movements (Alegre et al. 2003). Thus gamma and beta seem to have complimentary roles in motor coding both at the cortical and subcortical levels.

1.7.5 Tremor

As described previously it appears that tremor and bradykinesia-rigidity are subserved by different pathophysiological systems and therefore may require separate neurophysiological biomarkers to adequately capture them. At the cellular level Levy et al showed that in PD patients with tremor, there exists a subsection of neurons which discharge coherently with the limb tremor that are themselves characterised by both in and out of phase relationships to the tremor. In addition, they demonstrated

high frequency synchronization during tremor periods and suppression of synchronisation during voluntary movement (Levy et al. 2000; Levy 2002). Analysis at the level of the LFP has demonstrated increased signal at the tremor frequency and also double the tremor frequency (likely representing a harmonic) which was well localised within the STN and coherent with peripheral EMG (Reck et al. 2009). Investigation of activity at the cortex has also shown that this activity is coherent with the M1 motor area and extends out to a wider, diffuse network including other cortical areas, the cerebellum and diencephalon (Timmermann et al. 2003). Further work using non-linear techniques has revealed that the coupling in the theta band is bidirectional between the LFP and the peripheral tremor and there is significant delay (1-2 tremor cycles) for the brain to tremor driving signal (Tass et al. 2010; Wang et al. 2007). In addition to tremor frequency oscillations the beta band appears functionally related to tremor showing beta suppression prior to the onset of resting tremor (Wang et al. 2007). This effect which is opposite to the positive correlations already described between beta activity and bradykinesia-rigidity poses a problem for the use of beta as a biomarker in patients with PD, particularly those with tremor, and reinforces the need to individualise biomarkers according to clinical phenotype or to combine biomarkers. Overall, very little work has been done in terms of demonstrating a correlation between single unit or LFP activity and tremor severity over time.

1.7.6 Dystonia and Dyskinesias

Further aspects of Parkinsonism that may be reflected in the LFP are dystonia and dyskinesias. Alonso-Frech et al have investigated LFP signals whilst inducing dyskinesias in patients with PD through treatment with levodopa or Apomorphine (Alonso-Frech et al. 2006). They found that in patients who manifested dyskinesias there was a large increase in activity in the 4-10Hz band and when dyskinesias were present in just one limb, it was found that the 4-10Hz activity was present on the contralateral

side only, suggesting that it is specific to this clinical feature. On the other hand dystonia and dyskinesias have been inversely related to beta power levels (Silberstein, Oliviero, et al. 2005). This raises the possibility that the suppression of beta may favour the development of hyperkinesias, under some circumstances, and reinforces the view that closed loop control driven by a single biomarker such as LFP beta band power may be insufficiently nuanced to deal with all impairments. In addition, the relative merits of different basal ganglia targets for the sensing of biomarkers sensitive to dystonia and dyskinesia are unclear.

1.7.7 Gait and non-motor symptoms

The above characteristics refer to STN signals in relation to the classic triad of bradykinesia, rigidity and tremor. PD however extends to many other impairments including motor features like gait freezing, and non – motor symptoms such as depression, sleep disturbance, postural instability and autonomic dysfunction. Is it possible that specific biomarkers exist that may allow dynamic modulation of DBS specific to these impairments also? There has been little research as yet into specific physiological biomarkers of the non – motor symptoms; however progress is being made into a better understanding of the pathophysiology of gait with specific reference to a new subcortical target, namely the Pedunculopontine nucleus (PPN). Interestingly, this target is most effective when stimulated at low frequency and is found to have a specific therapeutic effect on gait and postural instability (Stefani et al. 2007). Both beta and alpha activity have been recorded in the PPN, and are at least partially dopamine dependent and coupled to cortical activity (Weinberger et al. 2008; Androulidakis, Mazzone, et al. 2008). Alpha power peaks correlated with gait speed and are shown to diminish at the point of gait freezing (Thevathasan et al. 2012). Additionally, there is now some early evidence of specific physiological markers of Parkinsonian neuropsychiatric sequelae. Subthalamic alpha activity

has been shown to differentially modulate in response to emotive stimuli and for these effects to correlate with depressive symptoms in PD (Huebl et al. 2011). Furthermore, impulse control disorders appear associated with an anatomically focal increase in theta-alpha activity (Rodriguez-Oroz et al. 2011). Therefore, it seems that some of the non – motor symptoms of PD may also have their own specific spectral characteristics that could potentially be captured in part with simple measures such as power spectral density.

1.7.8 Higher order spectral analyses

The above examples demonstrate that important and meaningful information regarding aspects of the concurrent pathological state can be derived from simple spectral analysis of the LFP signal. Activity has thus been divided in to individual frequency bands which have been related to different aspects of the disease / medication state through the use of correlations. However, this approach makes the assumption of a linear relationship between signal and clinical feature. Although some coding at the population level may occur in a linear manner this likely does not completely describe how the brain communicates and it is therefore possible that some valuable information regarding state is not being captured with these simple approaches (Friston 2000; Stam 2005). More sophisticated analyses have therefore been examined. The notion of "complexity" relates to dynamical systems theory and simply put, describes systems which are somewhere between simply predictable deterministic systems and those which show chaos. Complex systems appear to occur more readily in systems which are far from their natural equilibrium and can be recognised by characteristic features such as power law scaling (1/f), fractals and self-similarity (Bassett & Gazzaniga 2011). Quantitative measures of complexity have been developed and one such measure, Lempel-Ziv complexity, has been used to show that the complexity of the LFP in the beta frequency range negatively correlates with bradykinesia-rigidity at

rest, but not with tremor (Chen et al. 2010). As synchronised oscillatory activity increases, complexity falls, and the system becomes more deterministic and it is possible that complexity in the beta band directly relates to PD symptoms. Alternatively it may be that this complexity measure simply normalises the signal and thus avoids some of the experimental confounds highlighted above (e.g. stun effect and electrode targeting). Phase relationships between frequencies within the same signal may also be informative. Marceglia et al have shown using bispectral techniques that LFP signals become non-linearly correlated in the absence of dopamine and that this is particularly strong between low and high beta (Fig. 1.5)(Marceglia et al. 2006). The bispectrum relates to phase-phase interactions; however the introduction of the investigation of phase relationships raises other possibilities. Might phase-amplitude interactions between different frequencies also contain significant information? Indeed it has recently been shown that the degree of movement related modulation of high frequency oscillations by beta negatively correlates with bradykinesia/rigidity scores and that in the on medication state the high frequency oscillations are released from lower frequency coupling and demonstrated marked amplitude modulation related to movement (López-Azcárate et al. 2010). Phase-amplitude coupling has also been shown over the primary motor cortex and been found to be suppressed by subthalamic deep brain stimulation (de Hemptinne et al. 2013). Other work has examined the role of these high frequency oscillations themselves rather than their relationship to beta and has shown two distinct high frequency bands centred around 250Hz and 350Hz (Ozkurt et al. 2011). Moreover they found that the power ratio of these two bands correlated with UPDRS bradykinesia-rigidity at rest and that this was dopamine dependent and unrelated to beta. Non-linear analyses are potentially interesting but their correlation with motor impairment does not so far substantially differ from that seen with simple power measures and yet they come with a computational cost that may limit their application to clinical closed loop DBS in the near term. However, no study has so far directly contrasted correlations

between linear and non-linear measures and clinical impairment, nor determined whether those cases that contribute to correlations are the same for the two approaches. If not then the two approaches may prove complementary. Table 1.3 summarises the many studies that have related electrophysiological features to clinical state and highlights the relative lack of studies looking at correlations *within* subjects.

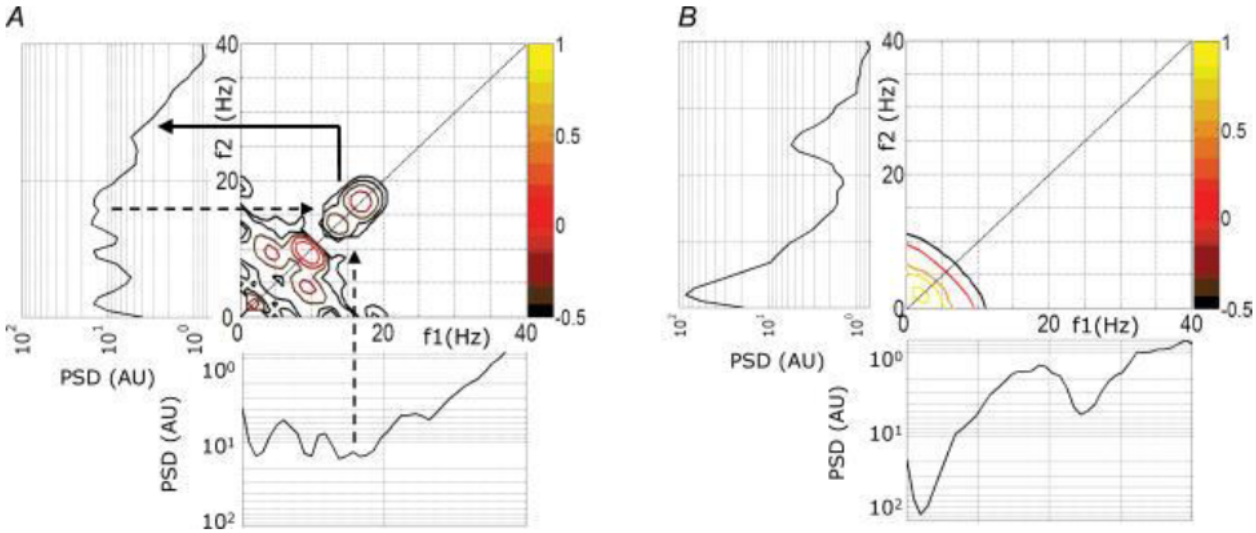

Figure 1.5. Bispectral analysis. Mean bispectrum from 13 subthalamic nuclei before (A) and after (B) levodopa administration. The central 2-D plot shows the mean bispectrum of the LFP signals as a function of frequencies f1 (x-axis, in Hz)and f2 (y-axis, in Hz).The level lines in the plot represent bispectrum values colour coded as indicated in the colour bar on the right (log transform of the average bispectrum, expressed in log arbitrary units, log AU). The mean power spectrum is also shown adjacent to each axis. The diagonal in the central plot defines the two regions of symmetry of the bispectrum. (A) Before levodopa administration, the arrows indicate the harmonic nonlinear correlation between the LFP rhythm in the low-beta range (13–20 Hz, dashed lines) and the LFP rhythm in the high-beta range (20–35 Hz, continuous line). This nonlinear correlation is evidenced by the bispectral peak (13–20 Hz, 13– 20 Hz). Note that this bispectral peak appears broad due to the frequency variability between nuclei. Bispectral peaks are also present in other regions; (2–7 Hz, 2–7 Hz), (8–12 Hz, 8–12 Hz), and (2–7 Hz, 8–12 Hz), suggesting the presence of nonlinear correlations between different LFP rhythms in the off Parkinsonian state. (B) After levodopa administration, bispectral peaks are suppressed. The mean spectral peak in the high-beta range is therefore now independent of activity at lower frequencies. Adapted from Ref (Marceglia et al. 2006).

TECHNIQUE / SITE	Correlation with treatment induced changes across subjects	Correlation with treatment induced changes	Correlation with absolute clinical state across subjects.	Correlation with absolute clinical state within

		within subjects		**subjects.**
CORTICAL				
EEG-EEG coherence (Silberstein, Oliviero, et al. 2005)	Reduction in EEG-EEG coherence (including beta) correlates with UPDRS improvement (levodopa & DBS). **No r values given**		Beta band EEG-EEG coherence correlates with UPDRS. **No r values given**	
MEG synchronisation likelihood (SL) (Stoffers et al. 2008)			Positive association with interhemispheric **(η^2=13.4%)** & intrahemispheric **(η^2=12.3%)** theta & interhemispheric beta **(η^2=9.2%)** SL measures.	
SINGLE/MULTI UNIT				
Single unit recordings (Weinberger et al. 2006)	Positive correlation between percentage of beta oscillatory cells with pre-op levodopa response **r^2=0.62**		Negative correlation between percentage of beta oscillatory cells with on drug motor UPDRS. **r^2=0.49**	
Spectral density estimation of raw multi-unit activity (Zaidel et al. 2010)			Spatial extent of STN beta oscillations positively correlates with improvement on DBS & levodopa **r^2 =0.45** Correlation between beta power off drugs with improvement in motor UPDRS with levodopa **r^2=0.2** or DBS **r^2 =0.3**	
LOCAL FIELD POTENTIALS				
LFP power spectral densities (Kühn, Kupsch, et al. 2006)	Reduction in beta with levodopa correlates with improvement in contralateral motor UPDRS Spearman's **rho=0.81**			
LFP power spectral	Reduction in beta levodopa correlates with			

densities (Ray et al. 2008)	improvement in contralateral bradykinesia/rigidity UPDRS **rho=0.7** Baseline beta power off medication correlates with improvements in motor symptoms **rho=0.68**			
LFP amplitude modulation by movement (cross correlation index). (Androulidakis, Brücke, et al. 2008)			Tapping performance vs. beta cross correlation index across patients (r^2=**0.15)**	Tapping performance vs. beta cross correlation index within patients r^2 **≤0.53**
LFP power spectral densities Asynchronous DBS/ LFP recording & Rotometer (Kühn et al. 2008)	Reduction in beta following DBS correlates with improvement in contralateral bradykinesia. r^2=**0.31**			
LFP power spectral densities (frequency aligned) (Kühn et al. 2009)	Reduction in beta with levodopa correlates with improvement in contralateral bradykinesia/rigidity UPDRS together R^2= **0.38,** rigidity alone R^2=**0.34** bradykinesia alone R^2=**0.17**			
LFP power spectra – high frequency oscillations (HFO) (López-Azcárate et al. 2010)			Movement-related modulation of the HFOs negatively correlates with rigidity/ bradykinesia scores R^2=**0.388 p=0.001**	
LFP Lempel-Ziv complexity (Chen et al. 2010)			Negative correlation in beta band with akinesia–rigidity **rho=–0.28**	

LFP power spectra – high frequency oscillations (HFO) (Ozkurt et al. 2011)			Power ratio of 250Hz & 350Hz HFOs correlates with UPDRS akinesia/rigidity **rho=0.36**	

Table 1.3. Table summarising studies that have investigated the relationship between LFP signals and clinical features. This demonstrates a clear relationship between LFP activity (particularly beta) and change in clinical features across subjects but highlights the very limited evidence for LFP signal correlations with clinical state within subjects. Within the beta band the sign of any correlation is always consistent with the fact that high levels of LFP activity are associated with a worse clinical state and bigger drops in LFP activity with treatment are associated with greater improvements in clinical state. Note that improvement is predominantly in bradykinesia-rigidity. Where possible, r^2, rho and η^2 values are given so as to show the proportion of the variance in clinical scores that can be predicted by the brain signals. Reprinted with permission (Little & Brown 2012).

1.7.9 Multiple sites

There is emerging evidence that signals at all levels including cortex, LFP and single units contain information that represents the clinical state and that excessively synchronised rhythmic activity appears to be related to Parkinsonism. As discussed above it is now becoming apparent that rhythms of different frequencies interact within the same signal. What of interactions between different signals at different sites; could these interactions be important in tracking clinical state in PD?

Phase coherence in the beta band across contact pairs within the same electrode separated by a few millimetres also correlates with bradykinesia-rigidity and this phase coherence has been found to account for up to 25% of motor variability (Pogosyan et al. 2010). What of locations that are much further apart? In addition to the evidence that local oscillations may signify something important about the Parkinsonian state, consensus is growing that oscillations may play a physiological role in the functional connectivity / binding of different spatially segregated neuronal populations across much greater distances (Fries 2005). Applying this to PD, we find that beta oscillations are coherent across bilateral STNs and cerebral cortices suggesting the existence of a bilateral network controlling beta (De

Solages et al. 2010; Silberstein, Pogosyan, et al. 2005). Moreover, the interactions between these spatially segregated rhythms (as measured through coherence) are dynamically modulated by movement and dopamine with phase lag and lead being frequency dependent (Litvak et al. 2011; Kühn et al. 2004; Williams et al. 2002). There is also evidence of complex non – linear interactions across sites with phase-amplitude coupling between the STN (phase) and cortex (amplitude) being excessive in PD (de Hemptinne et al. 2013). With one exception (cortico-cortico coupling) these measures of widely separated multisite interaction (coherence), although dopamine and movement responsive, have yet to be shown directly to be correlated with behavioural characteristics such as bradykinesia-rigidity (Silberstein, Pogosyan, et al. 2005). It remains to be established whether characterising interactions between widely distributed neuronal populations may give a more accurate representation of dynamic clinical phenotype particularly given the consideration that recording from more than one site raises practical implications such as increased risk of haemorrhage and infection.

1.7.10 Personal programming, dynamic optimisation and model based control

The aforementioned studies have been concerned with seeking reliable neurophysiological biomarkers that represent relevant clinical states and are consistent across time and across patients. This system of attempting to definitively identify well-defined signals can be contrasted with an alternative approach in which one uses learning algorithms to investigate LFP signal space in individual patients that then extract complex, non-linear multidimensional personalised signal characteristics from their LFP rather than using unitary biomarkers. Such approaches have been used elsewhere in brain computer interfacing (BCI) and software for this is now available through open source sites such as BCILAB (Delorme et al. 2011).

A learning paradigm of this sort requires a training period in which signals are correlated to clinical features and thus requires quantitative information on clinical features in a manner that is quick, continuous and reliable. Accelerometers can be used to give feedback information on limb tremor and joysticks or gyrosensors on bradykinesia (Deuschl et al. 2011; Allen et al. 2007; Kim et al. 2011). The real time continuous measurement of rigidity is more challenging and although quantification of rigidity has been achieved, these methods would need adaptation before implementation into a BCI (Prochazka et al. 1997; Endo et al. 2009). It would seem impractical to implant multiple bilateral devices to quantify motor impairment, but this approach could be realised by telemetrically downloading learnt algorithms after training periods in a clinical laboratory.

A further potential approach is to move away from static biomarkers for feedback control and to design computerised model-based control systems. These forms of systems are now ubiquitous outside of the health technology field (e.g. global positioning tracking and navigational systems, autopilot systems) but have yet to be fully implemented in medicine. The reason for the delay in uptake probably relates to previously insufficient computing power, inadequate neurophysiological models and the non-linearity in biological systems. All these obstacles are becoming surmountable and PD is theoretically well placed to benefit from this type of system given its ongoing dynamic nature. The field of model based control theory grew out of work by Kalman in the 1960s in which a maximum-likelihood filter was used to track a systems state and calculate changes that were needed to the system's control signals in order return it to a desired condition. With improvements in the implementation of these systems in non-linear environments with developments such as the unscented Kalman filter (UKF) they are now being implemented in realistic models of neuronal behaviour (e.g. Fitzhugh-Nagumo model). A substantial advantage of these systems is that they seek and utilise the best possible parameters for monitoring and control even if these do not represent a real bio-physical value but are merely

abstractions. In effect, the model (or control filter) is synchronised with the real system (basal ganglia) through continuous tracking and feedback. Additionally, the models allow one to monitor and record from just one site such as the STN and infer what the rest of the network is doing. Schiff has reviewed the history and development of model based control theory and discussed its application to PD and Feng et al have attempted to implement it in a model of PD to improve DBS stimulation through an evolutionary optimisation system for control of DBS stimulation parameters and separately through a non-linear feedback model (Schiff 2010; Feng, Greenwald, et al. 2007; Feng, Shea-Brown, et al. 2007). The elucidation of which is the best biomarker for closed loop DBS will take ongoing theoretical and empirical work and will look to balance strength of correlation to clinical state with simplicity and ease of computation.

1.8 Implementation of closed loop DBS in a model of Parkinson's disease

The validity of and technical feasibility of the biomarkers outlined above will likely only be clarified by further empirical study and by the attempt to utilise them within real, practical, closed loop systems firstly in non – human models. Rosin et al., have elegantly demonstrated effective closed loop stimulation in a non – human primate model of PD (Rosin et al. 2011). In this study they tested two monkeys rendered parkinsonian by the systemic application of the neurotoxin MPTP. The monkeys had surgical implantation of microelectrodes in the M1 area of the cortex and the globus GPi enabling recording from individual neurons at the two sites during stimulation of the GPi. The aim of their study was to assess whether delivering stimulation according to the pattern of firing of neurons (closed loop stimulation) was able to improve parkinsonism over and above that of normal, continuous (open-loop) high frequency stimulation. In addition they set out to determine if pattern triggered stimulation had dissociable effects on cortico-basal ganglia oscillations and neuronal firing discharge rates. A

number of different closed loop paradigms were examined with the most effective resulting from triggering from the firing of M1 neurons and stimulation in the GPi with short trains of seven pulses at 130Hz at a latency of 80ms. In the MPTP model the dominant circuit oscillation that results is 12.5 Hz and thus an 80 ms delay corresponds to stimulating at the start of the next oscillatory cycle (Fig 1.6).

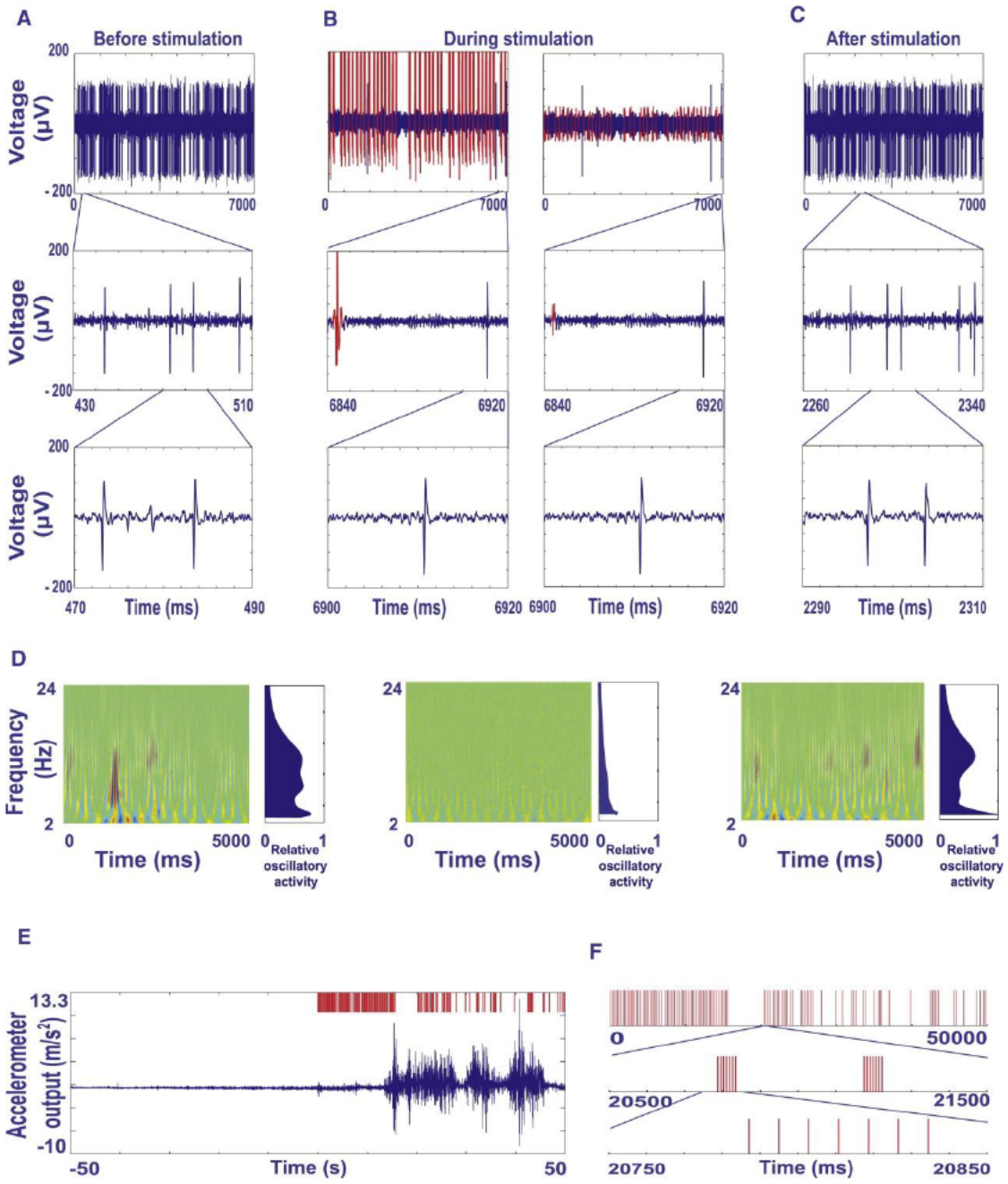

Figure 1.6. Closed-Loop GPtrain|M1 stimulation with 80 ms delay results in concurrent reduction of pallidal discharge rate, disruption of pallidal oscillatory activity, and alleviation of akinesia (A–C) An example of 7 s analogue traces of spiking activity of a GPi neuron before (A), during (B), and after (C) the application of the closed-loop GPtrain|M1 stimulus paradigm (train of seven stimuli delivered to the GPi triggered by M1 spikes, delay = 80 ms). Analogue data were filtered between 250 and 5000 Hz (Butterworth 4-pole software filter). The stimulus artefact is shown in red (B, left column), as is the residual artefact after artefact template removal (B, right column). Insets with higher temporal resolution (second and third rows) demonstrate stability of the single-spike waveform throughout the stimulation session and the adjacent spontaneous recordings. (D) Oscillatory activity depicted through wavelet spectrograms and displayed by frequency as a function of time, with blue to red colour indicating the intensity of activity. Spectrograms of activity before (left column), during (middle column), and after (right column) the application of the stimulus paradigm are shown. Power estimates averaged over time (to the right of each spectrogram) are relative to the maximal oscillatory power in the entire recording from this neuron. (E) Kinesis estimation: 100 s long trace of an analogue recording from an accelerometer fastened to the primate's limb contralateral to the stimulating electrodes, 50 s before the onset of stimulation and 50 s during stimulation. Stimulus raster is depicted in red in the upper trace. (F) Characteristics of the stimulus pattern: a highly irregular stimulus pattern and low stimulus rate (Rosin et al. 2011).

Neuronal activity was recorded in the GPi before, during and after stimulation. The clinical effect of stimulation was a marked reduction in akinesia as measured by accelerometry, which was most pronounced in the limb contralateral to the stimulation. Notably, akinesia improvement was substantially greater than that achieved with standard high frequency stimulation despite the significantly lower overall charge delivery. These compelling behavioural improvements were accompanied by a reduction in pallidal discharge rate and oscillatory activity which was more pronounced in the closed loop condition compared to the standard high frequency condition, despite the lower overall quantity of stimulation. Furthermore, they found that if the paradigm was changed so that sensing and stimulating both occurred in the GPi, akinesia was worsened. Importantly, this occurred in the context of firing rates that were still reduced but with increased oscillatory bursting. Indeed, the authors found no correlation between pallidal firing rate and oscillatory activity, suggesting independent mechanisms. As such, it appears that akinesia is related to oscillatory activity, not the firing rate, affording critical support for the concept that low frequency oscillations play a key patho-physiological role in PD. Additionally, it provides proof of concept that closed loop DBS can be

effective and most notably – can actually be more effective than conventional stimulation with less overall stimulation. The attempt to implement closed loop DBS in humans with PD is the subject of this current work.

1.9 Thesis objectives

This thesis aims to explore the rationale for and implementation of closed loop / adaptive (aDBS) in humans with Parkinson's disease. For this I shall aim to complete the following:

1. Review the current use of clinical DBS and the rationale for closed loop DBS in humans, including what is currently known about biomarkers of clinical state in PD (Chapter 1).
2. Investigate whether beta oscillations in PD are purely biomarkers or whether they play a role in the pathophysiology of the disease. We shall investigate what happens to clinical state when we augment beta with low frequency stimulation (Chapter 3).
3. Explore LFP biomarkers in PD and specifically to look for correlative evidence that beta oscillations correlate with clinical state across subjects (Chapter 4).
4. Investigate if the implementation of closed loop stimulation in humans is possible, efficacious and reduces electrical energy usage in a cohort of post-operative PD patients (Chapter 5).
5. Investigate whether the two bilateral basal ganglia systems function together or independently. This will inform on whether future aDBS systems use unilateral or bilateral triggering (Chapter 6).

Chapter 2 Materials & Methods

2.1 Patients

All subjects studied had advanced idiopathic PD diagnosed according to the Queen Square brain bank criteria (Lees et al. 2009)which was refractory to standard medical therapy. Indications for DBS included on / off motor fluctuations, dyskinesias, dystonias and medication resistant tremors (see individual chapters and subject descriptions). All subjects gave their informed written consent to take part in the studies, which were approved by the National Hospital for Neurology & Neurosurgery and Institute of Neurology Joint Research Ethics Committee, London UK, and the National Research Ethics Committee A, Oxford and the Ethics Committee of the Charité, University Medicine Berlin.

Experiments were carried out in the early post-operative period following electrode implantation and externalisation at the John Radcliffe hospital, University College Hospital (UCLH) and Kings College Hospital. Recordings were made between 3 – 7 days post-operatively on the morning following the overnight withdrawal of their parkinsonian medication to achieve a dopamine deficient and clinically OFF state (dopamine agonists have an extended half-life and therefore will not have been completely eliminated in all cases). We studied patients who had undergone implantation of the STN nucleus following the preferred practice of the neurosurgical teams with which we collaborated. GPi recordings were not made as the number of patients with GPi implantation was very low during the period of experimentation and as such we elected to exclude them in order to maintain a homogenous sample.

2.2 Surgical procedure

The electrode implanted was the Medtronic 3389 in all cases. These consist of 4 platinum-iridium cylindrical contacts measure 1.27 x 1.5 mm with a centre-to-centre separation of 2mm. Convention for electrode numbering holds that the lower most contact is labelled 0, increasing up to the uppermost contact, labelled 3. Placement in the STN aims for localisation of contact 0 below or in the lower border of the STN and the upper most contact (3) superior to, or at the upper most border of the STN. Electrode implantation and targeting is based on pre-operative imaging, which consists of stereotactic MRI in UCLH and combined stereotactic CT / MRI at the John Radcliffe hospital and at Kings College hospital. Targeting was calculated using navigation software with a double oblique course and entry point designed to avoid blood vessels, sulci, ventricles and caudate (Foltynie & Hariz 2010). Electrodes were connected to an external connection wire kit that could then be used to make recordings. Immediate post – operative imaging was performed to ensure that correct location of the electrode within the STN. At UCLH, this was performed using a fast spin-echo T2- weighted MRI with Leksell frame in situ (Foltynie & Hariz 2010). At the John Radcliffe hospital and at Kings College hospital post-operative CT scan was performed with frame in situ which was then fused with the pre-operative MRI (O'Gorman et al. 2009). Five to seven days later a second operation was performed in which the externalized extension wire was removed and the intracranial electrodes connected to a new sterile wire which was positioned subcutaneously towards the subclavicular area where it was connected to the pulse generator and battery pack. In addition to the anatomical targeting described, for choice of contacts we used contacts with the highest beta power as this has been shown to correlate well with the clinically efficacious contact as well as localisation within the dorsolateral STN (Pogosyan et al. 2010; Chen, Pogosyan, et al. 2006; Yoshida et al. 2010)

2.3 STN LFP recordings

With the externalised electrode wire, it is possible to connect the electrode to an amplifier in order to record the LFP. Both commercial and in house amplifier solutions have been used here. Passive LFP recordings, without stimulation (Chapter 6), were made on a commercial device – (Porti Amplifier, TMS international, Netherlands). This has the facility to record in a monopolar mode (common average rejection) in addition to having additional x4 DC inputs for sensors such as accelerometers, goniometers and strain gauges etc. This amplifier was also used, without LFP recordings, for measurement of force and angle in the assessment of rigidity in chapter 4. The Porti includes TMSi's proprietary "True Active Signal Shielding" technology, which results in a clean signal with low mains (50 Hz) interference. In order to remove mains artefacts, it employs common mode rejection whereby signal common to all electrodes is assumed to be artifactual and removed. This must be born in mind if there is a strong diffuse physiological signal being measured with a small number of electrodes, in which case the physiological signal might be "rejected". This can be avoided by adding extra electrodes, distant to the measured signal. This data were sampled at 2048 Hz and acquired using in house software. The data was high pass (> 1 Hz), notch (50 Hz) and low pass (anti – aliasing filter at 1000Hz) filtered to derive a clean signal. It was then saved and exported to Spike2 (Cambridge Electronic Design, UK) for further visualisation and analysis. The archival data studied in chapter 3 were sampled at 184 Hz and band pass filtered between 1 and 80 Hz (Biopotential Analyser Diana, St Petersburg, Russia).

All data were reviewed for electrical & movement artefacts which were subsequently removed prior to analysis. In the cases where monopolar recordings were made, these were converted to bipolar

montages by subtraction of recordings from adjacent contacts. Therefore 3 bipolar montages were derived for each 4-contact electrode 0-1, 1-2, 2-3.

Combined stimulation and recording was required for testing of closed loop stimulation and this required the use of an in house solution for both the amplifier and the stimulator. The amplifier has been extensively tested and reported upon previously (Eusebio et al. 2011). The amplifier routes monopolar stimulation (against shoulder pad reference) between the two recording contacts and performs common mode rejection across this recording pair in addition to steep low pass filtering in order to remove stimulation artefact. Therefore, despite stimulation voltages being around 1 million times greater than the underlying physiological signal, this artefact can be removed. Subsequently, there is a 5 stage differential amplifier with variable gain of 10,000 or 100,000 plus an analogue notch filter at 50 Hz. It is optically isolated from the output BNC which takes the signal to an analogue to digital (A/D) data acquisition unit (1401 Cambridge Electronic Design, UK) which saves the file and also allows simple visually guided data analysis.

2.4 Stimulator construction and safety

Medtronic provide an external stimulator which is for use in externalised patients in the immediate post-operative period. It allows the clinical evaluation of lead placement prior to placement of the pulse generator and battery pack. Using this device, it is possible to manually titrate up the voltage against side effects and clinical efficacy. However, with regards to using such a device for closed loop stimulation there are a number of problems. Firstly the speed at which this can be manually titrated is slow. If, in order to improve temporal resolution the stimulator is connected and disconnected very rapidly – patients experience unpleasant side effects related to this rapid shift in voltage. The ideal

device therefore, would be one in which it were possible to trigger rapidly, i.e. had good temporal resolution but additionally had the ability to ramp stimulation up and down gradually in order to avoid side effects such as paraesthesias. In the absence of such a commercial device, we designed and built a stimulator that matched these specifications in addition to being in accordance with current safety guidelines for medical devices. This stimulator was therefore constructed in order to reduce side effects to patients from rapid on / off switching and improve tolerability of closed loop DBS. In addition, the commercial external Medtronic stimulator allows for very high stimulation in a range that has been shown to cause neuronal damage. The new stimulator was constructed to be limited by design within stringent safety restrictions to prevent potential damage.

2.4.1 Regulatory framework

This was an in-house manufactured device to be used only for Professor Brown's research group, so in this case no CE marking or MHRA assessment was required as it was not designed to be sold or be used by other groups. Despite this, it was designed and built to comply with all safety guidelines to ensure the patients safety according to the following: Report 90 BS EN60601-1 *safe design, construction of medical equipment.*

2.4.2 Power and waveform specifications of stimulator

1. 2x9V batteries for power.
2. Current limited to ± 15 mA.
3. Output - 4 pin binder type connector for connection to DBS StimRecord amplifier.
4. DBS Wave 0- 5V, 100 μs, 130 Hz fixed with 250 ms ramping.
5. Symmetrically biphasic waveform shape.
6. Pulse and ramp modes

The stimulator has two modes. Pulse mode delivers a pulse for each individual input trigger and can be used for controlling each pulse independently at the required frequency / pattern. The second mode is ramp mode in which detection of a rise in the input trigger results in stimulation at 130 Hz for the duration that the input trigger stays high. In addition, this mode gradually increases the output voltage up to the set voltage over a variable ramping period. We found that a ramping period of 250 ms was optimal to minimise onset / offset paraesthesias whilst retaining good temporal resolution and this was therefore used heuristically for the duration of our experiments.

2.4.3 Electronic circuit design

See Fig 2.1 for circuit diagram in concert with functional description (Note, individual component labels from the circuit diagram are written in italics in brackets in the following description):

- A Peripheral Interface Controller (PIC) microprocessor unit *(U1)* generates 2 timing pulses at 100 μs with a 20 μs gap in between, and controls the pulse amplitude via the digital to analogue (D/A) converter (*SPI_DA)*.
- The output from the D/A is buffered and inverted by a duel op-amp (*U_AMP)*, the outputs from which go to the 2 channels of the metal–oxide–semiconductor field-effect transistor (*MOSFET)* switch.
- Optical isolation (*OP1)* from the PC to the PIC micro input (*RB0)* ensures patient isolation from any potential high voltage currents.
- When the input (*RBO)* is low the microprocessor produces 2 pulses of 100 μs every 7.5ms (133 Hz).

  The first pulse turns on the *MOSFET* switch to the -ve supply via a low pass

Filter (*R3-CF1)*. After a 20 μs delay the next pulse turns the other *MOSFET* switch to the +ve supply

via a secondlow pass filter (*R4-CF2)*. This results in a -ve output for 100 μs followed by gap of 20 μs and then a +ve output for 100 μs.

- While the microprocessor input *(RBO)* is low, the pulses will be repeated every 7.5 ms – this is the ramp mode. The maximum trigger rate is thus set to 133 Hz. When the circuit is in pulse mode – it will respond to input triggers at whatever pattern / frequency is passed into the input.
- In order to minimise unpleasant side effects for patients, in the ramp mode the voltage is ramped up from from 0 V to the set voltage over 250 ms and ramped down over 250 ms to zero volts on discontinuation. This is controlled through the *PIC* internal software. There is no ramping in the pulse mode.
- DC blocking capactors *(CPRO 1-4)* protect the patient in case of a fault inside the case that could lead to a direct DC current output (e.g. the timer becoming fixed at a high setting).
- A further filter (*R3,CF1)* is implented in order to protect the patient in the fault condition of timer malfunction resulting in potentially dangerously longer stimulation pulses.

(*With thanks to Spencer Neal for design and construction of the stimulator and assistance with description of circuit functioning.).*

A

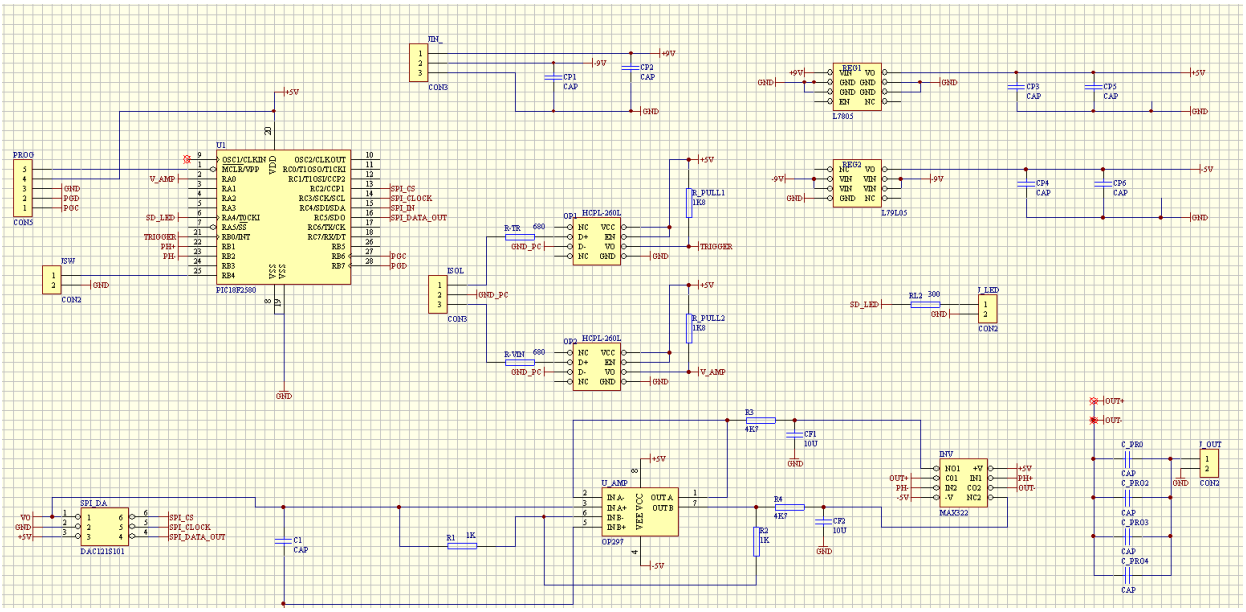

B

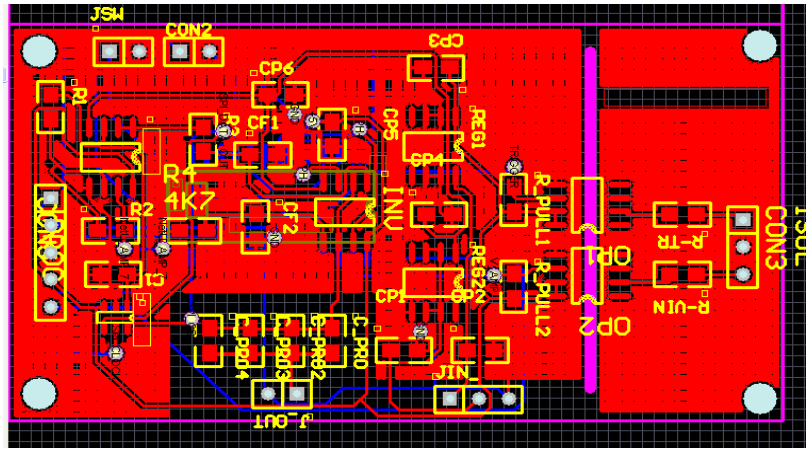
JSW
CON2
CP3
CP6
R2
CF1
CP5
REG1
CP4
R4
4K7
JINV
R_PULL1
OP1
R_TR
CON3
C1
CP2
R_PULL2
OP2
R_VIN
CP1
REG2
JIN
C_PRO
J_OUT

Figure 2.1. Circuit diagram (A) of stimulator and printed circuit board (B). Note physical optical isolation on circuit board for patient protection (purple vertical line).

2.4.4 Stimulator safety features

1. Type CF device built to the EN 60601-1 safety standard for human research.
2. Optical isolation of up to 1000 V from stimulator to outside components.
3. The stimulator is battery powered (+-9V) battery thereby limiting the maximum possible voltage exposure to within safe range.
4. DC blocking capacitors prevent and potential DC current between the stimulator and patient.
5. A current limit filter is in place in case of any potential timer faults to limit potential current exposure to the patient.
6. A watchdog timer is present within microprocessor so that should any software fault occur the microprocessor would automatically restart.
7. The maximum frequency stimulation rate is set and fixed to 133 Hz in ramp mode (when frequency is controlled internally by the PIC). This is triggered via the external trigger pulse and if the input frequency is higher than 133 Hz – it results in the output being disabled.
8. A fixed pulse width & frequency limits potential charge density < 30uQ/cm2 (see below).

The following diagram demonstrates the recommended stimulation parameters as defined by Medtronic following preclinical testing. Our in house stimulator is charge limited (unlike the commercial stimulator supplied by Medtronic) to be within the safe range only.

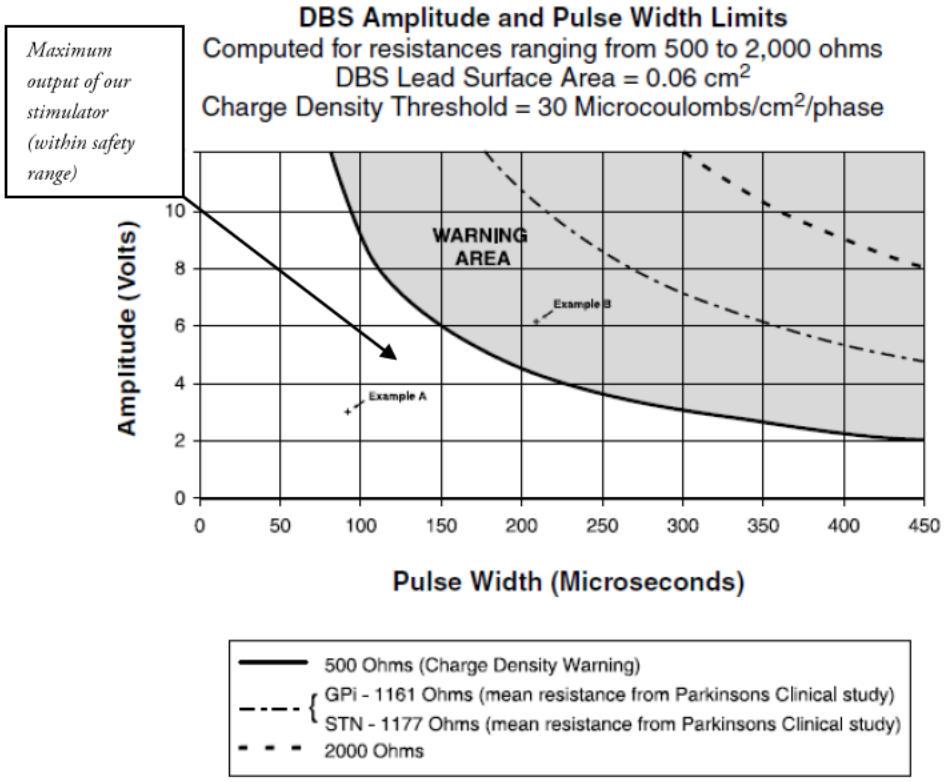

Figure 2.2 Charge density safety diagram with variable DBS parameters. The diagram shows the range of safe amplitude and pulse width in terms of charge density assuming a rate of 133 Hz and an impedance of 500 Ohms and safe cut off of 30 microcoulombs/cm^2/phase. Unsafe area shown in grey. Maximum values capable with our stimulator shown to be within the safe area even with most conservative impedance estimate of 500 Ohms. Example A and example B provided by Medtronic of safe and unsafe parameter setting respectively (Diagram produced by Medtronic and released as part of external stimulator documentation).

The absolute maximum charge density achievable with our stimulator can also be calculated numerically and also be shown to be well below the maximum of the 30 microcoulombs/cm2/phase:

- *Charge = 5V/500*100 s=* ***1000nQ per phase.***
- *Charge density=700nQ/0.06cm2=****16.6 µQ/cm2*** *(maximum is 30 µC/cm2)*

2.4.5 Pulse waveforms

Commercial DBS systems employ a biphasic charge balanced pulse design with cathodal pulse first. Studies have demonstrated however that the actual and idealised waveforms can vary substantially according to stimulator model (both across models and internal versus external stimulators), set parameters (V, frequency and pulse width) and across patients according to impedance. Our in vitro studies confirmed this heterogeneity using a Medtronic external stimulator (Butson & McIntyre 2007). We found that there was non – linearity between the set input voltage and the actual delivered voltage and that this was impedance dependent. We also found a tailing off of voltage during each individual pulse at higher voltage as well as moderate pulse shape distortion at high impedance.

Our stimulator also employed a biphasic charge balanced pulse (cathodal first) but was designed to avoid the features highlighted above in order to improve across subject comparisons and as such approximated an idealised biphasic waveform. This was tested in vitro under 500Ohms impedance and was found to have an excellent linear input output function in addition to minimal tailing off or pulse shape distortion at any voltage. Clinically, its effects were comparable to a Medtronic external stimulator.

2.5 Recording artefacts

There were a number of electrical artefacts which interfered with both passive recording and closed loop stimulation testing. The first of these related to mains interference at 50Hz. This was ameliorated by using common mode rejection on recording amplifiers, limiting mains powered devices in the vicinity, limiting wire length, and using bipolar montages plus large area reference pads. In addition, they were greatly attenuated by a narrow band notch filtered centred around 50 Hz. Artefacts due to

movement of wires were also minimised by asking patients to remain still during experimentation and by excluding from analysis low frequency components of the LFP which tend to be contaminated by movement (< 4 Hz). In addition, spike artefacts were visually removed in Spike2 (Cambridge Electronic design, UK). This resulted in clean data being available for further analysis, in the absence of stimulation.

The attempt to implement closed loop DBS introduced further difficulties with artefacts which were complicated by the need to sense from the signal in real time. Artefacts have the potential to inappropriately trigger stimulation when not indicated by the biomarker being followed, thereby reducing the sensitivity of the system to genuine fluctuations occurring within the basal ganglia network. There were three types of stimulation induced artefacts that were seen with our system. Firstly, in some patients there were increases in spike artefacts during stimulation which, in the spectrogram, could be seen to contain a broad frequency content (Fig 2.3). These were inconsistent, were not seen in all subjects and could be partially ameliorated by adjustment of cables and the reference pad. It was felt that these likely represented some breakthrough of the stimulation signal into the filtered LFP and resultant saturation of the amplifiers.

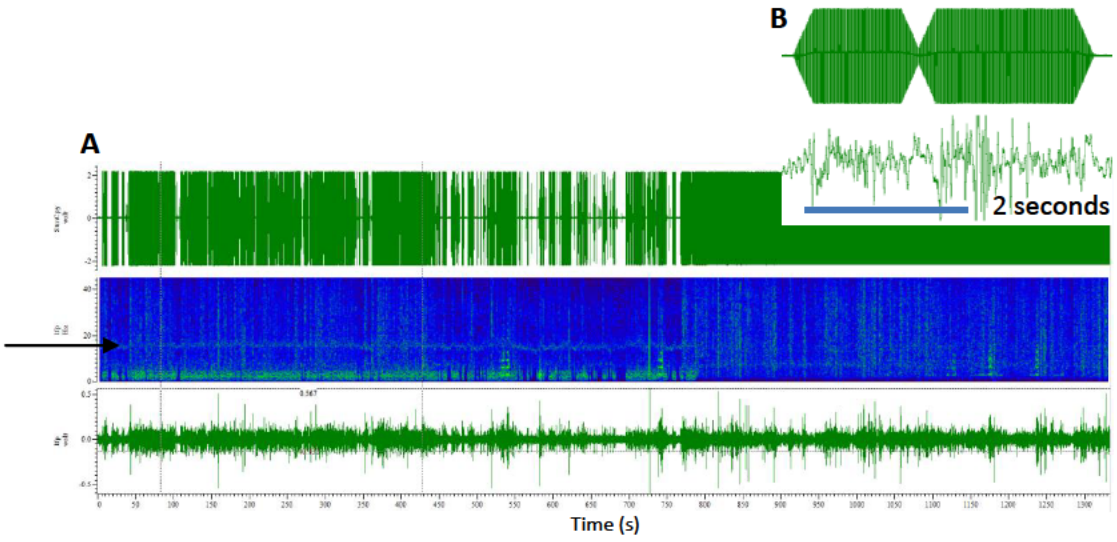

Figure 2.3. Diagram of electrical artefacts during DBS. (A) Compressed output (1300 s) of simultaneous stimulation and LFP recording in a subject from the closed loop DBS study (chapter 5). The bottom trace denotes the LFP, filtered between 3 – 37 Hz with spike artefacts visible. The middle channel consists of a spectrogram of the LFP demonstrating that these spikes have broad frequency components that includes the frequency of interest (beta oscillations seen as horizontal green line at 18 Hz, indicated by black arrow). The top trace is a copy of the stimulator output demonstrating that these spike artefacts can occur during intermittent stimulation (first half of trace) and during continuous stimulation (second half of trace). Figure B demonstrates a period of intense spikey artefacts close up during stimulation (bottom trace) with ramped stimulation seen above.

More concerning for potential closed loop DBS was the appearance of a consistent artefact in the bipolar recordings at both the onset and offset of stimulation. These were reproducible in a saline water bowl model when they were found to be affected by salt concentrations and duration of stimulation (Fig 2.4). Onset (first artefact) and offset (last artefact) are symmetrically inverted in the time series and when deconstructed using a spectrogram show a broad frequency makeup with decreasing amplitude as frequency increases. They were present with single pulses of stimulation, trains of stimulation and ramped stimulation but not during sustained bursts of continuous stimulation. Thus it appears that they are related to rapid change in stimulation state and have been reported previously by other groups (Fig 2.4) (Afshar et al. 2012). The consistency of these artefacts, inverted shape at onset and offset, reproducibility in a saline water bowl and dependence on electrolyte strength all point towards a

genuine effect at the tissue electrode interface, rather than an electrical artefact. As such it seems likely that they represent capacitance effects at the tissue-electrode interface, with charging and discharging of the capacitor at onset and offset respectively. These were found in all patients with differing magnitudes and could cause self-triggering by contaminating and increasing the beta signal being used to control the stimulation. The onset artefact was found to be less problematic as it was short lasting and the stimulator was switched on at this point in any case. The offset artefact did cause significant problems as it was at a time that stimulation was switch off and physiological beta amplitude was low. This had the effect of triggering stimulation and therefore in certain situations, stimulation became disconnected from physiological beta and was being triggered only by artefacts. This was not unsafe as continuous self-triggering simply results in standard continuous stimulation that is normally delivered clinically. It did mean however, that one was not able to test the efficacy of beta triggered stimulation as per the experimental design. A number of alterations were able to prevent self-triggering. Lowering the voltage of stimulation or increasing the threshold for triggering were both effective but limited the maximum voltage and time of stimulation that could be delivered. Changing the contacts of stimulation could also be effective in some cases, although this too could move the point of stimulation away from the optimal contact, decreasing the efficacy of the closed loop stimulation. Introducing a refractory period following stimulation allowed us to maintain high stimulation voltages and sensitive thresholds but at a cost of the temporal resolution of the system. The theoretical optimisation of these various parameters against each will need to be part of further studies.

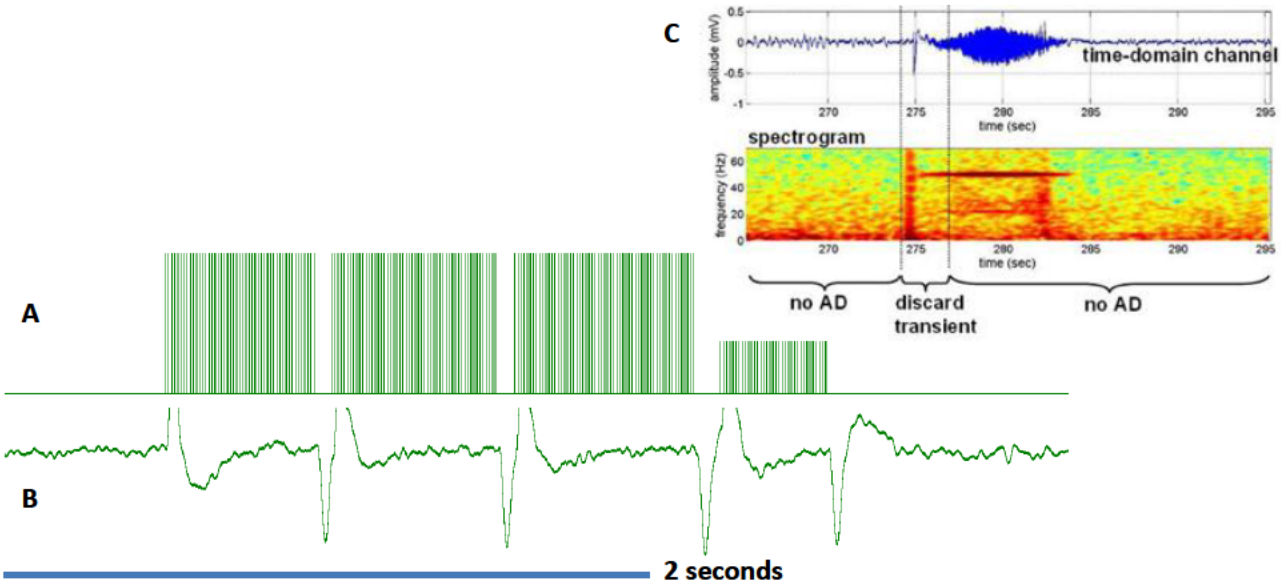

Figure 2.4 Figure demonstrating symmetrical inverted on / off burst artefacts in a water bowl during short bursts of stimulation. (A) shows the trigger channel with each vertical line corresponding to an individual pulse (note artefacts are present in the absence of ramping). (B) LFP channel recorded through the StimRecord device. Note – significant artefacts are present at the beginning and end of each burst of pulses but are absent during stimulation. (C) This figure shows a marked cross – frequency artefact at the onset of stimulation (275 s) in a sheep model of DBS in pre-clinical studies at Medtronic (Afshar et al. 2012).

2.6 Spectral analysis

LFP data is recorded as fluctuations in voltage over time. It is possible in some cases to see periodic patterns in raw data, however to extract more subtle regularities and to be able to quantify them, it is necessary to transform the raw time series into a new representation containing its constituent frequency components. A number of techniques have been used throughout the following chapters, the theory and application of which will be reviewed here.

The first technique to be discovered for decomposing continuous time series into frequency components was the Fourier transform. This comes from a theory developed by Joseph Fourier that states that it is possible to form any function f(x) as a summation of a series of sine and cosine terms of

increasing frequency. Euler's formula relates trigonometric functions, sin and cos, to the circular complex exponential function which is also convenient for times series analysis:

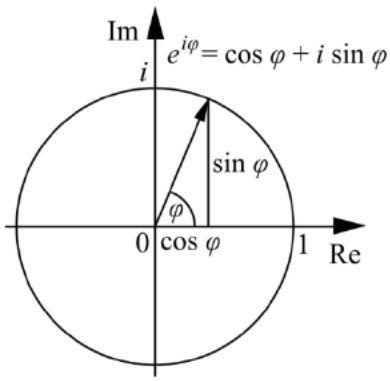

Figure 2.5 Schematic of Euler's theorem. Note the magnitude of the vector denotes the amplitude of the signal at any given moment and ϕ angle, the phase. Im = imaginary. Re = real.

The continuous Fourier transform assumes an infinite signal length that is then transformed to its constituent frequency components:

$$S(f) = \int_{-\infty}^{\infty} s(t).\, e^{-i2\pi ft} dt$$

Equation 2.1 The continuous Fourier transform.

The signal function s(t) at time is transformed to a complex representation S(f) which contains a real and imaginary component for each frequency (f). From the complex result one can derive the amplitude and phase at any given frequency. Normally only the amplitude value is used in Fourier analysis which is converted to power by squaring, which when performed at all frequencies, derives the power spectrum. The continuous Fourier transform assumes an infinite periodic signal but a special case can be derived for situations in which this does not hold – the discrete Fourier transform. This can

be used on sections of data and is implemented in a computationally efficient form as the fast Fourier transform algorithm.

A major assumption of the Fourier transform is that the signal is stationary within the period of analysis and as such it derives a single value for the amplitude and phase (at the start of the series) of the signal at each frequency. However, this is rarely true of physiological signals and indeed, much of the valuable information is hidden within the fluctuations in phase and amplitude over time. One solution is to use a short windowed version of the Fourier transform and repeat this after moving the window forward in a step – wise manner (Le Van Quyen & Bragin 2007). This takes advantage of local stationarity at short time windows, which has been shown to hold for EEGs but is as yet unproven for LFPs. This can be contrasted with a different method whereby a complex discrete periodic function is convolved against the time series to extract phase and amplitude information at all points in time. Such functions are called wavelets and a commonly used function in current neuroscience research is the Morlet wavelet which combines a sinusoid, windowed by a Gaussian kernel (Fig 2.6). When a family of wavelets with different fundamental frequencies are used, it is possible to extract amplitude and phase information at all points in time by taking the modulus of the analytic vector or the angle of the vector at time t. A third method which is similar, involves band pass filtering the original time series at each frequency of interest to derive a family of filtered time series. This is then convolved with the following function to derive the complex (analytic) series and this is known as the Hilbert transform:

$$h(t) = 1 / (\pi t)$$

Equation 2.2 The Hilbert transform can formally be realised as a convolution with the function shown.

The amplitude and phase can easily be extracted in the same manner as for Morlet wavelets. Although methodologically diverse, there is now theoretical work that implies that given certain conditions, these three different methods are formally equivalent (Bruns 2004). This similarity of methods is dependent on the matching of parameters across techniques which can be complex. As such, in general practical use, the different methods emphasise different components and have their own characteristics. Specifically Fourier based methods have a tendency to overfit data and are susceptible to noise, whereas wavelet based methods can have low frequency resolution over parts of the spectrum. The decision to use a particular method is often therefore influenced by user familiarity and the requirements of the analysis at hand. Using any of these three methods it is possible to extract the amplitude, and therefore power, in addition to the phase at all points in time. These can then be compared with clinical assessments and analysed by statistical techniques to derive correlations and test hypotheses.

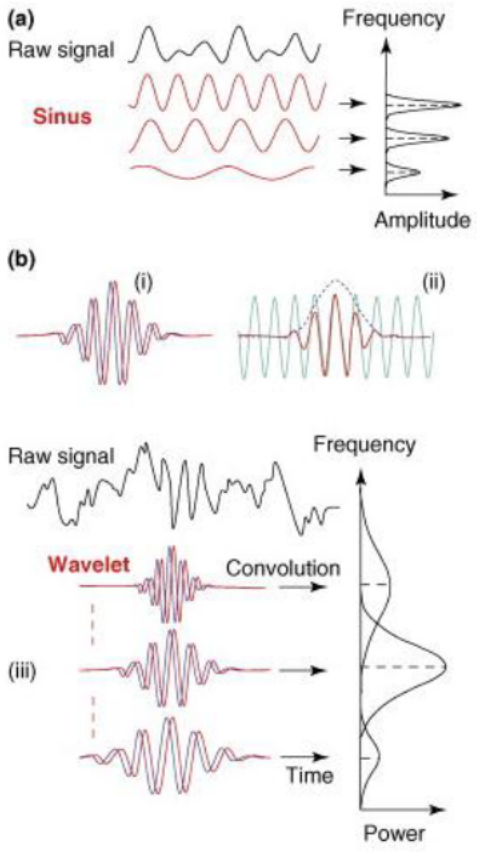

Figure 2.6 Schematic of Fourier versus wavelet analysis of time series. (a) The Fourier transform decomposes a signal into sinusoids of different frequencies, which sum to the original waveform. The spectral power (right) identifies their respective amplitudes. (b) In contrast to the classic Fourier transform, wavelets are a locally periodic wavetrain. For example, the wavelet shown in (i) is called the Morlet wavelet (the real component is shown in red and the imaginary component is shown in blue) and is a complex sine wave multiplied by a Gaussian (bell-shaped) envelope (ii). A family of wavelets is obtained by shifting and scaling a prototype wavelet, such that this set of functions adequately sample all the frequencies present in the signal. All wavelets of this family have, therefore, the same number of cycles for different frequency bands, resulting in different wavelet durations. A convolution, expressing the amount of overlap between the signal and this family of functions, gives time-varying amplitudes of the signal in frequency and time (iii). Adapted from Ref. (Le Van Quyen & Bragin 2007).

2.7 Clinical assessments

One of the aims of the present research was to explore neurophysiological biomarkers of PD. In order to do this, one must make recordings of neurophysiological signals and then compare them to clinical state. A key issue for successful identification of biomarkers therefore relates to the methods for quantification of clinical state. The most commonly used scale for the clinical evaluation of PD is the Unified Parkinson's Disease Rating Scale (UPDRS) with part III used explicitly for motor evaluation (Fahn & Elton 1987). Of the many scales available, the UPDRS has been found to have a relatively high internal consistency and inter–rater reliability (Ramaker et al. 2002). However, it has also been found to have significant redundancy and very strong emphasis on bradykinesia which makes up 40% of the total score of the UPDRS motor examination. In its original formulation, it is a qualitative scale with subjective rating between 0 and 4 indicating absent, slight, moderate, marked, severe presence of a range of symptoms. It is useful for chronicling disease progression and for quantifying changes in symptoms across a range of symptoms as used in chapter 3 & 5. In some studies, half points were used to improve sensitivity (Chen et al. 2010; Kühn, Kupsch, et al. 2006). In 2007, a study group for the movement disorders society modified the UDPRS in order to give more formal descriptions to the previous subjective grading system (Goetz et al. 2008).

Baseline UPDRS scores that are used in the correlation with beta variability (chapter 3) and stated as part of the clinical description of subjects in all other experiments were taken pre-operatively from the UPDRS part III scoring system following 12 hours of complete dopamine withdrawal and then repeated following administration of 200mg of levodopa (Fahn and Elton 1987).

Given that it is a subjective, bounded ordinal scale, it is not perfectly suited for the precise quantification of changes in specific motor subscores. In order to quantify objectively an individual feature of PD, it is necessary to employ a kinematic device which can directly measure the attribute of interest. This is relatively straightforward for the case of tremor, which can be simply and easily captured using an electronic tri-axial accelerometer (Weinberger, W D Hutchison, et al. 2009). The quantification of bradykinesia and rigidity is more complex. Bradykinesia is defined clinically as slowness of movement with progressive decrement of speed and amplitude and therefore contains multi-faceted aspects, which could all be assessed independently by quantitative metrics. A number of simple metrics have been developed including tapping time and rapid alternating movements although the correlation with clinical scores is somewhat poor (Kim et al. 2011; Jobbágy et al. 2005). The assessment of rigidity is more complex, necessitating the concurrent measurement of force and angle during passive limb displacement (Park et al. 2011; Endo et al. 2009). For our assessment of limb rigidity in chapter 4 during low frequency stimulation of the STN we used a rigidity assessment device that we designed and built for the purpose (see chapter 4). These metrics of clinical state were then taken forward for statistical analysis.

2.8 Statistical testing of hypotheses

Statistical testing was performed in SPSS v. 10 (SPSS INC., Chicaco, IL, USA) and Matlab (R2010b, The MathWorks, Natick, MA, USA) using the statistics toolbox. A variety of test modalities were used during the experimentation including Student t tests, multiple regression, ANOVA and correlation analysis. Both parametric and non – parametric testing were performed depending on the structure of the underlying data. Parametric testing has more statistical power but is more restrictive in its assumptions. The first assumption relates to the normality of data. Data is denoted as "normal" if it is symmetrically distributed around the mean with a variance structure defined by:

$$\mathrm{P}(x) = \frac{1}{\sqrt{2\pi}} e^{-\frac{1}{2}x^2}$$

Equation 2.3 Standard normal distribution. Simplest case of the normal probability distribution (P) of x in which the mean is equal to zero and the unit variance equal to 1.

2.8.1 Parametric testing and normality

Normal distributions are found to have approximately 2/3rd of samples (0.68) within 1 standard deviation and 95% of samples (0.954) within two standard deviations the mean. Assessment of normality can be made visually by looking at the shape of the distribution histogram or probability – probability curve. Alternatively, a more formal and quantitative measure is to test the structure of the sampling distribution with Kolmogorov – Smirnov testing. This method was used in our experiments due to its objective nature. A p value < 0.05 was used to reject the null hypothesis that the data were normally distributed. In cases of non – normality the data was transformed using power transforms or non-parametric testing performed.

The central limit theorem states that the means of samples taken from an underlying distribution will itself be normal if a sufficient number of samples are taken. This powerful concept allows one to use parametric testing on sampling distributions irrespective of the underlying (unknown) population distributions. Other assumptions of parametric testing include homogeneity of data which states that the variance must remain constant within the sample and independence of samples.

2.8.2 Student t tests

The student t test allows for the comparison of the means between two sets of samples and was used in Chapters 4,5 & 6. A p value of 0.05 was used as a cut off for rejection of the null hypothesis. One and two tail t tests were used according to the hypothesis being tested.

2.8.3 Analysis of variance (ANOVA)

Analysis of variance is valuable when a test is required to assess a group of means aginast each other. It operates by dividing up the variance for the whole population and then partitioning off the variance according to the different groups and comparing this partitioned variance to the group variance by means of a ratio – the F statistic. The statistical significance of the F value is dependent on the degrees of freedom for the sample. The validly of ANOVA testing is also dependent on a number of assumptions including normality and sphericity which equates to homogeneity of variance and can be tested with Mauchly's test. Our data did not violate sphericity and as such there was no need to adjust our degrees of freedom in assessing the significance of the F statistic. ANOVA was used in chapters 3, 5 & 6 and specifically, repeated measures ANOVA was used due to the use of multiple interventions on the same subjects.

2.8.4 Correlation & regression

Correlation coefficients measure the association between two variables and can take parametric or non-parametric forms. Pearson's product moment correlation coefficient measures the linear correlation between two parametric variables and is used in chapters 5 & 6. Spearman rank correlation coefficient is non-parametric and functions by comparing the ranking between two variables. It is utilised in chapters 3 & 4. In the case where there are multiple variables, it is possible to derive the independent effect of each variable by combining them in a multiple regression model that fits a linear equation to the observed data as in chapter 4.

2.8.5 Multiple comparisons correction

The foundation of scientific enquiry revolves around the falsification of hypotheses. Hypotheses are tested statistically following the empirical collection of data. If many hypotheses are tested, then the possibility of rejecting a null hypothesis by chance (Type 1 error) increases and the validity of our conclusions are significantly weakened. A structured, prospective approach to statistical analysis and the minimisation of the risk of Type 1 errors therefore significantly strengthens any analysis. As such, in these experiments, group level analyses by ANOVA were initially performed to establish a difference in means at the group level prior to secondary analysis of difference of means between subgroups. Secondly, if multiple tests were carried out, then the risk of type 1 error was controlled through use of multiple comparison adjustments. There are a number of ways of controlling the overall rate of type 1 errors when multiple tests are employed. This becomes particularly important when large datasets are used and very large numbers of tests are performed. The challenge for multiple comparison's procedures is to limit the chance of erroneously rejecting a null hypothesis (Type 1 error) whilst at the same time, minimising the likelihood of failing to detect a true difference (Type 2 error). The best

known procedure is the Bonferroni correction in which the p value, usually taken initially as 0.05, is reduced according to the number of tests performed. This does effectively limit the family wise type 1 error rate but at the cost of a high type 2 error rate. A more balanced approach has been developed relatively recently which controls f, the false discovery rate (FDR):

$$f = \frac{number\ of\ mistaken\ H_0\ rejections}{total\ number\ of\ H_0\ rejections}$$

By controlling the false discovery rate rather than the family wise error rate we still set an upper bound on false discovery but gain statistical power, the ability to detect an experimental effect if it does exit (Curran-Everett 2000). The FDR procedure controls the risk of erroneous results but also retains statistical sensitivity, thereby balancing the risk of Type 1 by Type 2 errors and is employed as the multiple comparison method of choice throughout these experiments.

2.9 Summary of limitations

The experiments carried out in this thesis were performed on a group of advanced PD patients chosen for DBS implantation and as such represent a select group of subjects. Inherent in these experiments therefore are a number of limitations that must be considered when interpreting the results. Due to the neurosurgical practice of the collaborating teams with whom this work was carried out, the majority of patients available for study had implantation of the STN not the GPi. Therefore in order to ensure a homogeneous dataset and correspondingly maximise our statistical sensitivity, the experiments were performed only on patients with STN implantation. Whether these results extend to DBS of other basal ganglia nuclei, most notably the GPi is at present unknown. There is good reason for optimism though, given the matching presence of beta oscillations in the GPi as with the STN, the similarity in

effect of clinical DBS at the two nuclei and the functional connectivity of the two sites (Brown et al. 2001).

Another possible limitation relating to patient selection involves the requirement for study off medication (withdrawn from levodopa). Patients who were not comfortably able to withdraw from medication were not tested and it is possible that this may have introduced a sampling bias towards less severely affected individuals, although the numbers that declined enrolment on the grounds of levodopa withdrawal were low (n=2). Relatedly, levodopa was withdrawn from the night before and clinically patients were checked to ensure that that they were clinically OFF prior to commencement of experimentation. However, it must be acknowledged that some of the medications taken the night before may have had extended half-lives (dopamine agonists and extended release levodopa) and consequently some patients were possibly not studied at their maximum possible physiological levodopa withdrawal. This is not believed to be a significant drawback given that the patients were clinically assessed to ensure that clinically they were showing the signs of significant relative dopamine deficiency but could have increased variability across subjects and slightly weakened the statistical significance of effects found.

Another significant consideration relates to the timing of the experimentation. The experiments in chapters 3,5 & 6 were all carried out in the acute post/peri-operative setting. The implantation of DBS electrodes causes focal damage and tissue oedema which is known to affect the physiology of the underlying networks and result in clinical improvement in the absence of any stimulation – the "stun effect" (Chen, Pogosyan, et al. 2006). However, recent studies have demonstrated that beta oscillations are stable for up to 7 years after initial implantation compared with peri-operative recordings, suggesting relatively good correlation between acute and chronic physiology (Giannicola et al. 2012).

Additionally, there is a good correlation between the acute physiological localisation of beta oscillations and the localisation of chronic stimulation contacts further suggesting that this link is robust (Yoshida et al. 2010). Given the improvements found due to implantation stun effects as described, it is possible that the results here presented underestimate the magnitude of the effects shown.

The slightly different operative procedures adopted at the different sites could also have possibly reduced the homogeneity of our samples. However, this is felt to be limited given the ubiquitous use of post-operative imaging to confirm electrode localisation in addition to the clinical testing of stimulation efficacy and localisation of the best placed electrode contact by beta peak detection during the off-line analysis regimes (Yoshida et al. 2010; Chen et al. 2006). The effect of the use of different amplifiers and recordings systems / sampling rates was reduced by normalisation of power spectral data within subjects and the downsampling of all data to a common sampling rate. Recording either in monopolar or bipolar format may however have slightly affected the estimation of beta amplitude across different studies due to the possibility of beta rejection if it were common across all contacts. Practically, this didn't appear to have been a significant problem given that beta was found in the vast majority of patients off medication and that monopolar recordings (TMS International, Netherlands) which were later converted to bipolar montages were found to be very similar to those recorded directly in a bipolar montage using the in-house StimRecord equipment.

A final possible critique that could be levelled at chapter 5, examining the effect of closed loop stimulation compared to conventional stimulation, is that we looked at only motor scores and did not perform any more complete assessments, either full UPDRS or PDQ-39. This was the case because we were limited by the acute nature of our experimentation due to the bench side equipment. The advent of miniaturisation of this equipment in the near future should allow for the assessment of closed loop

algorithms in chronic naturalistic settings to assess whether these results are translated into the real world and to quantify the benefit of closed loop DBS to patients in terms of quality of life improvement (Afshar et al. 2012).

Chapter 3. A torque-based method demonstrates increased rigidity in Parkinson's disease during low-frequency stimulation.

3.1 Introduction

Recordings of LFPs from the basal ganglia of patients with Parkinson's disease have shown prominent oscillatory activity at frequencies under about 30 Hz (Alonso-Frech et al. 2006; Bronte-Stewart et al. 2009; Brown et al. 2001; Cassidy et al. 2002; Foffani et al. 2006; Kühn, Kupsch, et al. 2006; Marceglia et al. 2006; Weinberger et al. 2006). Such activity is suppressed by treatment with levodopa and by clinically effective deep brain stimulation (Jenkinson & Brown 2011). Oscillatory activity has been shown to correlate with rigidity-bradykinesia both in the rest state and in response to treatment, although the frequency band of interest has varied between studies from 8 Hz up to 35 Hz (Brown & Williams 2005; Chen et al. 2010; Kühn, Kupsch, et al. 2006; López-Azcárate et al. 2010; Pogosyan et al. 2010; Ray et al. 2008; Zaidel et al. 2010). Indeed, to date, there is little evidence that any particular low frequency of oscillation is any more predictive of motor deficit than another (Kühn et al. 2009). The above correlative evidence of a link between oscillatory activity across a fairly wide range of low frequencies and bradykinesia has been strengthened by a number of interventional studies in which bradykinesia has been exacerbated by stimulation of the STN at 5, 10 and 20 Hz (Chen et al. 2007; Chen et al. 2011; Eusebio et al. 2008; Fogelson, Kühn, et al. 2005; Timmermann et al. 2004).

Hitherto, however, there has been no evidence to support a direct causal link between low frequency oscillatory activity and rigidity. Here we test for such a link by stimulating the STN at low frequencies in patients with Parkinson's disease while we assess rigidity with an objective mechanical device that allows continuous scalar estimates of tone. We examined patients on their usual anti-parkinsonian

medication, so as to avoid potential ceiling effects whereby rigidity could not worsen further with low frequency stimulation. We hypothesised that stimulation at frequencies ≤ 20 Hz would increase rigidity at the wrist, while stimulation at clinically effective high frequencies would reduce rigidity.

3.2 Methods

3.2.1 Subjects and Surgery

The study was approved by the local ethics committee and subjects gave their informed, written consent. Twelve patients (mean age 61.5 ± SEM 1.9 yrs.; disease duration 13.1 ± 1.6 yrs.; see Table 3.1 for further details) with idiopathic Parkinson's disease were investigated 2.9 ± 0.8 yrs. after implantation of bilateral DBS electrodes into the STN. Indications for surgery were advanced Parkinsonism with motor fluctuations and / or dyskinesias or tremor that could not be sufficiently controlled by drugs. The DBS electrode used was model 3389 (Medtronic Neurological Division, Minneapolis, USA) with four platinum–iridium cylindrical surfaces (1.27mm diameter and 1.5mm length) and centre-to-centre separations of 2mm. Contacts 0 and 3 were the most caudal and rostral contacts, respectively. STN electrode trajectories were aimed at the dorsolateral STN. The STN was identified on high-resolution T2 weighted axial, MR images. On the day of surgery, a Cosman-Roberts-Wells® (Radionics, Burlington, MA) stereotactic base ring was applied to the patient's scalp under local anaesthetic. A stereotactic CT was obtained and the images were fused to the MR using Radionics Stereoplan® software. The STN was identified and targeted visually although concordance with the Schaltenbrand and Wahren atlas (1977) was confirmed. The electrodes were introduced via a 2.7mm twist drill craniostomy in all cases. Correct placement of DBS electrodes in the STN was supported intraoperatively by loss of rigidity and/or tremor suppression with stimulation and

postoperatively by performing a stereotactic CT scan that was fused to the T2- weighted MR images as above. Operations were performed in two stages with implantation of the pulse generator after one week of testing to confirm clinical effect.

Case	Age (yrs.)	Disease Duration / Time since operation (yrs.)	Predominant symptom	Pre-op Levodopa challenge UPDRS part III on/off Ω	Rigidity (L+R arm) Off / On HFS*	Medication (total daily dose)	Chronic stimulation Parameters
1	65	24 / 2	Tremor (R side)	14 / 32	1.5/0	Co-beneldopa 1125mg Ropinirole 8mg Amantadine 100mg	L 3.1V 60us 130Hz R 2.6V 60us 130Hz
2	56	6 / 1	Tremor (R side)	22 / 43	5/2.5	Co-careldopa 1000mg Entacapone 800mg Selegeline 10mg Co-beneldopa 125mg	L 3.9V 60us 130Hz R 1.5v 60us 130Hz
3	60	11 / 6	R sided rigidity / tremor	28 / 45	3 / 2.5	Co-careldopa 312.5mg	L 3.4V 60us 180Hz R 2.9V 60us 180Hz
4	71	17 / 2	Dyskinesias	8 / 38	3 / 1	Co-beneldopa 1725mg Amantadine 200mg	L 2.8V 60us 130Hz R 3.3V 60us 130Hz
5	65	18 / 2	Rigidity L side	7 / 34	1.5 / 2	Co-beneldopa 1000mg	L 2.8V 60us 130Hz R 3.2V 60us 130Hz
6	68	10 / 0.5	Bradykinesia	2 / 17	0.5 / 1	Rotigitine 4mg Co-beneldopa 1000mg	L 3.4V 60us 130Hz R 3.4V 90us 130Hz
7	49	10 / 2	R leg dyskinesia.	10 / 35	2 / 0.5	Co-careldopa 500mg	L 2.6 V 90us 130Hz

			Bradykinesia / tremor			Pramipexole 2.1mg	R 2.3 V 60us 130 Hz
8	64	12 / 2	R sided rigidity	17 / 47	3 / 3	Co-beneldopa 500mg Tolcapone 300mg	L 3.6V 90us 130Hz R 3.2V 90us 130Hz
9	62	13 / 3	R sided tremor & dyskinesias	15 / 38	3.5 / 2	Co-beneldopa 1125mg Ropinirole 24mg	L 3.9V 90us 130Hz R 2.4V 60us 130Hz
10	56	19 / 10	Bradykinesia / rigidity	† / 51 (off)	4 / 4	Co-careldopa 375mg Ropinirole 8mg	L 3.5V 90us 185Hz R 3.1V 120us 185Hz
11	55	6 / 1.5	Leg tremors. Drug induced nausea	6/27	7.5 / 3.5	Co-careldopa 500mg	L 3.5V 90us 130Hz R 3.4V 20us 130Hz
12	67	11 / 2.5	Severe Off periods	7/23	2.5 / 0.5	Co-beneldopa 312.5mg Ropinirole 3mg	L 3V 60us 130Hz R 3.1V 60us 130Hz

Table 3.1 Table summarising the clinical features of subjects involved in the low frequency stimulation study

- * Assessed as item 22 of motor section of UPDRS.
- † UPDRS on drugs – pre – op off drugs score missing
- Ω UPDRS III tested after overnight withdrawal of all anti-parkinsonian medication and again after a test dose of a minimum of 200 mg levodopa. Test performed less than three months before surgery.

3.2.2 Protocol

All patients were assessed on their usual medication. They were studied with the STN stimulation switched off and during bilateral STN stimulation at 5Hz, 10Hz, 20Hz, 50Hz and their usual therapeutic high frequency setting. The latter will be termed 130Hz, although in two patients

therapeutic stimulation was delivered at a higher frequency (see Table 3.1). The order of stimulation frequencies (including no stimulation) was pseudo-randomized across patients, with the exception that, to minimise protocol length, the final block was always the therapeutic high frequency setting. Stimulation contacts, amplitude and pulse duration remained the same as utilized for chronic therapeutic stimulation in each patient (see Table 3.1). The study was performed in a double blind manner with both the patient and assessor of rigidity unaware of which stimulation frequency was being used between 0-50 Hz. Eight minutes elapsed after changing stimulation settings before testing rigidity.

3.2.3 Rigidity assessment

Rigidity at each wrist was clinically assessed with item 22 of the motor section of the UPDRS. Half points were used to increase sensitivity (Chen et al. 2010; Kühn, Doyle, et al. 2006). However, clinical assessment alone has poor sensitivity as well as high inter-rater and intra-rater variability (Patrick et al. 2001; Prochazka et al. 1997). We therefore followed clinical assessment with an objective mechanical assessment of rigidity at each wrist that afforded continuous scalar estimates. This was preferred to an index of rigidity derived from EMG, as several studies have confirmed that torque-based methods of quantification are more strongly related to clinically determined rigidity than EMG based metrics (Endo et al. 2009; Levin et al. 2009; Park et al. 2011). We assessed wrist torque in response to externally based displacement imposed by the examiner rather than by a motor. The former was preferred so as to limit anxiety and re-enforcement related to use of a motor and fixed manipulandum. Angular displacement was measured using an electronic goniometer across the wrist (TMS International B.V., Netherlands) that was calibrated using a manual goniometer for each patient across the whole angular range of displacement. Force was measured using a strain gauge (Omegadyne

LCM201-100N) mounted between two horizontal aluminium bars (Fig 3.1A). The strain gauge had a linear range from 0 to 100N ±1%. Force and angle measures were low pass filtered at 1kHz, sampled with a frequency of 2048 Hz and recorded through a commercial amplifier (TMSI Port 7, TMS International B.V., Netherlands).

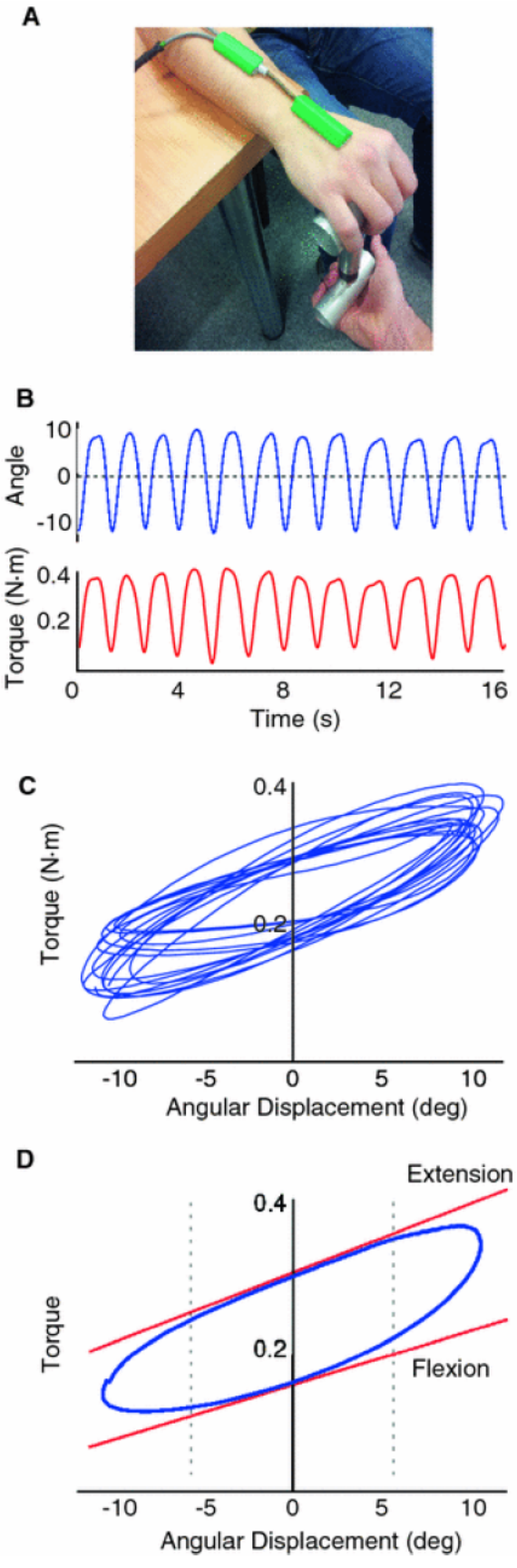

Figure. 3.1 Device and method for determining rigidity (A) Photograph of mechanical rigidity device. (B) Time series of force and displacement during stimulation at 5 Hz from subject 7 (UPDRS—clinical rigidity score—1). (C) Superimposed torque–angular displacement cycles during stimulation at 5 Hz. d Schematic of analytical method for determining rigidity coefficients in flexion and extension. A single displacement cycle is shown from stimulation at 5 Hz (blue line) with linear regression of mid-cycle phase (dashed lines 50 % of cycle) for both flexion and extension (red line). The gradient of the regression line is taken as the rigidity for that cycle. Reprinted with permission (Little, Joundi, et al. 2012).

The metacarpo-phalangeal (MCP) junction of the subject's hand was rested on the top bar of the device while the bottom bar was controlled by the experimenter. The distance between the MCP joint and the wrist was used to calculate torque (force x distance). Patients were requested to look straight ahead and minimise speech movement and speech. The hand was then passively flexed and extended as the experimenter applied force in a sinusoidal, vertical, manner. Velocity was controlled by delivering a fixed displacement at a set frequency of 0.75 Hz using a visual metronome which was visible to the experimenter but not the patient. This frequency falls in the range used clinically to determine rigidity with the motor UPDRS (Shapiro et al. 2007). The experimenter moved the wrist through half the full range of comfortable displacement around the horizontal plane. Patients were encouraged to fully relax and not to assist with movement. Active assistance was identified by subjective reduction in force on the strain gauge device prior to the start of a cycle and these sections were removed and rigidity assessment repeated after patient re-instruction. A minimum of 14 cycles per condition were performed.

3.2.4 Analysis

We derived the elastic coefficient of the wrist calculated from unit torque / unit angular displacement (Endo et al. 2009; Powell et al. 2012). Rigidity was calculated offline in MATLAB (v. 7.11.0, R2010b, The Mathworks, Natik, MA, USA) using custom written scripts. The oscillatory time series of both torque and angular displacement were pass-band filtered between 0.25 Hz and 1.25Hz using a 4^{th} order Butterworth filter to remove offset, noise and any super-added tremor. Continuous oscillatory traces were broken into individual cycles using the phase determined through a Hilbert transform. Displacement was plotted against torque (x and y, respectively) for the central 50% of each cycle and this was fitted with a linear regression line (Fig 3.1B). The gradient of this line was taken as the elastic

coefficient, and the procedure repeated for each cycle of movement. The mean elastic coefficient of the last 12 cycles performed in each experimental run was taken as our index of rigidity for that condition. Exclusion of the first few movement cycles allowed the subject to relax before assessments were made. This procedure was separately performed for both the flexion and extension phase of each cycle.

All rigidity values were normalised to the OFF stimulation state [(stim off – stim (f) / stim off)] to determine percentage change compared to baseline, and signs inverted so that a positive % change represented an increase in rigidity. Kolmogorov-Smirnov tests confirmed the normality of the % changes estimated with the device, and so stimulation frequency effects were evaluated with t-tests. Significant effects were reported if they remained significant according to the False Discovery Rate procedure and t-tests were two tailed. Changes in clinical assessments of rigidity were assessed with non-parametric Wilcoxon signed ranks tests. Clinical assessments of rigidity were logarithmically transformed prior to correlation with device measurements, given the known logarithmic nature of psychophysical observation (Weber's law). Correlations were performed using Spearman's correlation. Statistical analysis was performed in the Statistical Program for Social Sciences (SPSS) statistical software (version 17.0, SPSS Inc., Chicago, IL, USA).

3.3 Results

Our *a priori* hypothesis was that the effects of stimulation at frequencies ≤ 20Hz would be related and lead to an increase in rigidity, whereas the effect of stimulation at 130 Hz would lead to a decrease in rigidity at the wrist. Objective assessment of tone with our device bore this out (Fig 3.2). The effects of stimulation at 5, 10 and 20 Hz all correlated with one another, whether extension or flexion were tested (mean Fisher transformed r = 0.725 ± SEM 0.016 and 0.568 ± 0.009, respectively, all

correlations individually significant, $p < 0.05$). However, correlations between the effects of stimulation at 5-20 Hz with those of stimulation at 130 Hz were weak ($r = 0.229 \pm 0.042$ and $r = 0.308 \pm 0.121$ for extension and flexion, all but one non-significant). The similarity in the response to low frequency (5, 10 and 20 Hz) stimulation in flexion and extension seen at the group level (Fig 3.2) was also found at the level of individual limbs. Thus the maximum rigidity in the low frequency blocks in flexion was at the same stimulation frequency as in extension in 19 out of 24 sides (Fisher's exact test, two-tailed $p = 0.0032$, compared to the 8 out of 24 instances expected by chance). Across movement phases the maximum rigidity in the low frequency blocks was at 5 Hz on 17 sides, 10 Hz on 17 sides and 20 Hz on 14 sides.

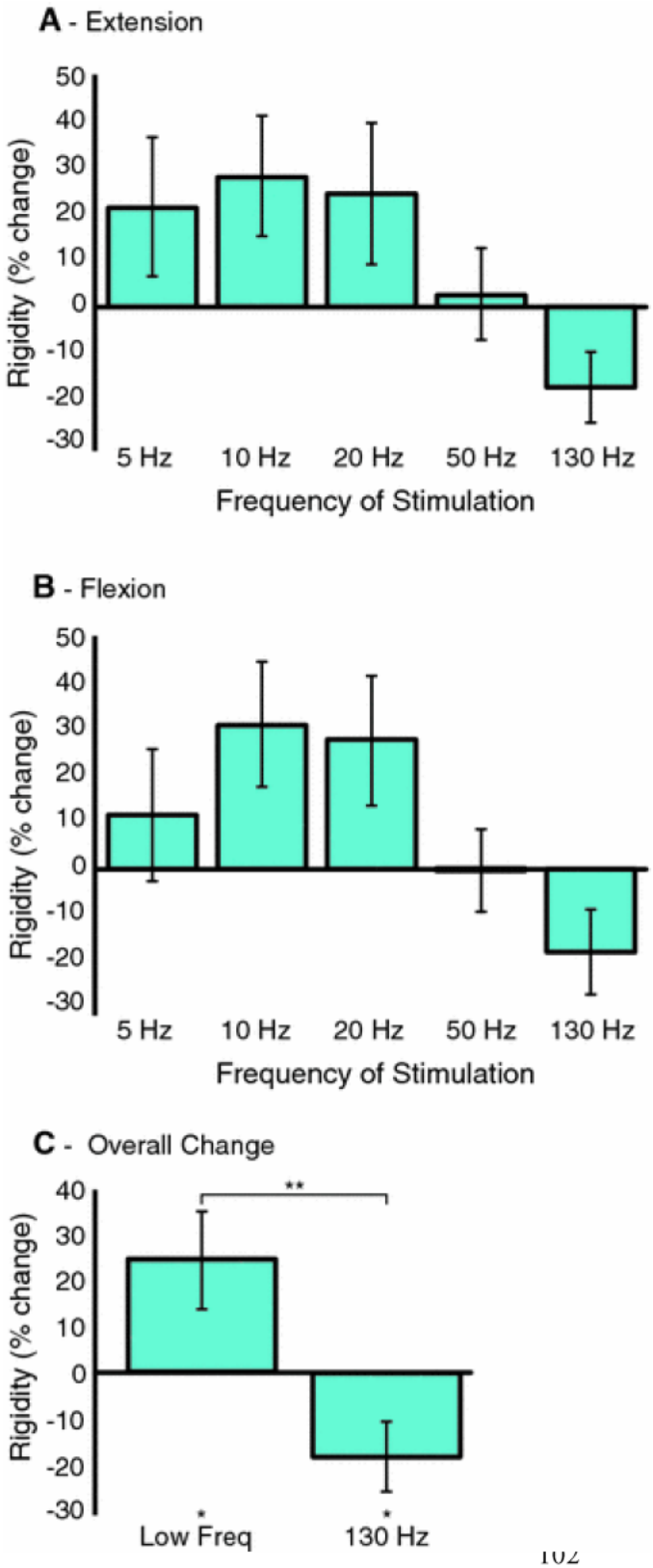

Figure. 3.2 Effects of bilateral stimulation of the STN at different frequencies on quantitative rigidity compared to off-stimulation state. A Mean (±SEM) percentage change in extension coefficients. B Percentage change in flexion coefficients. Stimulation at frequencies ≤20 Hz exacerbates rigidity, whereas stimulation at the therapeutic frequency of 130 Hz tends to improve rigidity. The pattern is similar for extension and flexion. C Percentage change of averaged low-frequency (5,10 and 20) flexion/extension coefficients with significance. Low-frequency stimulation significantly increases rigidity (*$p < 0.05$), and high-frequency stimulation significantly reduces rigidity (*$p < 0.05$). Low-frequency and high-frequency stimulation are significantly different (**$p < 0.01$). Twenty-four upper limbs were tested with patients on Parkinsonian medication. Reprinted with permission (Little, Joundi, et al. 2012)

Thus effects on flexion and extension were very similar (contrast Fig 3.2A and B), and so in subsequent analyses we averaged changes across flexion and extension. Thereafter, we averaged the effects of 5-20 Hz stimulation and compared this to baseline (no stimulation) and to the effect of stimulation at therapeutic frequency, 130 Hz. Low frequency stimulation (5-20 Hz) increased rigidity by 24.0 % (one-sample t-test, $t_{df\,23} = 2.240$, p=0.035), whereas high frequency stimulation reduced rigidity by -17.8 % (one-sample t-test, $t_{df\,23} = -2.284$, p=0.033). The effects of low and high frequency stimulation were also different (paired t-test, $t_{df\,23} = 3.511$, p = 0.002).

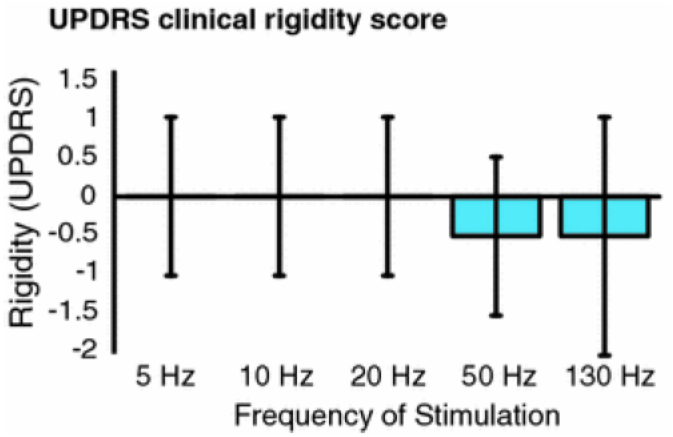

Figure 3.3 Effects of bilateral stimulation of the STN at different frequencies on clinical UPDRS rigidity scores compared to off-stimulation state. Median and inter-quartile ranges are shown. Rigidity was assessed using item 22 of the motor UPDRS. Twenty-four upper limbs were tested with patients on Parkinsonian medication. Reprinted with permission (Little, Joundi, et al. 2012).

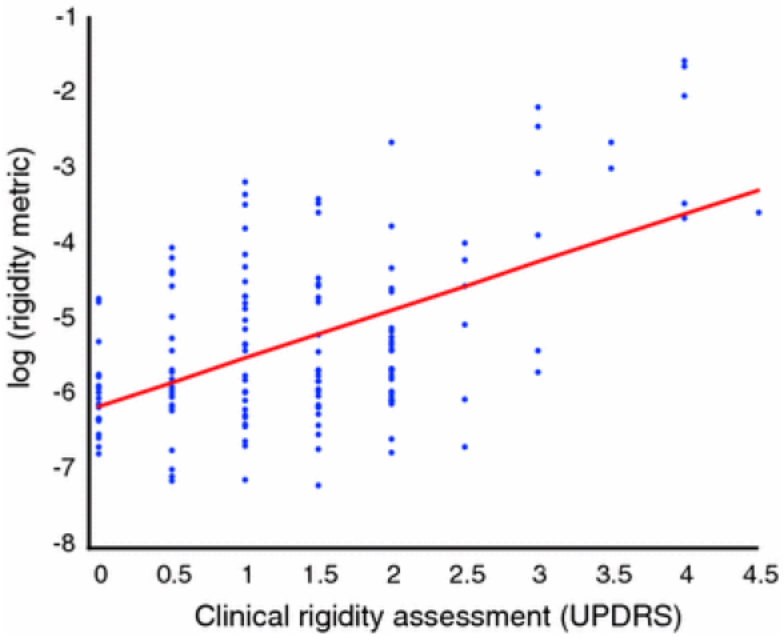

Figure. 3.4 Scatter plot of clinical rigidity assessment versus log quantitative rigidity scores. There is a correlation between clinical rigidity scores and log rigidity scores, rho = 0.361, p = 0.002. Rigidity was clinically assessed using item 22 of the motor UPDRS. Data are compiled from 24 upper limbs and five different stimulation frequencies (including 0 Hz). Patients were on Parkinsonian medication. Reprinted with permission (Little, Joundi, et al. 2012)

We were unable to demonstrate an effect of low frequency stimulation when using double-blinded clinical assessment of rigidity (Fig 3.3). As above, we averaged the effects of 5-20 Hz stimulation and compared this to baseline and to the effect of stimulation at therapeutic frequency, 130 Hz. Low frequency stimulation increased rigidity by 1 % (Wilcoxon test, p=0.87), whereas high frequency stimulation reduced rigidity by 45 % (Wilcoxon test, p=0.002). The effects of low and high frequency stimulation were also different (Wilcoxon test, p = 0.002). Clinical and device assessments were significantly correlated, although the relationship was not strong (Spearman's rho= 0.382, p=0.002; Fig 3.4).

3.4 Discussion

This study shows a worsening of objectively recorded rigidity in patients with Parkinson's disease during low frequency stimulation of the subthalamic nucleus, and thus provides further evidence for a causal role for these oscillations in the pathophysiology of the condition. Recordings of the effects of low frequency stimulation were made under double-blind conditions. Clinical assessment of tone made under the same conditions, however, did not reveal any change, -perhaps because of the acknowledged poor sensitivity and high variability of this technique (Patrick et al. 2001; Prochazka et al. 1997). The latter may also explain the relatively modest correlation between mechanical and clinical assessments of rigidity in the present investigation. Such modest but significant correlations between objective and clinical assessments of rigidity have also previously been reported in the setting of DBS (Levin et al. 2009). Previous studies have investigated the effect of low frequency stimulation on bradykinesia in patients with Parkinson's disease and generally found a modest effect with stimulation over 5-20 Hz (Chen et al. 2011). The results presented here are remarkable for a larger effect size (24%) and for extending evidence of a causal link between low frequency oscillations and impairment to rigidity. As previous studies have all been performed off medication it is possible that a floor effect limited the size of previous results, though it is also possible that rigidity is more sensitive than bradykinesia to low frequency stimulation. On the other hand, a floor effect might have led to an under-estimation of the therapeutic effects of high frequency stimulation on rigidity in our series of patients on medication, although it should also be noted that assessment of stimulation at 130 Hz was performed last and was not double-blinded.

Our data reinforce those studies showing a correlation between low frequency synchrony and aggregate measures of bradykinesia and rigidity (Brown & Williams 2005; Chen et al. 2010; Kühn, Kupsch, et

al. 2006; López-Azcárate et al. 2010; Pogosyan et al. 2010; Ray et al. 2008) and of rigidity alone (Hammond et al. 2007; Zaidel et al. 2010). One of the latter studies reported peak correlations with rigidity at 15 Hz (Zaidel et al. 2010). With respect to rigidity, it is possible that low frequency synchrony in basal ganglia-cortical loops may, under physiological conditions, promote postural activity through the upregulation of the effects of sensory inputs that reinforce such activity (Androulidakis et al. 2006; Gilbertson et al. 2005; Lalo et al. 2007). This upregulation may be further heightened when low frequency synchrony is exaggerated in Parkinson's Disease (Hammond et al. 2007).

Finally, the present study introduces a new method of rigidity assessment in patients with Parkinson's disease which, although simple to implement, -mimicking clinical evaluation,- affords objective, continuous scalar estimates of tone, rather than the bounded, ordinal clinical assessment using the motor UPDRS.

Chapter 4. Beta band stability over time correlates with Parkinsonian rigidity and bradykinesia.

4.1 Introduction

There is an increase in correlative evidence suggesting that exaggerated oscillatory synchronisation in the beta frequency band may be related to motor impairment in patients with Parkinson's Disease (Jenkinson & Brown 2011). Such synchronisation is usually indirectly measured as the average spectral amplitude or power of beta frequency band activity in the LFP recorded in basal ganglia sites targeted during functional neurosurgery. LFP fluctuations largely reflect the temporal and spatial summation of presynaptic neuronal activity (Goldberg et al. 2004; Magill et al. 2004; Mitzdorf 1985) and therefore LFP amplitude or power indexes the strength of synchronisation, the density and (up to an electrode dependent limit) the spatial extent of the involved neural pool. However, a further variable is often overlooked, and this is the constancy of these features over time. Synchronisation and the size of the affected neural pool can change from moment to moment, leading to fluctuations in spectral amplitude or power over time that affect the average signal. Consider, for example, two networks. One is almost completely synchronous or very extensive for a brief instant, and then barely synchronous or very small for the rest of the time. Another network is modestly synchronised and extensive throughout. The two networks may lead to similar time averaged LFP power but the impact upon normal functioning may potentially be very different. We have previously reported that the spatial extent of beta band phase synchronisation in the region of the STN correlates with rigidity –

bradykinesia (Pogosyan et al. 2010). We now test whether the temporal stability of synchronisation as inferred from LFP amplitude also correlates with rigidity – bradykinesia.

A correlation between the temporal stability of beta band amplitude and motor impairment would be important for several reasons. First, fluctuations in amplitude might imply the existence of processes that can disrupt pathological synchrony, which might provide clues for new therapeutic approaches, as in epilepsy (Loddenkemper et al. 2001). Secondly, the temporal stability of beta band amplitude might provide a faithful indicator of current motor state suitable as a feedback signal in the closed loop control of therapeutic deep brain stimulation (Rosin et al. 2011). Temporal stability might provide a faithful feedback signal in its own right, or, if proven to carry non-redundant information, through combination with other measures.

We elected to assess the temporal stability of the amplitude of the LFP in the beta range with a simple measure, the standard deviation of the time varying beta band amplitude normalised by the mean beta band amplitude, otherwise known as the coefficient of variation (CV). There is some hope that the CV of LFP amplitude might correlate with clinical state, given the correlation of a complexity measure of beta activity with motor impairment (Chen et al. 2010). However, the CV and complexity, as estimated using the Lempel-Ziv complexity are not equivalent. The Lempel-Ziv complexity captures not only linear dependencies in the structure of the LFP over time but also nonlinear interactions between frequencies (Chen et al. 2010) making it a more difficult statistic to estimate and a less intuitive one. We also elected to assess the strength of correlations between motor impairment and CV in the lower and upper beta frequency band, and to investigate this both with respect to the off medication state and change with medication, -aspects not explored with the Lempel-Ziv complexity. Consideration of the lower and upper beta frequency bands was motivated by studies which suggest a

differential functional and pathological significance between these frequency ranges (López-Azcárate et al. 2010; Foffani et al. 2006; Marceglia et al. 2006; Marceglia et al. 2007).

4.2 Methods

4.2.1 Patients & Surgery

We investigated the relationship between time related fluctuations in the amplitude of the beta band signal and motor impairment, as indexed by the motor UPDRS, in the off medication state at rest and in response to levodopa treatment in two independent archival datasets; an intraoperative off medication rest dataset and a post-operative dataset which included data from on and off medication. The surgical target was the STN and the DBS electrode used was model 3389 (Medtronic Neurological Division, Minneapolis, USA).

4.2.2 Rest OFF medication Dataset

Eighteen patients with advanced idiopathic PD were recorded intra-operatively in the off medication state (mean age 60.4 ± (SEM) 7.0 yrs, disease duration 15.2 ± 5.4yrs, mean pre-operative UPDRS motor score 42.9 ±15.7 off drugs and 11.1 ± 7.4 after levodopa challenge). These patients have been reported previously (Pogosyan et al. 2010); however, the earlier study only investigated the correlation between LFP phase coherence and clinical features. LFPs were recorded from bipolar pairs of adjacent electrode contacts to maximise spatial selectivity. This afforded a series of three bipoles, 01, 12 and 23, from the four electrode contacts of each electrode, where contact pair 01 was the most caudal. Intra-operative recordings involved a staged descent in 2 mm steps from above the STN with periods of recording at each level. All patients showed a step increase in beta power between contacts 01 on entering the STN of at least 100%. This depth has been termed the physiologically defined target level

(Yoshida et al. 2010). Full details of the patients, surgery, recordings and physiological targeting are included in the previous report (Pogosyan et al. 2010). Data from this cohort were amplified, pass band filtered between 1 and 80 Hz and sampled at 184 Hz (Biopotential Analyser Diana, St Petersburg, Russia). Thereafter LFPs were examined off-line in Spike2 software (Cambridge Electronics Design, Cambridge, UK).

4.2.3 On-Off Medication Dataset

Ten patients (20 sides) were recorded in the off state and following levodopa challenge in the post-operative period prior to battery and stimulator implantation (age 60.6 ± 2.5 yrs, disease duration 11.9 ± 1.4yrs, pre-operative UPDRS motor score 45.1 ± 2.5 off drugs and 22.4 ± 4.1 after levodopa challenge). Full details of patients, surgery and recording have previously been reported separately for nine of the subjects (Kühn, Kupsch, et al. 2006) and one subject (case 5 in (Kühn, Doyle, et al. 2006)). LFPs were recorded from bipolar pairs of adjacent electrode contacts as above. Data from this cohort were amplified and filtered at 1-250 Hz using a custom-made, high impedance amplifier (which had as its front end input stage the INA128 instrumentation amplifier, Texas Instruments Incorporated 12500 TI Boulevard Dallas Texas, USA) and recorded through a 1401 A-D converter (Cambridge Electronic Design, UK) onto a computer using Spike2 software (Cambridge Electronic Design, UK). Signals were sampled at ≥ 625 Hz.

4.2.4 Spectral analysis

Spectral decomposition with a continuous wavelet transform was performed for both datasets using a Morlet wavelet, due to its efficient time frequency resolution and lack of assumptions regarding stationarity (Muthuswamy & Thakor 1998; Pogosyan et al. 2010). Convolution of each LFP time series for each subject was carried out with an array of appropriately scaled wavelets to generate a

complex time series for each frequency band between 1-80Hz for the duration of each recording, the modulus of which denoted the instantaneous amplitudes for each frequency at all points during the recording. The wavelet transformation is in a sense therefore a band-pass filtering of the LFP such that the resulting time series shows the magnitude of oscillations over the time of the recording in the specific filtered frequency (Fig 4.1). As can be seen, there was variation in the amplitudes at the specific frequencies that then were used to calculate the coefficient of variation (CV) by dividing the standard deviation of each frequency specific amplitude time series by the corresponding mean amplitude. This afforded a single value of each frequency for the duration of the whole record. As such, for each subject a single value of amplitude variability (CV) was obtained for each frequency resulting in 80 frequency specific CVs (1-80Hz) per subject for further correlation.

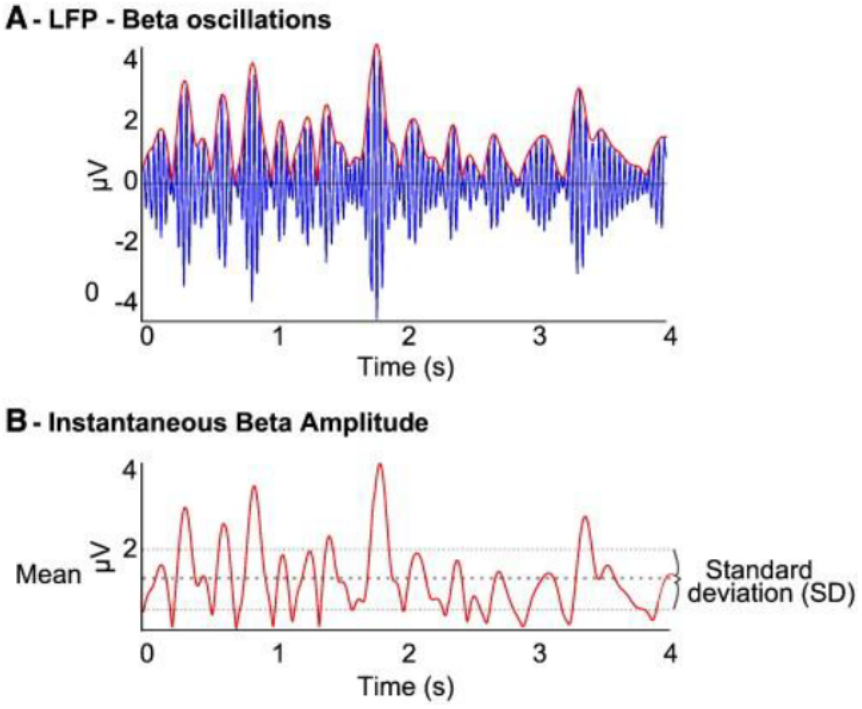

Figure 4.1 Schematic showing amplitude variability in beta in one subject and corresponding instantaneous amplitude time series. [**A**] Filtered beta LFP signal from subject 12 (intraoperative rest data) demonstrating marked fluctuations in beta amplitude over time and a low hemibody UPDRS score = 23. [**B**] Instantaneous amplitude time series with mean amplitude (thick dashed line) and standard deviation also illustrated (thin dashed lines). Instantaneous amplitude is calculated by convolution of the LFP with an

appropriately scaled / frequency specific wavelet to determine the amplitude of the selected frequency band at all points in time. The standard deviation of the instantaneous amplitude time series captures the variability of amplitude over time for that frequency. This is then normalised by the mean amplitude in that frequency band to derive a scale invariant measure of amplitude variability – the coefficient of variation of amplitude over time (CV), for each record. Reprinted with permission (Little, Pogosyan, et al. 2012)

The CV is therefore scale invariant and relatively immune from confounds introduced at the between subject level such as differences in stun effects or small variation in targeting between sides and subjects. Recording lengths were 65 ± 2.4s (SEM) for the intraoperative dataset and 286 ±15s (SEM) for the levodopa response dataset. Processing was performed in MATLAB (v. 7.11.0, R2010b, The Mathworks, Natik, MA, USA) with custom written scripts.

4.2.5 Correlations

The CV averaged across the frequencies within the low beta (beta 1 = 12-20 Hz) and high beta (beta 2 = 21-33 Hz) frequency bands for each side was correlated with clinical scores derived from the motor UPDRS across subjects. The clinical scores were total hemibody score (sum of unilateral UPDRS motor score sub-items 20-26), rigidity-bradykinesia hemibody score (sum of unilateral UPDRS motor score sub-items 22-26) and rest tremor hemibody score (sum of unilateral UPDRS motor score sub-items 20 and 21 for arm and leg) contralateral to the recording site. The percentage change of UPDRS for each item was calculated as ([hemibody scoreON - hemibody scoreOFF] / hemibody scoreOFF) x 100. Similarly, percentage changes in the CV was calculated as [CVON - CVOFF] / CVOFF and in the signal amplitude as [AmplitudeON - AmplitudeOFF] / AmplitudeOFF.

Kolmogorov-Smirnov testing revealed that the intra-operative rest data were not normally distributed and therefore correlations were performed using Spearman's correlation coefficient (rho) and data normalised using a Boxcox power transformation (lamda=0.3) prior to multiple linear regression. The

treatment change dataset fitted a normal distribution (KS $p>0.05$) and therefore was not transformed prior to multiple regression. Statistical analyses were performed using SPSS version 19 (SPSS Inc., Chicago, IL, USA).

4.3 Results

4.3.1 Intra-operative rest recordings off medication (18 subjects, 36 sides)

Spectral analysis of the LFP recorded at the physiologically defined target level revealed that all 18 subjects had at least one spectral peak within the beta band (13-35 Hz). The power spectrum averaged across all records demonstrated two defined peaks at 16 Hz and 25 Hz, within the low beta (beta 1) and high beta (beta 2) frequency bands, respectively (Fig 4.2A).

The CV of intra-operatively recorded amplitude was calculated with 1Hz resolution over 1 to 80 Hz and correlated against the presurgical motor UPDRS score. The correlation between the CV of the amplitude envelope and UPDRS scores was significant and broad, albeit restricted to the beta 2 range (Fig 4.2B, C). This relationship was strongest at the frequency of the peak (25Hz) in the beta 2 range of the group mean power spectrum (rho = -0.75, $p<0.001$; Fig 4.3). Correlations were negative so that a higher CV was associated with more modest motor impairment in the contralateral limbs.

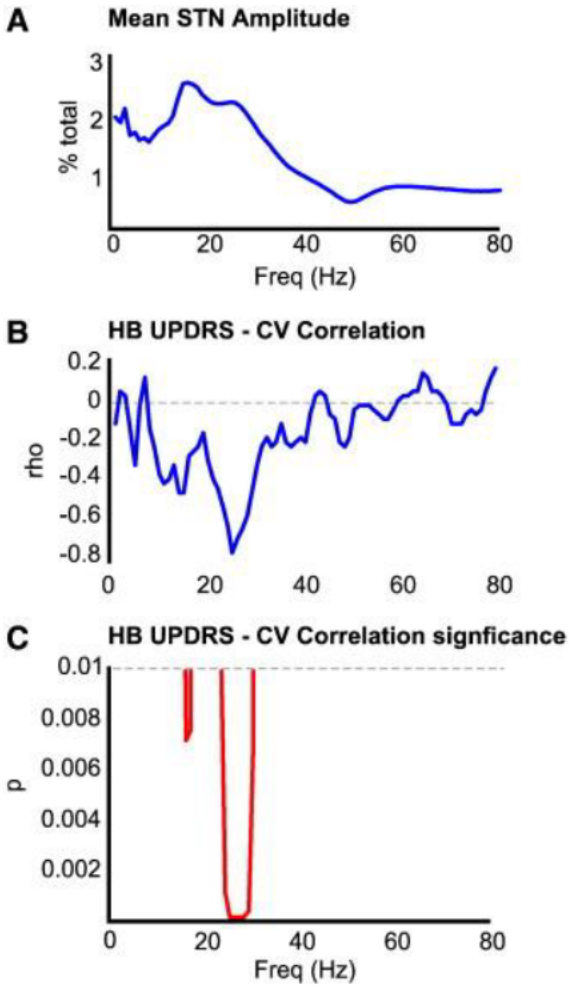

Figure 4.2 Spectral correlations. [**A**] Mean STN LFP amplitude spectral density across all subjects, shown as % of total in each 1Hz frequency band. There are peaks at 16 and 25 Hz, in the beta 1 and beta 2 ranges, respectively. [**B**] and [**C**] show Spearman's correlation coefficient (rho) and its significance between the CV of STN LFP amplitude at a given frequency and contralateral hemibody (HB) motor UPDRS scores. There is a strong and broad correlation between the STN LFP CV at a given frequency and contralateral hemibody motor UPDRS scores in the beta 2 range. Reprinted with permission (Little, Pogosyan, et al. 2012)

Having confirmed a correlation between hemibody motor UPDRS scores and the temporal variability of oscillatory activities in the beta frequency band, we separately calculated the mean CV across the frequencies within the beta 1 and beta 2 ranges and correlated these against total hemibody motor UPDRS scores. The Spearman's correlation coefficient (rho) of mean beta 1 CV vs. UPDRS was -0.44 ($p=0.008$) and -0.59 for mean beta 2 CV ($p<0.001$). This procedure was repeated for alpha (7-11 Hz)

which demonstrated a weaker correlation with borderline significance (rho = -0.34, p=0.044) and for gamma (40-80 Hz), which revealed no correlation (rho= -0.08, p = 0.65).

The relationship between beta CV and clinical features was not only frequency but also impairment selective. Correlations between beta 1 and beta 2 CV and contralateral rigidity-bradykinesia hemibody scores alone were significant (rho = -0.45, p = 0.006 and rho = -0.53, p < 0.001), but there was no relationship between beta 1 and beta 2 CV and contralateral tremor hemibody scores (rho = -0.26, p = 0.11 and rho = -0.24, p = 0.16). Correlations were also found to be highly focal. The primary analysis was conducted using STN recordings made at the physiologically defined target level (Yoshida et al. 2010). We therefore repeated the analysis using data recorded from 2 mm above the physiological target level and correlations were absent for both beta 1 & beta 2 (rho = -0.22, p = 0.2 and rho = -0.18, p = 0.3).

CV is relatively scale independent, as it is normalised by mean amplitude. To be sure that we were not confounding our predictions of the variance in clinical state with a dependency of the latter on amplitude, we further performed multiple regression analysis using CV and amplitude in the two beta sub-bands. The overall model accounted for 41% of the variance in contralateral hemibody UPDRS scores (r^2 = 0.41; F(4,31) = 7.060, p < 0.001) and 29% of contralateral rigidity-bradykinesia hemibody UPDRS scores (r^2 = 0.29; F(4,31) = 4.622, p = 0.005). However, only the CV in the beta 2 band strongly correlated with contralateral hemibody UPDRS scores and was a significant predictor of clinical impairment (standardised *b* coefficient -0.54, p=0.009), when accounting for the remaining variables in the regression model.

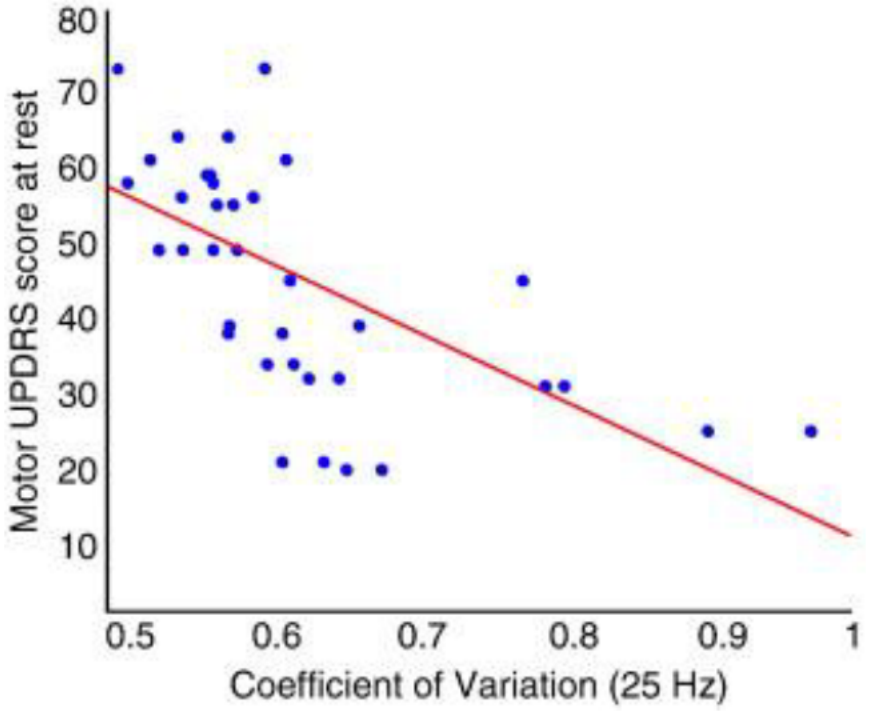

Figure 4.3 Scatter plot of CV and contralateral hemibody motor UPDRS off medication. Shown for the frequency (25 Hz) of the peak of activity in the Beta 2 range in the group mean spectrum (Fig 4.2A). There is a negative correlation between CV and UPDRS off medication (rho = -0.75, p<0.001). (Little, Pogosyan, et al. 2012)

4.3.2 ON / OFF dataset (10 subjects, 17 sides)

We next investigated whether treatment with levodopa increased the CV and did so in proportion to treatment induced improvement in rigidity-bradykinesia. To this end we analysed a second archival dataset that recorded STN LFPs in patients both off and on levodopa, concurrently with clinical assessments. Two recordings were found to not show a distinct peak within the beta range and were therefore excluded from further analysis. The CV estimated for a further recording was identified as a significant outlier and was excluded following examination of residuals (Cook's score 4.6). An ANOVA of amplitude in the remaining 17 sides, with factors medication and beta frequency range (beta 1 or beta 2), revealed an effect of levodopa ($F(1,16) = 6.57$, $p = 0.021$) and a trend towards

interaction between medication and beta range ($F(1,16) = 3.29$, $p = 0.089$) but no main effect of beta frequency range. Post-hoc t-tests showed that there was a significant reduction in beta 1 amplitude (38%; $p = 0.03$) and a smaller but significant reduction in beta 2 amplitude (21%; $p = 0.042$). An ANOVA of CV with the same factors revealed no main effects or interactions.

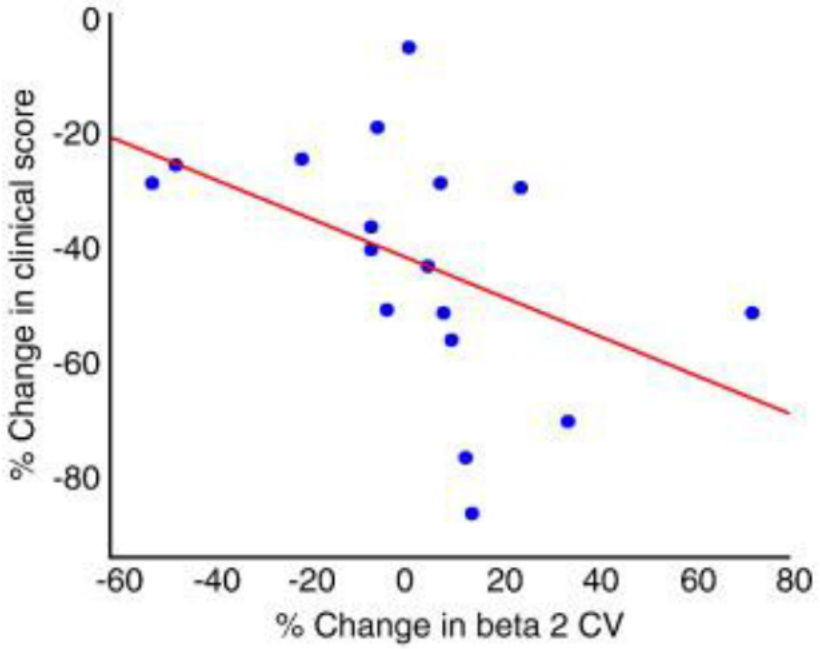

Figure 4.4 Scatter plot of change in mean beta 2 CV and change in contralateral hemibody rigidity-bradykinesia score in response to levodopa. The patients with the best improvement (more negative % change) in rigidity-bradykinesia have the greater increase in beta 2 CV. (Little, Pogosyan, et al. 2012)

Despite the above, we found a significant negative correlation between the levodopa-induced change in mean beta 2 CV and the change in contralateral rigidity-bradykinesia scores ($rho = -0.66$, $p = 0.004$; figure 4.4). Greater increases in CV upon treatment were associated with greater improvements in rigidity-bradykinesia upon treatment. This was again found to be symptom selective as there was no relationship between beta 2 CV and contralateral tremor hemibody scores ($rho = 0.14$, $p = 0.6$). There was also no significant association between change in beta 1 CV and change in clinical state. Note too that the change in CV cannot alone account for improvement in clinical state with medication, as a

minority of patients showed modest improvement despite drops in CV after treatment. On two sides, each from different patients, the drop in CV after treatment related to the complete suppression of the beta 2 peak that was formerly present in the off medication state.

Levodopa-induced changes in beta band amplitude are known to correlate with improvements in motor signs. We therefore reprised our previous multiple regression analysis, but using levodopa-induced changes in amplitude, CV and clinical state. The overall model accounted for 44 % of the variance in contralateral hemibody rigidity-bradykinesia scores (r^2 = 0.44, F(4,12) = 4.20 p = 0.024). However, only the change in CV in the beta 2 band was correlated with the change in contralateral hemibody UPDRS (Standardised *b* coefficient -1.08, p = 0.019), when accounting for the remaining variables in the regression model.

4.4 Discussion

This study demonstrates that the normalised variability (CV) of the beta frequency band component of the STN LFP over time strongly predicts the variance between patients in rigidity-bradykinesia. Specifically, the greater the CV at rest and the greater the increase in CV following levodopa treatment, the lower the bradykinesia-rigidity score at rest and the greater the improvement in rigidity-bradykinesia with treatment. These effects were found to be frequency and impairment specific, as well as focal.

There are several reports that treatment induced suppressions of beta amplitude or power in the STN LFP correlate with treatment induced clinical improvement (Kühn, Kupsch, et al. 2006; Kühn et al. 2009; Ray et al. 2008). However, it has been less clear whether beta amplitude or power in the off medication state correlates with motor impairment. Several studies found no such correlation (Kühn,

Kupsch, et al. 2006; Kühn et al. 2009; Ray et al. 2008). In contrast, two studies have reported significant, correlations between beta band power and rigidity-bradykinesia in the off-medication state (rho = 0.428 in (López-Azcárate et al. 2010) and rho = 0.329 in (Ozkurt et al. 2011)).Two other studies have reported correlations under similar circumstances using the Lempel-Ziv Complexity measure in the beta band (Chen et al. 2010) or LFP phase synchronisation across electrode contacts (Pogosyan et al. 2010). A number of other studies have shown correlations between independent specific force parameters and power in different frequency bands. Rapid force decrement in a sustained grip task has been shown to be correlated with beta power (Tan, Pogosyan, Anzak, Foltynie, et al. 2013), gamma has been shown to scale with maximal effort (Anzak et al. 2012) force movements and beta / gamma have been shown to have complementary associations with low and high motor effort, respectively (Tan, Pogosyan, Anzak, Ashkan, et al. 2013).Our study reinforces these findings by demonstrating that the CV of beta 2 band LFP activity, in particular, correlates off medication with rigidity- bradykinesia (rho = -0.59), and extends them by showing that, like treatment induced changes in beta band amplitude or power, treatment induced changes in CV also correlate with treatment induced changes in bradykinesia and rigidity (rho =-0.66).

Thus another feature of synchronisation, its temporal variability, may impact on clinical state. Time averaged LFP power/amplitude estimates index the strength of synchronisation, the density and spatial extent of the involved neural pool and the constancy of these features over time. However, power/amplitude estimates cannot infer the relative contributions of these different features and their relative pathophysiological importance remains unclear. Thus, measures reflecting individual features, like the spatial extent of phase synchrony in the beta band (Pogosyan et al. 2010) and the CV of beta band activity may potentially provide complementary, rather than redundant, information about clinical state. This raises the possibility that measures can be combined to strengthen clinical

correlations. Özkurt et al showed this with beta power and the high frequency oscillation power ratio, and here we demonstrate that combining beta amplitude and beta CV in a multiple regression model accounts for 41 % of the variance in contralateral hemibody UPDRS scores off medication (Ozkurt et al. 2011). Similarly, combining levodopa-induced change in beta amplitude and beta CV in a multiple regression model accounts for 44% of the variance in change in contralateral hemibody rigidity-bradykinesia scores. This multivariate approach may prove useful in selecting feedback signals that faithfully reflect current motor state and are therefore suitable for closed-loop control of DBS (Rosin et al. 2011). This may be particularly the case with beta amplitude and its CV, as both are computationally simple to calculate, potentially limiting drains on battery power, and correlate over a large spectrum of clinical state as suggested by the correlations evident with rest and treatment induced changes. Nevertheless, it is important to stress that although beta amplitude and CV have been shown to explain a significant portion of the variance in rigidity-bradykinesia across patients, this has yet to be demonstrated within subjects, a necessary pre-requisite for any signal or signal combination to be used in closed loop control.

It should be noted that the OFF drug motor UPDRS scores contrasted with the first intra-operatively recoded LFP data set were assessed a median of 2 months prior to surgery (range 1 day–6 months). This is likely to have, if anything, led to an under-estimation of clinical correlations with CV. Still, other studies demonstrating a correlation between drug-induced change in beta band LFP activity and change in bradykinesia-rigidity have been based on motor examinations that were performed up to a few months before surgery and have shown no difference in the residuals from the correlations between patients examined in this way and those assessed on the same day as electrophysiological recordings (Ray et al. 2008; Kühn et al. 2009). This may be because the changes in UPDRS motor scores over comparable time intervals can be small and insignificant (Olanow et al. 2004).

An interesting aspect of the current study that has thus far not been discussed is the relative focussing of correlations with bradykinesia-rigidity in the beta 2 rather than beta 1 frequency band. This is in accord with the differential reactivities in these two bands under different experimental conditions, including a more pronounced response to treatment with levodopa in the beta 1 than beta 2 range (López-Azcárate et al. 2010; Marceglia et al. 2006; Marceglia et al. 2007; Priori et al. 2004). Of the two bands, STN activity in the beta 2 band is most synchronised with cortical activity (Hirschmann et al. 2011; Litvak et al. 2011) and may therefore have the greater facility to directly disrupt motor function. However, it has also been suggested that it is not so much the precise frequency of synchronisation in the beta band that may be important, but rather how strong synchronisation is (Kühn et al. 2009). For the moment, the relative contributions of beta 1 and beta 2 frequency bands, if any, to motor impairment remain to be clarified.

Where does the temporal variability of beta activity arise? Could it be an emergent property of stochastic noise in the underlying neural networks, or secondary to deterministic processes? Modelling studies have suggested that beta oscillations in basal ganglia networks are at the boundary of synchronous and non-synchronous regimes in Parkinson's disease, and that small fluctuations in intermittent synchrony can be generated just by moderately increased coupling strength in the basal ganglia circuits due to the lack of dopamine (Park et al. 2011). Dopaminergic therapy suppresses tonic levels of beta (Hammond et al. 2007) and it has recently been suggested that the phasic release of endogenous dopamine in response to salient cues in the internal and external environment causes moment-to-moment fluctuations in beta activity in the basal ganglia (Jenkinson & Brown 2011). Smaller CVs might then reflect greater attenuation of reactive dopamine release secondary to greater dopaminergic denervation.

Correlation does not necessarily imply causation and whether the behaviour of neuronal populations in the beta band is causally linked to bradykinesia and rigidity or the relationship between the electrophysiological and clinical state is epiphenomenal remains to be established (Weinberger, William D Hutchison, et al. 2009; Jenkinson & Brown 2011; Timmermann & Florin 2011). Assuming that temporal variability in the degree of synchronisation is causally important, how might this come about? Our data would suggest that it is not simply secondary to increasing levels of background beta synchrony, as the correlation between temporal variability and motor state persisted when we normalised variability by amplitude, and remained significant in a multiple regression model that included amplitude. The implication is that there may be something disadvantageous to basal ganglia function about loss of spontaneous beta reactivity that is relatively independent of the absolute level of beta synchrony. One possibility is that predictive preparation for voluntary action is diminished without phasic modulation of dopamine and beta (Jenkinson & Brown 2011).

Chapter 5. Adaptive deep brain stimulation in advanced Parkinson disease

5.1 Introduction

Deep brain stimulation is an established treatment for severe Parkinson disease (PD), dystonia, and tremor, and has an emerging role in a range of other neurological and neuropsychiatric conditions (Hariz 2012). However, its widespread adoption is at present limited by cost, side effects, and partial efficacy (Little & Brown 2012) In many brain disorders, for example PD, symptoms fluctuate on a moment-by-moment basis depending on factors such as cognitive and motor load and concurrent drug therapy. If it were feasible to track these fluctuations with a suitable feedback signal and stimulate only when necessary, it might be possible to improve therapeutic efficacy while preserving battery life and limiting side effects (Modolo et al. 2011) A recent study in nonhuman primates suggested that adaptively controlled DBS triggered by feedback from the spikes of a single motor cortical neurone was even more effective than standard continuous high-frequency stimulation in a model of PD (Rosin et al. 2011).

In developing adaptive DBS (aDBS) for clinical use, two challenges must be overcome. First, the feedback signal must be robust over time. Second, neurosurgical intervention in the brain should be minimized so as to limit surgical risks, preferably only using a single surgical site. One possible solution to these issues is to record the LFP directly from the stimulating electrode and to use this as the feedback signal to control when stimulation is delivered. Increasing evidence suggests that beta frequency band (13–30Hz) oscillations in the LFP can be consistently picked up in the subthalamic nucleus (STN) of patients with PD and that their level correlates with motor impairment, with and

without treatment (Little & Brown 2012). The LFP recorded in this way is robust over time, and developments in amplifier systems have enabled the recordings of beta oscillations in the LFP while simultaneously delivering high-frequency stimulation, despite the voltages used for the latter being around 1 million times greater than the LFP oscillations (Abosch et al. 2012; Giannicola et al. 2012; Eusebio et al. 2012).

Here we test whether a BCI system that uses the beta activity in the LFP recorded directly from the stimulating electrode in the STN to control when stimulation is delivered can be more energy efficient than and clinically superior to current standard continuous DBS.

5.2 Patients and Methods

We recorded 8 patients (Table 5.1) with advanced idiopathic PD with motor fluctuations and/or dyskinesias who gave their informed consent to take part in the study, which was approved by the National Research Ethics Service Committee South Central–Oxford A. Patients underwent DBS surgery on the STN as previously described (Foltynie & Hariz 2010). In Cases 2, 7, and 8 (see Table 5.1), the locations of the electrodes were confirmed with immediate postoperative fast spin-echo T2-weighted MRI with a Leksell frame still in situ. In the remaining cases, locations were confirmed with immediate postoperative CT with a Leksell or CRW frame (Integra Radionics, Burlington, MA) still in situ. CT scans were then fused with preoperative T2-weighted MRI (O'Gorman et al. 2009). Electrode extension cables were externalized through the scalp to enable recordings prior to connection to a subcutaneous DBS pacemaker, implanted in a second operative procedure up to 7 days later. The permanent quadripolar macroelectrode used was model 3389 (Medtronic Neurologic Division,

Minneapolis, MN), featuring 4 platinum–iridium cylindrical surfaces. Its contacts are numbered 0, 1, 2, and 3, with 0 being the most caudal and contact 3 being the most cranial.

Case	Age, yr	Disease Duration, yr	UPDRS Off	UPDRS On	Site	First Symptom	DBS Indication	Drugs (total daily dose)
1	59	12	42	20	Oxford	Right arm bradykinesia	On/off fluctuations, tremor bradykinesia	L-dopa 900mg, rasagiline 1mg
2	62	10	20	8	UCLH	Left arm bradykinesia/tremor	On/off fluctuations, tremor	L-dopa 1,000mg, trihexyphenidyl 3mg
3	67	7	43	14	Oxford	Right side rigidity/pain	On/off fluctuations, dyskinesias	L-dopa 1,000mg, ropinirole 10mg, amantadine 200mg
4	49	10	42	6	Oxford	Right arm tremor	Tremor	L-dopa 300mg, trihexyphenidyl 2mg
5	49	10	58	23	Kings	Right arm rigidity/pain	On/off fluctuations, tremor	L-dopa 1,100mg
6	63	3	18	8	Oxford	Tremor	Tremor/bradykinesia	L-dopa 800mg
7	67	14	63	24	UCLH	Shoulder pain/stiffness	On/off fluctuations	L-dopa 650mg, pergolide 9mg
8	57	8	43	17	UCLH	Stiffness/tremor	Severe off periods, on/off fluctuations	L-dopa 1,500mg, rotigotine 16mg, rasagiline 1mg, entacapone 1,000mg

DBS = deep brain stimulation; UCLH = University College London Hospitals; UPDRS = United Parkinson's Disease Rating Scale.

Table 5.1 Clinical details of patients in aDBS study

We recorded bipolar LFP activity from contacts 0–2 and 1–3 of the electrodes in the STN after overnight withdrawal of antiparkinsonian medication between operations for electrode placement and pacemaker implantation. LFPs were band-pass filtered between 3 and 37Hz and amplified (×9,100) using a 3-stage common mode rejection amplifier. The system and its validation have previously been described in detail (Eusebio et al. 2011). Recordings from all the STNs exhibited beta activity in the LFP. We determined which contact pair of 0–2 and 1–3 exhibited the greater beta (13–35Hz) amplitude on the side contralateral to the most affected upper limb from recordings made with the patient at rest, unstimulated and off medication. We then determined the frequency of the peak beta

value in the frequency spectrum of the LFP from the selected bipole and filtered the signal around this as specified for each subject in Table 5.2. Next, the voltage for test stimulation was determined using continuous DBS (cDBS) at 130Hz. The contact selected for stimulation was that which lay in between the bipolar contact selected above for recording (e.g., contact 1 or contact 2)(Eusebio et al. 2011). Stimulation was begun at 0.5V and increased by 0.5V increments every 3 to 4 minutes until clinical benefit was seen, without side effects such as paraesthesia. This voltage was then fixed across the subsequent test conditions. Finally, prior to presentation of test blocks, the stimulation trigger threshold that achieved a reduction of stimulation time of approximately 50% while maintaining clinical effect was heuristically determined.

	Online Filter, Range (Hz)	Stim, V	Stim Site	Stim Contact	aDBS, % Time on Stim	Random, % Time on Stim	aDBS, Time between Stim Bursts, s	Random, Time between Stim Bursts, s
Case 1	16–22	2.7	L	1	44.2	44.5	1.09	1.19
Case 2	19–25	1.8	R	1	35.5	34.1	0.64	0.75
Case 3	23–29	1.8	R	2	43.4	42.6	0.47	0.69
Case 4	17–24	1.6	L	2	46.4	46.5	0.45	0.50
Case 5	16–18	2.1	L	1	42.1	45.2	0.94	0.86
Case 6	28–34	2.6	R	1	57.7	45.8	0.73	0.64
Case 7	17–22	2.4	R	2	37.1	40.8	0.64	0.65
Case 8	16–20	2.7	R	1	47.6	46.7	1.75	1.53
Mean	22	2.1			**44.3**	**43.3**	**0.84**	**0.85**
SEM	1.8	0.2			2.4	1.5	0.2	0.1
p						**0.58**		**0.81**

Two-tailed, paired *t* tests showed no difference between time on stimulation in aDBS and random stimulation modes or length of time between stimulation bursts. Stimulation voltage was the same for all stimulation conditions.
aDBS = adaptive deep brain stimulation; L = left; R = right; SEM = standard error of the mean; Stim = stimulation.

Table 5.2 Stimulation details for the 8 patients in aDBS study. Filtered LFPs were rectified and smoothed using a moving average filter of 400-millisecond duration to produce an online value of beta amplitude. The

latter was used to control triggering of stimulation via a user-defined threshold through a portable computer (Fig 5.1). The trigger output was passed via an optically isolated input to the stimulator. The delay between crossing of threshold to stimulation onset was 30 to 40 milliseconds. Stimulation was delivered by a custom-built battery-powered (±9V) stimulator specially constructed for this series of experiments. It used an embedded microprocessor and a digital-to-analogue converter for stimulation control that delivered a biphasic charge balanced symmetrical pulse waveform. The stimulator was extensively tested in vitro, and its design was subject to external review (Dr S. Wang, Suzhou Institute of Biomedical Engineering and Technology, Chinese Academy of Sciences). Stimulation once triggered was sustained until beta amplitude fell below threshold again (Fig 5.2). Stimulation was delivered monopolarly, at 130Hz, with a pulse duration of 100 microseconds and ramped up and down over 250 milliseconds at onset and offset. The 250-millisecond ramping was necessary to avoid paraesthesias induced during the switching on and off of stimulation (see Table 5.2). The stimulator provided a continuous readout of the stimulation voltage, which could then be tracked throughout the experiment. For safety, charge densities were limited to <30μQ/cm2, and DC currents were blocked with a DC-blocking capacitor. The input–output voltage function was linear, and there was no pulse shape distortion when this was tested in vitro (0.5kΩ impedance). All connections to the patient were optically isolated, and the stimulator met the EN60601-1 medical safety standard. Estimates of time on stimulation in the aDBS mode included an additional 250 milliseconds per stimulation block to allow for the linear ramping up and down.

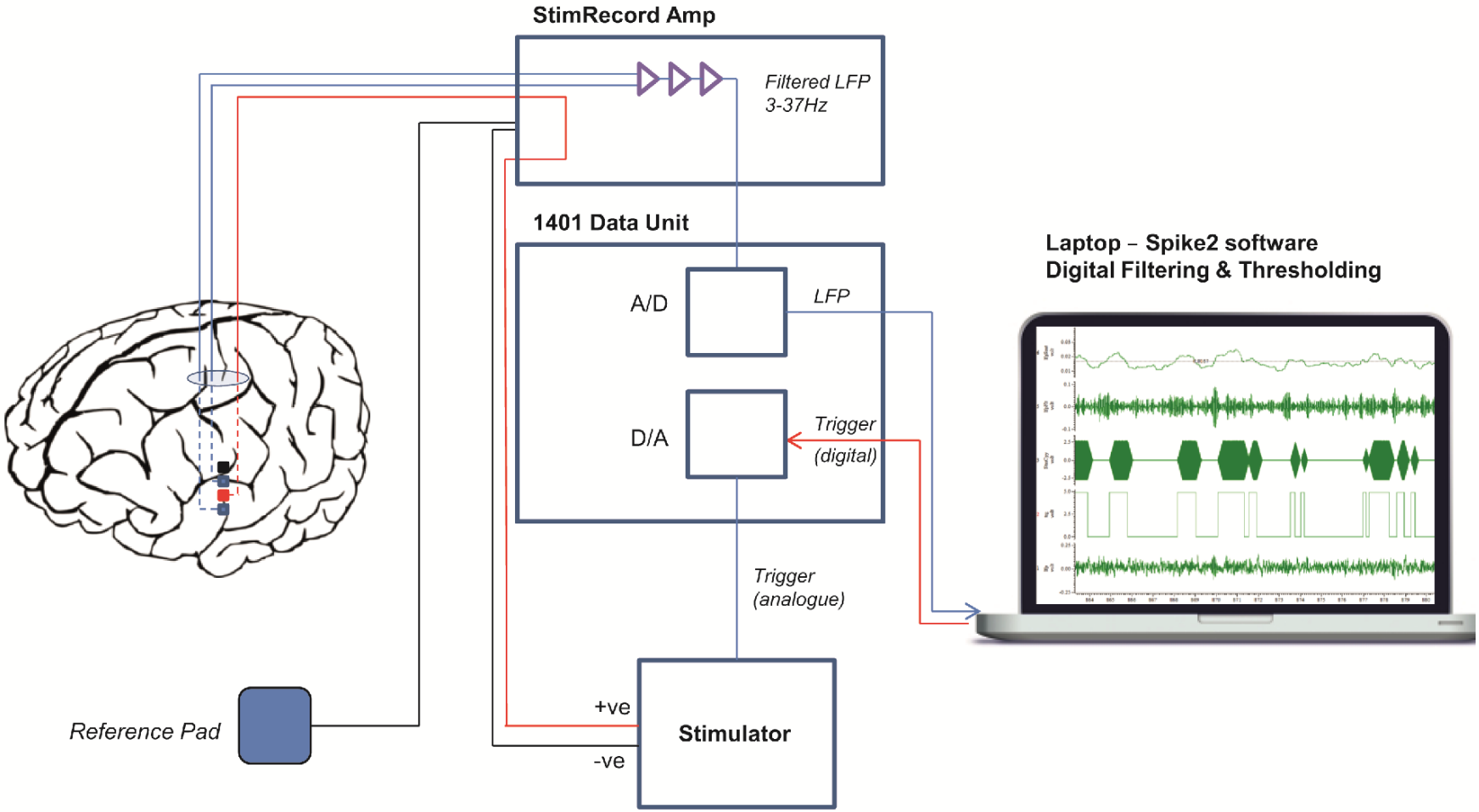
StimRecord Amp
Filtered LFP
3-37Hz
1401 Data Unit
A/D
LFP
D/A
Trigger
(digital)
Trigger
(analogue)
Laptop – Spike2 software
Digital Filtering & Thresholding
Reference Pad
+ve
-ve
Stimulator

Figure 5.1 Experimental setup for adaptive deep brain stimulation in externalized subjects. Bipolar local field potential (LFP) is passed through a custom built StimRecord amplifier that filters (3–37Hz) and amplifies (×9,100). The analogue (A) output is passed to a 1401 data acquisition unit (Cambridge Electronic Design, Cambridge, UK), which converts it to a digital (D) signal that is displayed on a portable computer using Spike2 software (Cambridge Electronic Design, Cambridge, UK). The signal is digitally filtered around the beta peak in real time and converted to beta amplitude by rectifying and smoothing. A threshold is set that triggers stimulation in a monopolar montage between the 2 bipolar recording electrodes when beta power crosses the threshold. Stimulation terminates when beta power drops again below threshold.

Patients were clinically tested off stimulation and with conventional cDBS, aDBS, and random stimulation (random bursts of stimulation not triggered by beta amplitude rise). Experimental conditions were randomized in order across patients, and each condition was performed once. About 5 minutes rest without stimulation was given before each experimental condition. The mean amplitude threshold for triggering stimulation in this mode was 3.9 ± 3.8% above the mean beta amplitude of the LFP and corresponded to a peak-to-peak amplitude of the beta filtered signal of 2.6 ± 0.6μV. Mean ± standard error of the mean of duration of rest, aDBS, cDBS, and random blocks was 629 ± 102 seconds, 640 ± 143 seconds, 507 ± 37 seconds, and 515 ± 32 seconds, respectively. Subjects were clinically assessed at least 300 seconds into each condition. Temperli et al have shown that the change in tremor, rigidity, and bradykinesia following the onset or offset of STN DBS follows an approximately exponential course, with, judging from their published figure, about 50% of the total change achieved after 5 minutes (300 seconds), (Temperli et al. 2003) and others have made similar observations (Lopiano et al. 2003; Blahak et al. 2009). For clinical assessment, we used a subsection of the hemibody motor United Parkinson's Disease Rating Scale (UPDRS; items 20, 22, and 23) for the upper limb contralateral to the side of stimulation. These assessments were also recorded with a digital video recorder and blindly rated by 3 experienced movement disorder specialists who were not part of the clinical or research team, with an inter-rater reliability of 0.52 (Ebel 1951) Although patients were implanted bilaterally, we only evaluated stimulation contralateral to the worse affected hemibody, so as

to limit patient fatigue and due to time constraints in the perioperative period. Total electrical energy delivered per unit of time was calculated assuming an impedance of 0.5kΩ (Blahak et al. 2011; Volkmann et al. 2002) Physiological data were analysed in MATLAB (version 7.10; MathWorks, Natick, MA) using custom-written scripts and wavelet convolution. Statistical analyses were performed in SPSS Statistics 19 (SPSS, Chicago, IL). Clinical data were normally distributed (single-sample Kolmogorov–Smirnov tests $p > 0.05$), and therefore means, standard error of the means, and parametric statistical analyses are presented. Where Mauchly's test of sphericity was significant ($p < 0.05$) in repeated measures analyses of variance (ANOVAs), Greenhouse–Geisser corrections were applied (and degrees of freedom adjusted accordingly).

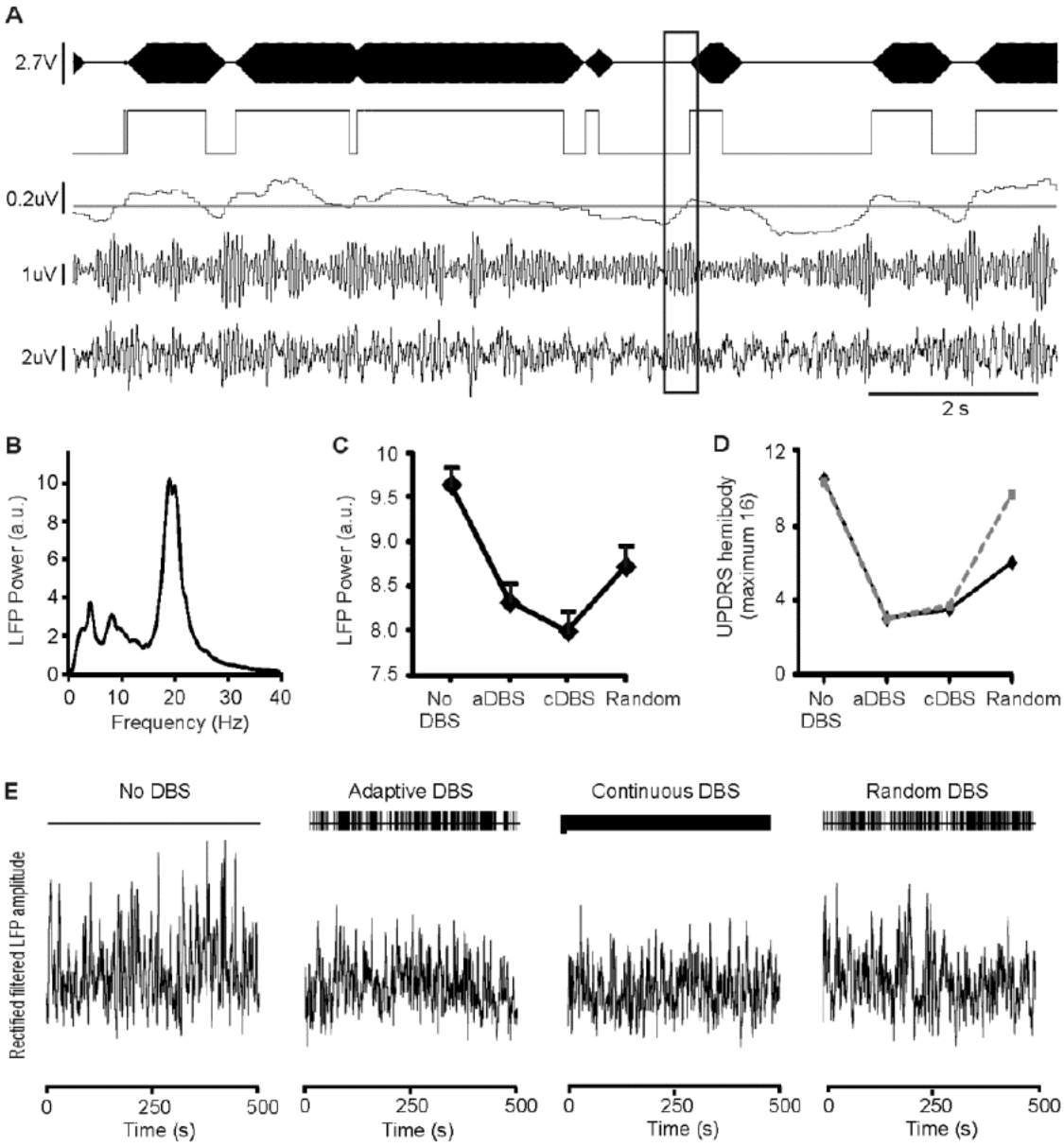

Figure 5.2. Results of aDBS in Case 1. (A) Sample section of adaptive deep brain stimulation (aDBS) recordings. Channels are from bottom to top: analogue filtered local field potential (LFP; bipolar contacts 0 and 2), LFP digitally filtered about the beta peak, running average of rectified, beta filtered, amplitude with triggering threshold superimposed, stimulation trigger signal and stimulation (130Hz, 100μS, monopolar contact 1). Boxed area shows a beta burst. Time for this to cross threshold depends on LFP amplitude at onset of beta burst, but thereafter there was only a 30- to 40-millisecond delay to stimulation onset. Note stimulation is ramped, and can be triggered by bursts of beta that are of variable duration, but often last <1 second (see also Table 5.2). (B) LFP power spectrum without DBS. (C) LFP power changes in different stimulation modes. (D) Motor impairment in different stimulation modes. Solid black and interrupted grey lines are unblinded clinical and blinded video scores, respectively. (E) Sections (500 seconds) of rectified beta-filtered LFP amplitude in each stimulation mode. a.u. = arbitrary units; cDBS = continuous DBS; UPDRS = United Parkinson's Disease Rating Scale.

5.3 Results

5.3.1 Clinical effect

Mean baseline (without stimulation or medication) UPDRS hemibody subscores (bradykinesia, rigidity, tremor) were 5.8 ± 0.8 and 6.3 ± 0.7 in unblinded and blinded postoperative clinical assessments. Repeated measures ANOVA demonstrated a significant main effect of stimulation condition within subjects in both unblinded and blinded assessments ($F_{df\ 1.7,11.9} = 13.7$, $p = 0.001$ and $F_{df\ 3,21} = 10.5$, $p < 0.001$, respectively).

Both aDBS and cDBS improved motor scores (Fig 5.3). The mean reduction in unblinded and blinded UPDRS scores relative to the unstimulated state was 66.2% (unblinded assessment) and 49.7% (blinded assessment) for aDBS. However, the improvement with cDBS was significantly less at 54.3% (paired t test, 2-way, $t_7 = 2.78$, $p = 0.028$) and 30.5% ($t_7 = 3.7$, $p = 0.007$) in unblinded and blinded assessments, respectively. The average improvement in motor scores in the aDBS condition compared to the cDBS condition was 28.7 ± 10.6% ($p = 0.03$) and 27.0 ± 7.8% ($p = 0.005$) in unblinded and blinded assessments, respectively. This effect was maintained if rigidity scores were excluded from the blinded assessments, with a 22 ± 10.6% ($p = 0.04$) improvement in motor scores with aDBS compared to cDBS.

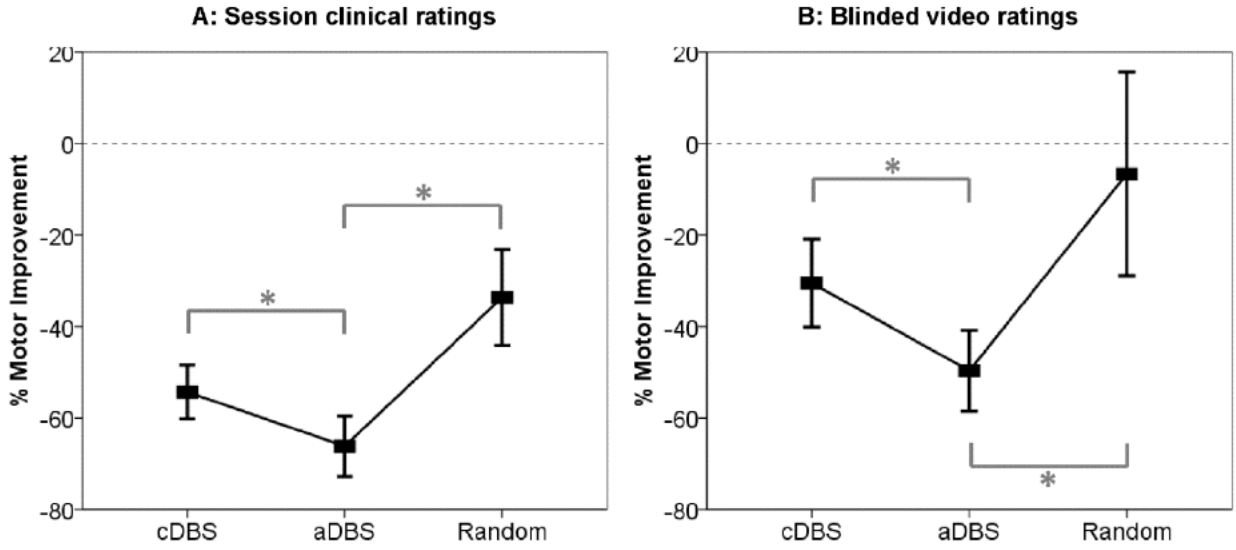

Figure 5.3. Clinical assessments with stimulation. Mean ± standard error of the mean percentage change in hemibody United Parkinson's Disease Rating Scale scores (items 20, 22, and 23) with different stimulation conditions as assessed unblinded during the experimental sessions (A) or from video recordings by blinded experts (B). Asterisks denote significant differences following correction for multiple comparisons by the false discovery rate procedure. All changes were significant from the unstimulated state, with the exception of the blinded score for random stimulation. aDBS = adaptive deep brain stimulation; cDBS = continuous deep brain stimulation.

Random intermittent stimulation lead to a motor score reduction of 33.7% and 6.7% in unblinded and blinded assessments, which was significantly less than the improvement found with aDBS (paired t test, 2-way, unblinded $t7 = 4.2$, $p = 0.004$; blinded $t7 = 2.17$, $p = 0.03$).

5.3.2 Power savings and adaptive effect

The mean total electrical energy delivered with aDBS (132 ± 21μW) was significantly less than that with cDBS (270 ± 37μW; $t7 = 7.4$, $p < 0.0001$), so that the better improvements in clinical score were achieved with less than half the total electrical energy delivered. Similarly, when averaged over the whole block of stimulation, aDBS was only on 44.2 ± 2.4% of the time. This was well matched by random DBS, which was on 43.3% ± 1.5% of the time (paired t test, 2-way $t7 = 0.57$, $p = 0.59$; see Table 5.2). Moreover, time on stimulation tended to progressively drop during stimulation in the

aDBS mode. This was despite the use of a fixed beta threshold, suggesting that beta bursts became less frequent over the course of aDBS. The mean correlation coefficient between percentage stimulation time over each 10 seconds and total duration of DBS up to that point was −0.23 across subjects (2-tailed, 1-sample t test, $t7 = 3.2$, $p = 0.01$). This correlation was also individually significant in 3 of the 8 cases (Pearson test, $p < 0.01$; Fig 5.4).

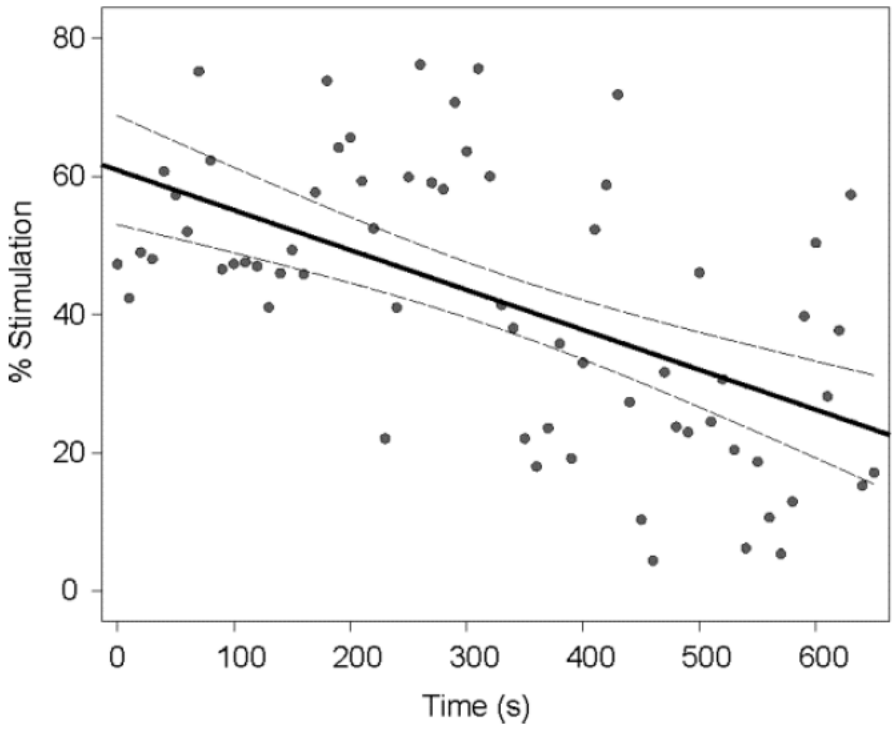

Figure 5.4. Decline in triggered stimulation duration over time. Dependency of proportion of time stimulated (% per 10-second block) on duration of adaptive deep brain stimulation is shown for Subject 5. Solid and interrupted lines are result of linear regression and 95% confidence intervals, respectively. $r = -0.567$, $p < 0.001$.

5.3.3 Beta suppression

The suppression of beta peak amplitude averaged across the duration of a given block type and then averaged across subjects correlated with the mean clinical improvement in those blocks (Pearson test,

$R2 = 0.99$, $p < 0.001$, and $R2 = 0.85$, $p = 0.08$ for blinded and unblinded clinical assessments, respectively).

5.4 Discussion

In this proof-of-principle study, we demonstrate successful BCI-controlled deep brain stimulation in patients with PD. We show that this approach can be about 30% more effective than conventional high-frequency stimulation, despite delivering <50% of the stimulation of current DBS. The latter is of critical importance, as it impacts on both side effects and the lifetime of implanted battery systems.

The scale of our treatment effects is particularly encouraging, as we only tested unilateral stimulation. However, it should be noted that we evaluated only selected motor UPDRS items over stimulation blocks of about 10 minutes. These methodological features stemmed from time constraints related to fatigue in postoperative patients and the non-ambulatory nature of our BCI-controlled control system. Nevertheless, aDBS had beneficial effects on all 3 of the cardinal signs of Parkinsonism: rest tremor, bradykinesia, and rigidity. Moreover, the scale of (contralateral) improvement with cDBS was similar to that previously reported, despite the above limitations related to postoperative assessment. Most studies of the efficacy of chronic continuous bilateral DBS use unblinded clinical assessments off medication and rate improvement as between 28 and 71%, which compares favourably with the 54% improvement seen here with continuous stimulation (Benabid et al. 2009). Relatively few trials have assessed the acute benefit of continuous DBS in the chronically implanted system through the blinded assessment of videos. These report lower treatment effects ranging from between 25.3 and 30%, (Temperli et al. 2003; Lopiano et al. 2003) similar to the 30.5% reduction shown with cDBS

determined through blinded assessment in the current study, although less than the 49.7% reduction found with aDBS (Ford et al. 2004; Castrioto et al. 2011).

The random stimulation mode, in which random intermittent DBS was delivered for similar periods of time as aDBS, served to exclude the possibility that intermittency itself is the key determinate of the efficacy observed with aDBS. This might arise, for example, if the effect of continuous high-frequency stimulation was subject to accommodation. However, the random mode was less than half as efficient as aDBS, implying that intermittent stimulation has to be triggered by beta bursts to have its optimal effect.

Improvements in motor deficits were mirrored by proportionate changes in beta power across the different stimulation conditions. The efficacy of triggering DBS off beta bursts (over and above that of random intermittent stimulation), together with the correlation between treatment effects and beta power reduction, provides further evidence that the oscillatory synchronization indexed by beta activity in the STN LFP is at the very least a faithful biomarker of Parkinsonian impairment, if not causally important (Jenkinson & Brown 2011) An additional interesting observation that needs to be substantiated in further trials is that the proportion of time involving stimulation in the aDBS mode tended to progressively fall as this mode was maintained. Given the constant trigger threshold, this result suggests that aDBS may lead to positive adaptive effects whereby pathological Parkinsonian networks become less prone to produce phasic increases in beta activity. Such an antikindling effect has also been noted in computational studies of desynchronizing brain stimulation, including DBS (Hauptmann & Tass 2006). The presence of adaptive effects further raises the possibility that clinical improvement with aDBS may be even greater when this intervention is sustained for periods longer than those utilized in our study.

Improvements in clinical efficacy were achieved despite significant reductions in power usage, with an overall reduction in stimulation time in the aDBS condition of 56%. This equated to a mean decrease in total electrical energy delivered of 132μW, and energy saving would have been even more marked had we employed higher-stimulation voltages, as energy is proportional to voltage squared. Against this should, however, be offset the additional power requirements of the low-energy circuits necessary to deliver feedback-controlled stimulation and ramping in a clinical system. For a single-channel power classifier, this should be no more than about 10μW, leaving the aDBS mode overall power savings sufficient to double the battery life of the implantable pulse generator in addition to the improvements in clinical efficacy shown (Afshar et al. 2012). Conventional cDBS is associated with an average battery life of <4 years, with replacement usually necessitating general anaesthesia and incurring substantial hardware costs (Bin-Mahfoodh et al. 2003). Therefore, a halving of power consumption would reduce the number of replacement battery operations required, limiting surgical risk and significantly reducing costs of overall treatment. Alternatively, the interval between recharging would double if rechargeable implantable pulse generators are used instead, although these are not suitable for all patients with PD (Timmermann et al. 2013).

The delivery of substantially less stimulation energy with aDBS has an additional implication, not evaluated in the current study. DBS-related side effects critically depend on stimulation parameters, including the energy delivered. Thus, aDBS may be associated with fewer side effects than conventional stimulation, although this remains to be confirmed. In particular, periods of nearly normal functioning will not be compromised by DBS when the delivery of this is controlled by a BCI (Chen, Brücke, et al. 2006). Such periods of normal functioning include those induced by antiparkinsonian medication, which when effective is associated with suppression of beta activity in the

STN (Brown et al. 2001; Priori et al. 2004; Alonso-Frech et al. 2006; Kühn, Kupsch, et al. 2006; Kühn et al. 2009; Ray et al. 2008).

We have demonstrated that it is possible to track an LFP biomarker from the site of stimulation and use this to successfully control stimulation in patients with a continuously fluctuating neurological condition such as PD. Power savings were substantial, and efficacy was found to be superior to standard stimulation. Although not directly tested in this study, it is hoped that the reduced time on stimulation will result in side effects being proportionately reduced once chronic aDBS is possible. Our approach does not complicate the surgical procedure, which still involves implantation of a single brain target. This and other observations suggest chronic aDBS is feasible; beta activity in the LFP is robust over time (Abosch et al. 2012; Giannicola et al. 2012) and reported in a mean of 95% of STN at rest in the off-medication state by 5 groups, (Little & Brown 2012) and of 60% of STN by 1 group (Giannicola et al. 2012; Priori et al. 2004; Giannicola et al. 2013; Rosa et al. 2011). Implantable DBS systems with the capability to deliver feedback-controlled stimulation are already in technical development (Afshar et al. 2012). Thus, our acute study should in time be replicable in a chronic setting.

Several aDBS parameters, including the level of smoothing of beta activity to be applied and the target level of on-stimulation time, remain to be optimized, so that the gains in terms of efficacy and efficiency seen here may be further improved in time. Our threshold crossing of beta amplitude as the stimulation trigger affords a good starting point for algorithmic control, although this may be further improved upon in the future with more sophisticated classifiers based on the use of multiple LFP features to track clinical state. Equally, our intervention, discontinuous but regular stimulation at high frequency, may be bettered in time by stimulation regimes that specifically target pathological rhythms

through phase cancellation or disruption (Brittain et al. 2010). Nevertheless, our simple and tractable system was able to outperform standard continuous stimulation in efficacy and power consumption, potentially offering a major advance in electrical neuromodulation therapy for PD. The same approach may also prove beneficial in other fluctuating movement and neuropsychiatric disorders.

Chapter 6. Bilateral functional connectivity of the basal ganglia in patients with Parkinson's disease and its modulation by dopaminergic treatment

6.1 Introduction

The basal ganglia are comprised of a distributed network of subcortical nuclei with well described anatomical inter-connections and connections to and from the cerebral cortex, thalamus and brainstem (Tepper et al. 2007). These anatomical links are complemented by a flexible functional connectivity characterized in part by oscillatory synchronization (Williams et al. 2002; Litvak et al. 2011). Elucidating the behaviour and structure of such oscillatory activity is important for understanding basal ganglia function and for identifying reliable biomarkers of disease states that could be used to inform treatment.

Recordings from DBS electrodes in patients with PD demonstrate excessive beta oscillations (13-32 Hz) throughout the basal ganglia and have shown that these beta oscillations are suppressed by movement, levodopa and by DBS (Amirnovin et al. 2004; Hammond et al. 2007; Priori et al. 2004; Kühn, Kupsch, et al. 2006). Increases in beta power, recorded from a single site, are indicative of increased spatial-temporal neuronal synchrony in the localised vicinity of the recording electrode. Many reports have highlighted the correlation between local beta synchronization (and its surrogates), and clinical severity across sides, both with respect to the off-levodopa state and to levodopa-induced changes in both synchronization and clinical impairment (Little & Brown 2012). It has also been

found that there is bilateral coherence in the beta range between STNs in the majority of PD patients when studied off medication (De Solages et al. 2010). This demonstrates that synchrony within the beta band is not only present at the local mesoscopic level but also occurs at the macroscopic level, resulting in a widespread distributed beta network. Inter-hemispheric coherence has correspondingly been found at the cortical level in PD and been shown to be suppressed by levodopa administration (Silberstein, Pogosyan, et al. 2005). Whether, the bilateral subcortical beta network is similarly modulated by dopamine is as yet unknown and investigated in this study.

Previous investigations have often considered the beta band as a single functional unit, however there is mounting evidence of dissociable functional characteristics between low beta (13-20Hz; beta 1) and high beta (21-32Hz; beta 2) activities, with regard to movement induced desynchronisation (Priori et al. 2002) and suppression by levodopa (Little, Pogosyan, et al. 2012; López-Azcárate et al. 2010; Marceglia et al. 2006). Studies considering the different beta subbands have thus far only examined local synchrony within a hemisphere and it is therefore unknown whether there is a differential effect of dopamine on interhemispheric subcortical coupling in the low and high beta subbands. This too is investigated in the current study.

Finally, coherence, although a sensitive and well validated method for quantifying functional connectivity between different sites, is partly limited by being a composite measure which conflates both phase and amplitude correlation. A further pertinent question therefore, which we address here, is whether coherence can be deconstructed into independent phase synchronization and amplitude co-modulation, and whether these are similarly affected by dopamine? Addressing this question may help clarify the fundamental mechanisms employed by the brain for long distance connectivity at subcortical levels, and may also have practical implications. Recent work has shown the potential

benefits of using beta oscillations to control the delivery of DBS (Rosin et al. 2011; Little et al. 2013). In PD patients this was achieved with unilateral DBS in which stimulation was delivered in response to beta amplitude threshold crossing. Advancing aDBS towards clinical application however will require a better understanding of how the basal ganglia systems on the two sides interact. Specifically, it remains to be determined how best to trigger bilateral adaptive stimulation and whether this would be optimally achieved by synchronous or asynchronous (independent) stimulation across the two sides. The identification of strong bilateral amplitude co-modulation of subcortical beta activity might encourage trials that involve a simpler, unilateral sensing of beta amplitude that then controls bilaterally synchronous DBS.

In this study we investigate a cohort of PD DBS patients on and off medication and analyse STN LFPs in an attempt to characterize the bilateral subcortical functional connectivity of the basal ganglia in the two beta sub-bands and their response to dopamine. In addition, we aim to deconstruct bilateral coherence into independent amplitude co-modulation and phase synchronization to ascertain which is driving the subcortical beta network and whether these aspects of connectivity have a differential response to dopamine.

6.2 Material and methods

6.2.1 Patients and surgery

We investigated the bilateral connectivity between STNs in a cohort of 23 subjects with PD on and off levodopa. This comprised 10 subjects who were studied in the United Kingdom (UK) and 13 patients who were recorded in Germany. All subjects had advanced idiopathic PD with motor fluctuations

and/or dyskinesias. The average age was 59 ± 1.9 years and the preoperative score on the motor section of the Unified Parkinson's Disease Rating Scale (UPDRS), (Fahn & Elton 1987) was 42 ± 3.1 off medication and 17.3 ± 2.4 on medication. The mean disease duration at the time of surgery was 11.5 ± 0.7 years. The mean equivalent levodopa dosage was 1220 ± 132 mg at the time of surgery. UK patients underwent bilateral DBS surgery on the STN as previously described (Foltynie & Hariz 2010). The German operative procedure was similar (Kühn, Kupsch, et al. 2006). Eighteen of the subjects have been previously reported as part of earlier studies; nine in (Kühn, Kupsch, et al. 2006), two in (Kühn, Doyle, et al. 2006), one in (Doyle et al. 2005) and six in (Anzak et al. 2012).

All subjects gave their informed written consent to take part in the study, which was approved by the National Hospital for Neurology & Neurosurgery and Institute of Neurology Joint Research Ethics Committee, London UK and the ethics Committee of the Charité, University Medicine Berlin.

6.2.2. LFP recordings

All subjects were recorded after overnight withdrawal of antiparkinsonian medication (off state) and following levodopa challenge equivalent to their standard morning medication (on state, minimum dose 100mg) in the post-operative period (days 3-7), prior to battery and stimulator implantation. Improvement with medication was confirmed through assessment of finger tapping, wrist rigidity and tremor (using the corresponding items of the motor UPDRS). Subjects rested in a chair with their eyes open. They were asked to remain quiet and still, and rest was confirmed by visual inspection. Periods of voluntary movement detected by the examiner on visual inspection were noted and excluded from further analysis. However, periods of rest tremor or dyskinesias were not rejected.

In the United Kingdom bilateral STN LFPs were low pass filtered at 1 kHz, sampled with a frequency of 2,048 Hz and recorded in a monopolar configuration (contacts 0-4) through a commercial amplifier

(TMSI Port 1, TMS International B.B., The Netherlands). Subsequently they were converted to 3 bipolar montages by subtraction of the signals from adjacent contacts and high-pass, notch and low-pass filtered at 1 Hz, 49-51 Hz and 100 Hz, respectively.

In Germany LFPs were recorded directly from bipolar pairs of adjacent electrode contacts bilaterally. Data were amplified and filtered at 1–250 Hz using a custom-made, high impedance amplifier (which had as its front end input stage the INA128 instrumentation amplifier, Texas Instruments Incorporated 12500 TI Boulevard Dallas Texas, USA) and recorded through a 1401 A-D converter (Cambridge Electronic Design) onto a computer using Spike2 software (Cambridge Electronic Design). Signals were sampled at ≥625 Hz. Given the differences in recording techniques we only contrasted normalised measures (percentage total power, coherence and correlation) and not absolute power levels in later analysis.

The first 74s (minimum recording length across subjects) was taken from each recording, separately off and on levodopa, to allow for comparison of coherence within and between subjects.

6.2.3 Data analysis and statistics

Bipolar LFP time series were imported into Matlab (version 7.10) and analysed with custom written scripts evoking functions from the Matlab signal processing toolbox. Power spectral analysis was calculated using an average periodogram method with a 1s Hamming window and 50% overlap yielding a frequency resolution of 1Hz. Low frequencies (<4Hz) were ignored due to possible contamination by movement artefacts such as those due to dyskinesias. Power was normalized as the percentage total power between 5 and 90 Hz (excluding a 49-51 Hz band contaminated by European line noise) prior to visualization and further analysis. The power spectra of all six bilateral bipolar channels were analysed for peaks in the beta range (13-32 Hz, function - 'findpeaks.mat' - returns local

maxima, defined as a bin which is larger than its two neighbours, with a set minimum inter peak distance of 4 Hz). For the power spectral analysis and beta peak count, the presence and position of the beta peak was then confirmed by visual inspection of the power spectral density function. The bipolar channel on each side with the highest amplitude beta peak was used for further analysis, in line with evidence that beta activity is focused in the STN, especially in its dorsolateral 'motor' portion (Chen, Pogosyan, et al. 2006; Yoshida et al. 2010). The beta band was subdivided into low (13-20 Hz; beta 1) and high (21-32 Hz; beta 2) ranges for further analysis (Priori et al. 2002; Little, Pogosyan, et al. 2012; Hirschmann et al. 2011). Co-modulation of STN activities across the hemispheres in the gamma band is the subject of another study.

6.2.4 Coherence

The squared coherence of the bilateral signal pairs was determined using a mean squared average periodogram method (1 s Hanning window, 0% overlap) which again yielded a 1 Hz frequency resolution. The theoretical upper limit of the 95% confidence interval (CI) for the coherence was defined as $1-p^{1/(N-1)}$ where p = 0.05 and N was equal to the number of windows in the periodogram (Halliday et al. 1995). By itself, this method does not compensate for multiple comparisons across different frequencies. Accordingly, we defined a significant elevation / peak as one that exceeded the 95% confidence limit over at least two consecutive frequency bins. As our frequency range of interest was the beta band (20 points, 13-32 Hz), this restricted the family wise rate to 0.05 (Type 1 error p = probability of obtaining two adjacent points in the beta band greater than 95% CIs by chance = (0.05^2)*20 = 0.05). We also confirmed that this approach was conservative by demonstrating that the 95 % CI derived above exceeded those derived from a surrogate dataset using a previously described method (De Solages et al. 2010). For this second method the phase components of the two signals

were randomly phase shuffled in the frequency domain before using the inverse Fourier transform to recreate 1000 surrogate pairs of time series that were then analysed to determine the empirical sampling distribution of the coherence. Statistical significance was assessed in each frequency bin by comparing the actual coherence with the 100(1-p) percentile from the sampling distribution, where p = 0.05.

6.2.5 Amplitude Co-modulation

The amplitude envelope of the signal was assessed for all frequencies by taking the modulus of the pass-band filtered and Hilbert transformed signal. Pass-band filtering was performed in both the forward and reverse directions, to achieve zero phase distortion, using a fourth order Butterworth filter with a pass-band of 1 Hz. Co-modulation of amplitude was determined by dividing the amplitude envelope into windows and averaging the amplitude within each window. The co-modulation index was defined as the Pearson's correlation coefficient of the averaged windowed amplitude series from the two STNs. This was repeated for all frequencies within the beta range. We tested windows of 0.5, 1, 5 and 15 s duration and found no significant difference between correlations. Only data for 1 s windows are presented. We determined whether the co-modulation index was different to that expected by chance by comparison with a surrogate dataset. The sampling distribution for the amplitude co-modulation was determined by calculating the correlation coefficient at each frequency between the windowed averaged amplitudes for 1000 pairs of time shuffled pairs of time series. Statistical significance was assessed in each frequency bin by comparing amplitude co-modulation with the sampling distribution of surrogate data, as above.

6.2.6 Phase locking

Phase information was extracted following passband filtering and Hilbert transformation of both time series at all frequencies (Fig. 6.1). Phase synchronization was calculated according to the phase locking value (PLV) method, also known as the mean phase coherence or synchrony factor, which is a measure of how the relative phase is distributed over the unit circle (Lachaux et al. 1999; Pereda et al. 2005). The phase difference of the two unwrapped phase signals was computed and the modulus (2 π) taken to create a time series of phase differences at all points in time on the unit circle. The phase difference vectors at all points in time were then averaged and the length of the average vector (between 0 and 1) was taken as the measure of phase synchronization. This was repeated for all frequency pairs:

$$\gamma_{n,m} = \sqrt{\left| \left\langle e^{i\varphi_{n,m}(t)} \right\rangle \right|} = \sqrt{\left\langle \cos \varphi_{n,m}(t) \right\rangle^2 + \left\langle \sin \varphi_{n,m}(t) \right\rangle^2}$$

Equation 6.1. Phase locking value (PLV). $\phi_{n,m}(t)$ represent the relative phase difference at all points in time, *t* for the two signals n and m.

The statistical significance of this phase locking value (PLV) was again estimated using a surrogate dataset. The sampling distribution of the PLV was determined by randomly shuffling the time points of the two signals and calculating the PLV between these two time-shuffled series. This was repeated 1000 times and the 95% CI for the PLV determined as above. Note that frequency co-modulation across the two STN was not studied here, as it does not directly relate to coherence.

Statistical analyses were performed using SPSS version 19 (SPSS Inc., Chicago, IL, USA) and Matlab (version7.10) statistics toolbox. Data were normally distributed or transformed so that they became normally distributed (see results for relevant transforms; single sample Kolmogorov-Smirnov tests $p > 0.05$, following False Discovery Rate (FDR) correction for multiple comparisons) (Curran-Everett

2000). Means, standard error of the means and parametric statistical analyses (including Pearson's correlation) are presented. Repeated measures two factor ANOVAs were tested and post-hoc tests presented as significant if they survived FDR correction for multiple comparisons.

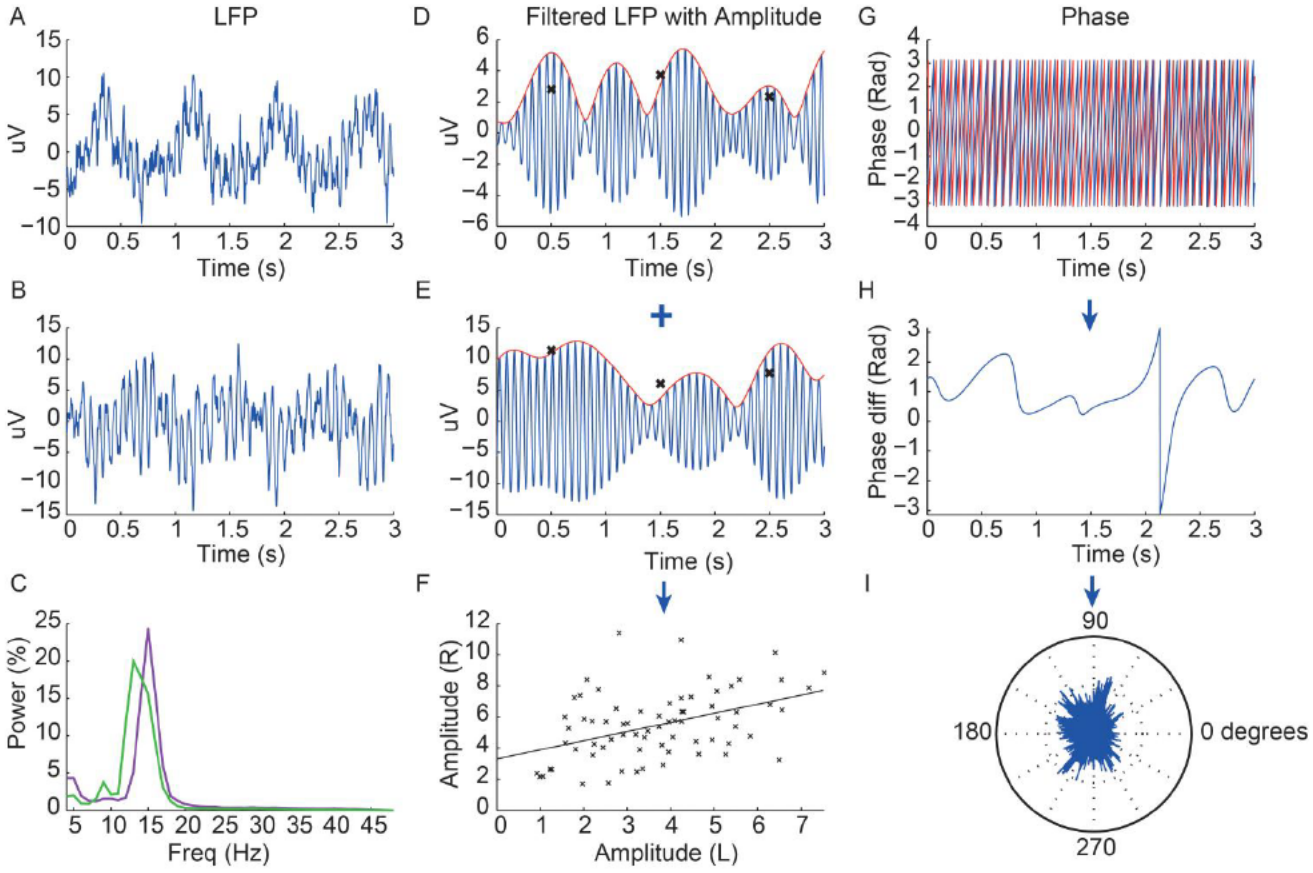

Figure 6.1. Data from one subject off levodopa showing LFPs with extracted amplitude and phase. The first column shows 3s of unfiltered bipolar LFPs from the two STN (A= left STN, B= right STN) and their respective power spectra (C; left STN - purple, right STN - green). The second column shows the LFP pass-band filtered around the corresponding beta peak (blue) of each STN (D= left STN, E= right STN) with the amplitude shown in red. The crosses show the average amplitude for each 1 second window and the final graph shows the correlation of these 1s average amplitudes across the two sides over 74 s duration record, with a linear regression line through them (F). The r value of this linear regression line is taken as the value of the amplitude co-modulation for any given subject. In this example $r = 0.57$, $p < 0.001$. The right column shows the superimposed phase of the two LFP signals (red = left STN and blue = right STN) over 3s (G) with the phase difference over this period shown below (H). A rose plot underneath shows the proportion of phase difference vectors at all points for the whole recording around the unit circle (I). The length of the average of these vectors is then taken as the value of the phase locking value (PLV), which in this case was 0.22. Note low frequency oscillations at about 1 Hz likely to be cardiac pulse artefact in A and B. Despite this, modulations in the amplitude envelopes of the beta band filtered LFP activity shown in D and E are not time-locked to the low frequency cardiac pulse artefacts in 1A and B.

6.3 Results

6.3.1 Power spectra

Group data for patients on and off medication are presented in Fig 6.2. Power spectra demonstrated beta peaks off medication on both sides in 22 subjects and on one side only in one subject. The mean beta peak frequency was 22 ± 0.84 standard of the mean (SEM) Hz. Log transformed power was analysed by repeated measures two factor ANOVA (factors beta sub-band and levodopa) and demonstrated a main effect of levodopa ($F_{(df\ 1,22)}$=17.5, p<0.001), but no effect of frequency band ($F_{(df\ 1,22)}$=2.3, p=0.14). There was a significant interaction between frequency and levodopa ($F_{(df\ 1,22)}$=4.6, p=0.044). Post hoc analysis (two tailed paired t tests) revealed a reduction in beta 1 power after levodopa (t_{22}=-4.4, p<0.001) but no significant change in beta 2 (t_{22}=-1.5, p=0.4). The beta peak frequencies across the two sides were strongly correlated (r = 0.70, p<0.001).

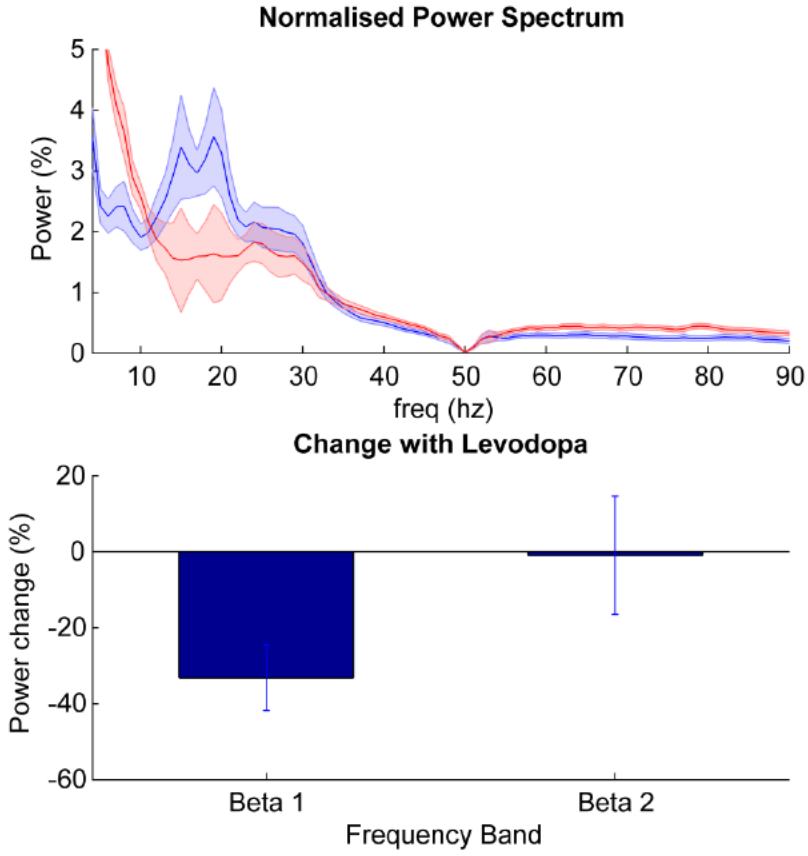

Figure 6.2. Spectral power changes in the STN with levodopa. Top panel shows mean ± SEM power spectral density of all 23 subjects in the off (blue) and on (red) medication state. Bottom panel shows the mean ± SEM % change between the two states (on – off medication) in the beta sub-bands. Only the power suppression in the beta 1 band following levodopa was significant (t_{22}=-4.4, p<0.001).

6.3.2 Coherence

Group data for patients on and off medication are presented in Fig 6.3. There was significant coherence between the STN sides in the beta range in 19 out of the 23 subjects in the off medication state. The mean frequency of the coherence peak was 20.6 ± 1.3 Hz, with a mean maximum coherence of 0.15 ± 0.02 across the whole beta band. On levodopa the number of subjects with significant bilateral coherence dropped to 15 (mean frequency of coherence peak 23.3 ± 1.2 Hz and mean

maximum coherence 0.11 ± 0.02 across the whole beta band). Differences in Fisher transformed coherence averaged across beta sub-bands were analysed with repeated measures two factor ANOVA (factors beta sub-band and levodopa) and demonstrated a main effect of levodopa ($F_{(df\ 1,22)}$=4.5, p<0.046) but no significant effect of frequency ($F_{(df\ 1,22)}$=3.0, p=0.10). There was an interaction between levodopa state and frequency ($F_{(df\ 1,22)}$=5.7, p=0.026). Post hoc tests confirmed a significant reduction in beta 1 coherence with levodopa (t_{22} = -2.7; p=0.01), but no change in beta 2 coherence (t_{22}=-0.4; p=0.69).

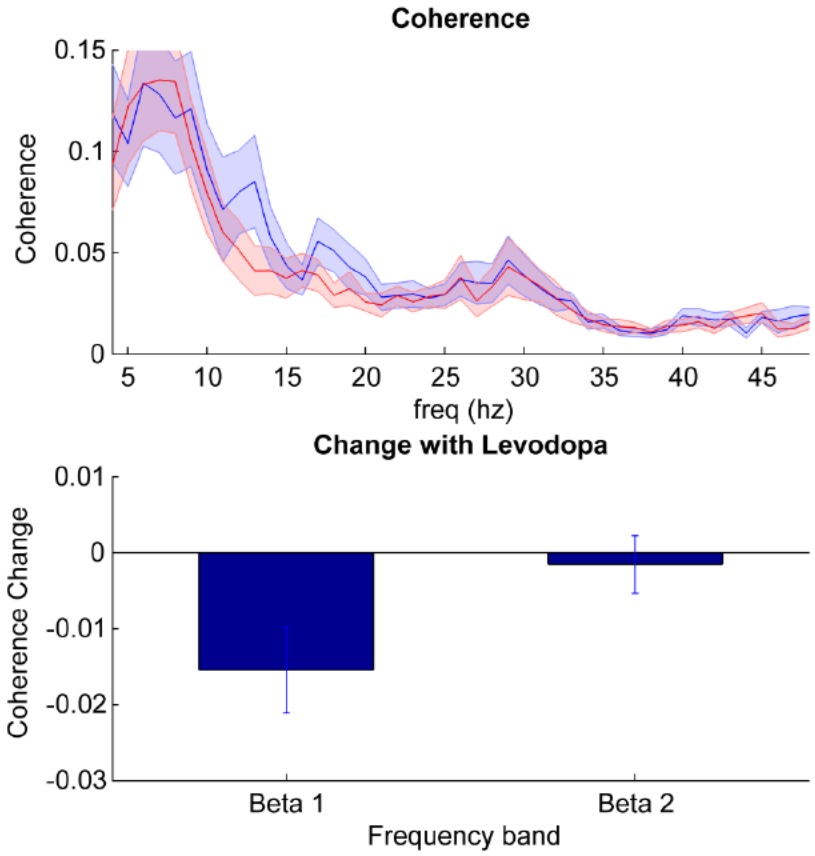

Fig 6.3. Coherence change between STNs. Top panel shows mean ± SEM coherence of all 23 subjects in the off (blue) and on (red) medication state. Bottom panel shows the mean ± SEM % change between the two states (on –off medication) in the beta sub-bands. Only the coherence suppression in the beta 1 band following levodopa was significant (t22 = -2.7; p=0.01).

6.3.3 Amplitude Co-modulation

Group data for patients on and off medication are presented in Fig 6.4. The correlation between the fluctuations in the amplitude envelopes in the beta range on the two sides was calculated independent of phase and compared against a surrogate dataset using the same window (1s) as for the coherence analysis. We found that off medication 17 subjects showed a significant positive beta amplitude co-modulation peak with an average r value of 0.40 ± 0.03 and mean peak frequency of 21.7 ± 1.3 Hz across the whole beta band. This reduced to 10 subjects on medication with an average peak r of 0.34 ± 0.02 and mean peak frequency of 22.1 ± 1.2 Hz. Group analysis of Fisher transformed correlation coefficients with repeated measures ANOVA (factors beta sub-band and levodopa) did not demonstrate a main effect of either levodopa ($F_{(df\ 1,22)}$=3.0, p=0.10) or frequency ($F_{(df\ 1,22)}$=1.5, p=0.23), nor any interaction between levodopa and frequency ($F_{(df\ 1,22)}$=0.04, p=0.84).

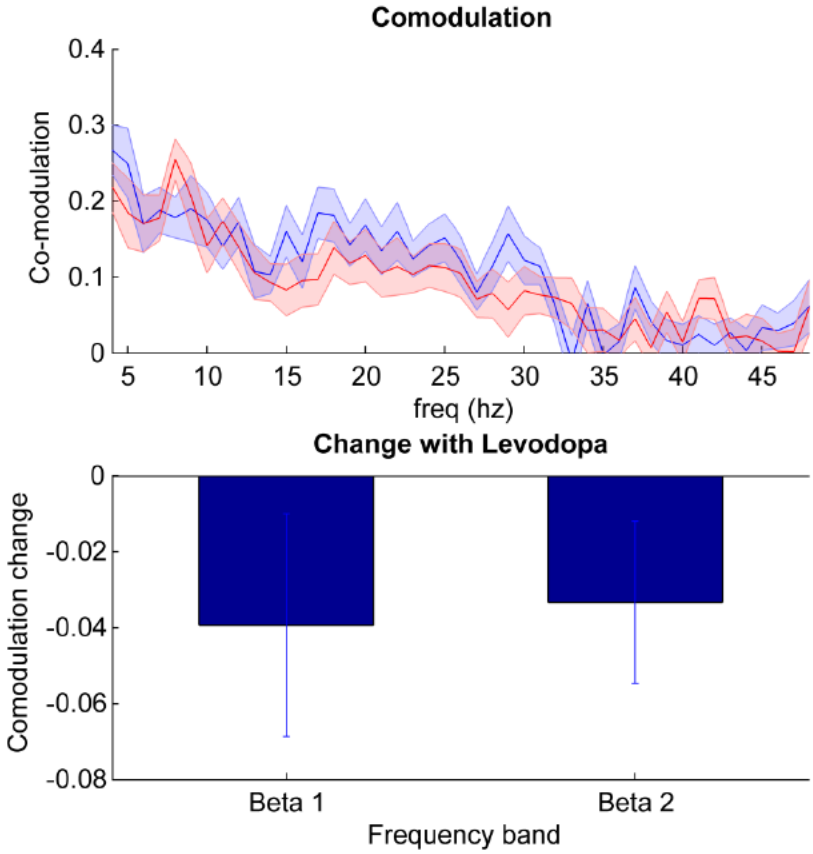

Fig 6.4. Amplitude co-modulation between STNs. Top panel shows mean ± SEM amplitude co-modulation of all 23 subjects in the off (blue) and on (red) medication state. Bottom panel shows the mean ± SEM % change between the two states (on – off medication) in the beta sub-bands. There was no significant effect of levodopa, frequency band or interaction between the two (see results).

6.3.4 Phase Locking Value

Pure phase synchronization, independent of amplitude co-modulation, was assessed using the phase locking value (PLV) in the beta range (Fig 6.5). This revealed significant phase locking in 16 subjects off medication, with a mean peak PLV of 0.29 ± 0.02 and mean peak frequency of 21.4 ± 1.4 Hz across the whole beta band off medication. This reduced to 12 subjects and to a PLV of 0.26 ± 0.15 following levodopa (mean peak frequency of 24.9 ± 1.4 Hz). A repeated measures ANOVA of PLV

(factors beta sub-band and levodopa) revealed a borderline main effect of frequency ($F_{(df\ 1,22)}$=4.3, p=0.051) and an interaction between levodopa and frequency ($F_{(df\ 1,22)}$=7.3, p=0.01). There was no main effect of levodopa ($F_{(df\ 1,22)}$=1.8, p=0.20). Post hoc testing demonstrated a reduction of phase locking with medication in the beta 1 range (t_{22}=-2.8, p=0.01) but no effect in beta 2 (t_{22}=0.8, p=0.41). Rayleigh's test confirmed a non-uniform distribution of phase differences between STN beta oscillations around the unit circle (p<0.001) and a histogram of phase differences demonstrated a peak centred around zero phase lag (Fig. 6.6). The mean phase lag (-0.026 rad / -14^0) was found to be not significantly different from zero (one sample circular t-test, n=23, p=0.21).

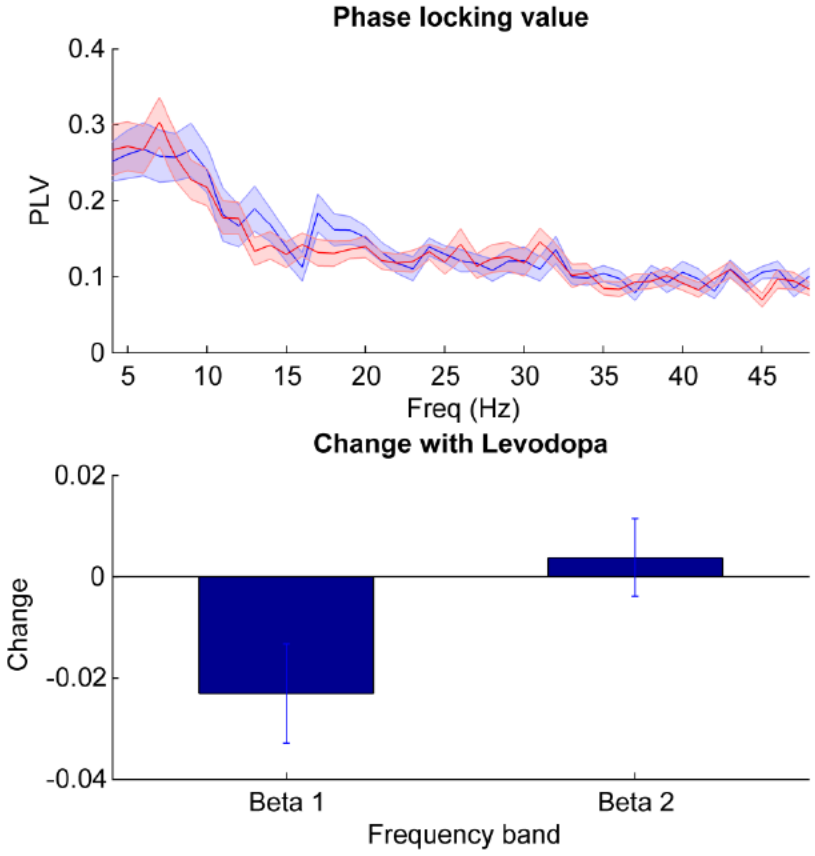

Fig 6.5 Phase synchronisation between STNs. Top panel shows mean ± SEM amplitude PLV of all 23 subjects in the off (blue) and on (red) medication state. Bottom panel shows the mean ± SEM % change in PLV between the two states (on – off medication) in the beta sub-bands. Only the beta 1 band PLV was suppressed following levodopa (t_{22}=-2.8, p=0.01).

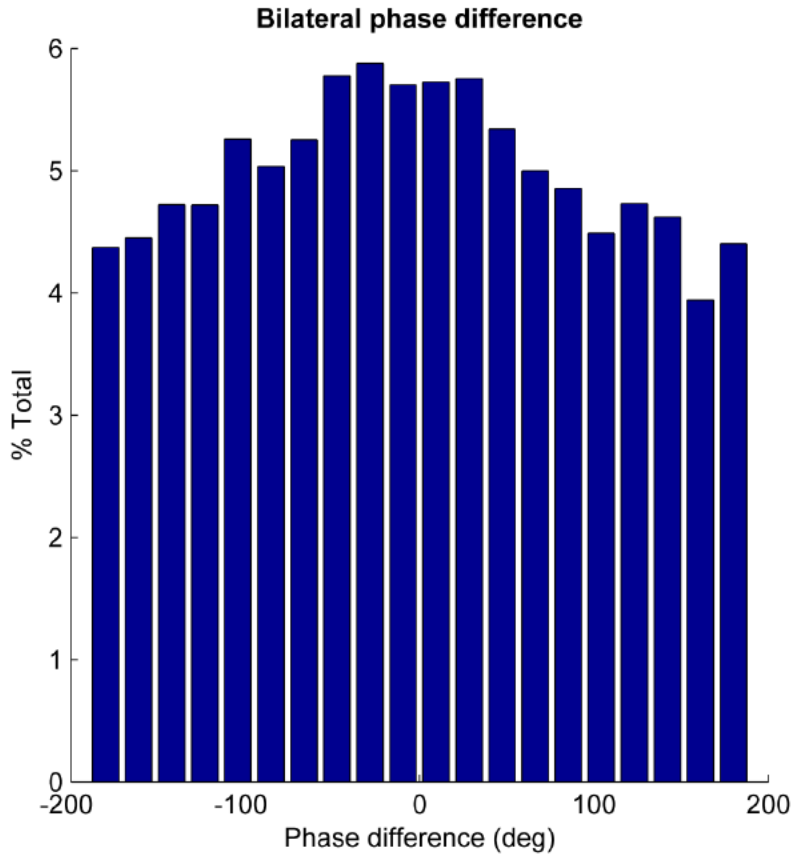

Fig 6.6 Histogram of beta phase differences between bilateral STN. Histogram of all phase differences across 23 subjects at peak beta frequency off medication, demonstrating predominance of zero phase lag.

6.4 Discussion

In this study we investigated the bilateral functional connectivity of the subthalamic nuclei on and off levodopa in a cohort of patients with PD. We confirmed the previously described subthalamic beta range coherence between the left and right STNs in the off medication state (De Solages et al. 2010), and further demonstrated an acute and relatively selective suppression of phase locking in the lower beta range in response to levodopa. This suppression mirrored the effect of levodopa on local power in

the STN in this sub-band. Although amplitude co-modulation of beta was present between the two sides, this was not significantly affected by levodopa in either the lower or upper beta range.

A distributed cortical beta network has been shown previously to be present in Parkinson's disease, to be modulated by dopamine and to correlate with disease severity (Silberstein, Pogosyan, et al. 2005). This study is the first to examine the beta network subcortically in response to dopamine. Our data parallel that found at the cortex and therefore extends the concept of distributed, dopamine responsive, beta synchronisation to subcortical structures. Widespread beta synchronisation could represent a purely pathological response to dopamine withdrawal. However, it should be noted that despite a robust reduction in beta 1 coherence at the group level in response to levodopa, there still remained statistically significant residual beta coherence peaks in the majority of subjects. Although this could be explained by an insufficient levodopa dosage in some patients it also raises the possibility that widespread beta connectivity is not simply pathological but plays a physiological role, at least at lower levels of coherence.

From coherence alone it is difficult to deduce the exact physiological mechanism of connectivity and, specifically, whether coupling takes the form of amplitude co-modulation and/or phase synchronization. Both have been suggested as providing potential coding schemes (Friston 2000). Phase synchronization, in particular, leads to coordinated neuronal firing and the synchronous arrival of multiple excitatory post-synaptic potentials (EPSPs) onto target neurons. Given the short half-life of EPSPs this temporal summation promotes efficient information transfer from one population to the next (Brittain & Brown 2013; Buehlmann & Deco 2010). However, when exaggerated as in PD, phase synchronisation potentially leads to a loss of information coding space or entropy (Hanslmayr et al. 2012). Although it remains to be proven whether amplitude co-modulation is exaggerated in PD, this

form of interaction may also have physiological bounds, and when pronounced across mesoscopic signals like the LFP may necessarily entail attenuation of time varying amplitude modulation on finer spatial scales. Here, we provide evidence that interactions in the beta band occur within a distributed bilateral network, as well as at the local basal ganglia level (Pogosyan et al. 2010). Only that cross-hemispheric interaction expressed through phase synchronization (and, secondarily to this, through coherence) was significantly attenuated by dopaminergic input, and even then, only in the low beta range. Amplitude co-modulation in the same frequency band was relatively unaffected by acute dopaminergic therapy. Dopamine may therefore primarily modulate functional connectivity between the STN on the two sides through changes in the co-ordination of phase between sites. This ability of dopamine to acutely change functional connectivity with a time-course that excludes structural change has previously been noted in ipsilateral basal ganglia-cortical circuits, both empirically and in modelling studies (Cassidy et al. 2002; Litvak et al. 2012; Marreiros et al. 2013).

This study is consistent with a growing body of evidence that demonstrates a functional dissociation between low and high beta range activities, highlighted by their differential sensitivity to dopaminergic therapy (Priori et al. 2002; Little, Pogosyan, et al. 2012) and the preferential coherence between the STN and cortex in the upper beta range (Litvak et al. 2011; Hirschmann et al. 2011). Here we extend those studies which examined local synchrony as found in the single site LFP recordings and show that distributed bilateral coherence is characterized by a fixed, dopamine unresponsive peak in the high beta range and a second dopamine reactive frequency band in the low beta range.

The anatomical pathways sub-serving the functional connectivity between the STNs are currently unclear as there is no known direct anatomical inter-hemispheric connection between these nuclei in the primate (Carpenter & Strominger 1967; Carpenter et al. 1981). Although limited activity in the

contralateral STN can be evoked at very short-latency by stimulation of the ipsilateral nucleus, possibly through stimulation of fibres of passage (Brun et al. 2012; Walker et al. 2011), the bulk of modulatory effects of stimulation of one STN upon the other are of much longer latency than the temporal difference between STNs reported here, and are compatible with indirect communication between the two STNs (Brun et al. 2012). Potentially, the bilateral coherence shown here and elsewhere (De Solages et al. 2010) could also be mediated by indirect poly-synaptic pathways, although the centring of phase lags between the STN near zero places an upper limit on the delays involved in such indirect connectivity. Alternatively the two STN could be synchronized through common input to both from one or more additional structures. One candidate common input might be cerebral cortical activity in the beta frequency band, given that this is coherent with and leads that in STN and so may plausibly drive subcortical oscillations in the beta range (Williams et al. 2002; Litvak et al. 2011; Fogelson et al. 2006). Contralateral cortico-striatal connections have been identified and these, through the indirect pathway, could provide the anatomical underpinning for this common beta input (Nambu et al. 1996; Takada et al. 1998). An alternative might be bilateral projections in the hyperdirect pathway, although these are as yet unconfirmed in the human. However, as previously noted, coherence between the cortex and STN preferentially occurs in the upper beta range (Litvak et al. 2011; Hirschmann et al. 2011), so that a common input from cortex may not necessarily explain the coupling between the two STN at lower beta frequencies.

With the advent of aDBS, the question of whether basal ganglia on the two sides act as a separate or a single functional network is important from a translational perspective. Given recent work showing efficacious aDBS triggered off beta amplitude in PD patients (Little et al. 2013) it is necessary to know whether any coupling of amplitude across the two sides is sufficient to control bilateral aDBS from ipsilateral recordings. We find that, although statistically significant, the peak level of co–modulation

was low and therefore unilateral monitoring would not be appropriate for bilateral triggering of stimulation off individual beta bursts (Little et al. 2013).

This study is the first to demonstrate the effect of levodopa on subcortical beta functional connectivity in PD with levodopa suppressing coherence in the low beta band. We show that this beta connectivity is driven by both significant amplitude co-modulation and phase synchronisation but that it is the phase effects that are predominantly modulated by dopamine. Bilateral coherence is also characterized by a functional dissociation of the high and low beta sub-bands in response to levodopa with a fixed unreactive peak in the high beta range and a dopamine responsive frequency region in the low beta range. Coupling, although robustly significant, was in absolute terms relatively weak and thus with respect to progressing aDBS from unilateral to bilateral stimulation, the two basal ganglia networks may have to be approached separately with independent sensing and stimulation.

Chapter 7. Discussion

The core aim for this thesis was to explore and test the implementation of adaptive deep brain stimulation in subjects with PD. Towards this aim, I commenced with a review of the range and scope of potential biomarkers that could be used to inform an adaptive, responsive closed loop system in PD. This review emphasised the strength of population based neurophysiological metrics such as the LFP which combine excellent temporal precision in addition to long term stability. The association between LFP based measures of neuronal synchronisation, as reflected in spectral power, and clinical state was highlighted, with specific emphasis on the correlation between beta oscillations and Parkinsonism. The question of whether oscillations, as manifest in metrics such as beta power, are causally important or merely epiphenomena was then investigated with a study which augmented beta oscillations through low frequency DBS. This showed a significant reinforcement of rigidity with low frequency stimulation, further suggesting that beta likely has a causal role in the generation of PD symptoms and signs. The relationship between change in beta and change in clinical state with treatment is now well established; however the data correlating beta power at rest across subjects with symptoms of PD is conflicting. Therefore, an exploration of a new biomarker of PD, namely the temporal variability of beta amplitude, was then studied and shown to correlate across subjects both at rest and in response to treatment with levodopa. Beta oscillations were then utilised as a biomarker of clinical state in PD for a study of adaptive deep brain stimulation in the post-operative period. This study, the first to implement aDBS in patients with PD, showed a reduction in time on stimulation, improved clinical outcome compared to standard stimulation and suppression of beta oscillations in proportion with motor improvement. Finally, an exploration of the bilateral subcortical beta network was presented which demonstrated that although there is statistically significant functional connectivity between the two STN in the majority of subjects, the absolute levels are relatively low which implies a need for

bilateral sensing and triggering in bilateral closed loop aDBS. The successful implementation of aDBS in PD has implications both for our understanding of the mechanisms of basal ganglia function and for the future treatment of patients with PD.

7.1 Basal ganglia function

Albin and DeLong's elegant and now classical model of the basal ganglia appeared to explain many of the clinical manifestations of movement disorders, including PD, through imbalance between the direct and indirect pathways (Albin et al. 1989). However, as discussed in the introduction, it fails to align well with modern data on discharge firing rates and paradoxical outcomes from DBS stimulation of sites such as the GPi (Basso et al. 2008). Additionally, the anatomical inter-connections are clearly more complex than originally conceived (Nambu et al. 2002). A subsequent modification of the standard model of basal ganglia function therefore incorporated the hyperdirect pathway and other neurophysiological data and is described as the *centre-surround model* (Mink 1996). In this model, the striatum acts to provide highly focal inhibition of the output nuclei of the basal ganglia in contradistinction to the STN which delivers widespread facilitation. The outcome of this schema is that "wanted" movements are disinhibited and released whereas "unwanted" movements are supressed in a centre-surround fashion, thereby giving the basal ganglia a central role in action selection. This model has broader explanatory power than the earlier Albin and DeLong model in that it explained a wider range of motor disorders including dystonia and tics but also gives some insight into normal physiological movements. Like the earlier model, its coding scheme is purely rate based and it makes no allowances for changes in firing pattern. However, physiological studies have not confirmed the expected negative correlation in firing rates in pallidal neurons engaged in competing actions that is predicted under the model (Bar-Gad et al. 2003).

There is now compelling evidence that disorders of movement and in particular PD are characterised by changes in neuronal firing pattern in addition to changes in firing rate (Bergman et al. 1994; Brittain & Brown 2013). The development of models of the basal ganglia that incorporate the importance of temporal patterning of firing across wide networks in addition to the effect of learning has begun, but is likely to evolve as more data on the effect of synchronisation at the individual neuron and population levels becomes available (Israel & Bergman 2008). The work presented here on beta oscillations and their application to aDBS may therefore inform on the role of synchronisation in the basal ganglia both in health and disease.

7.2 The functional role of beta oscillations in Parkinson's disease

Early classic accounts of the basal ganglia therefore highlighted the role of anatomy and rate coding in the functioning of the motor system. This understanding however, has now been complimented by an appreciation of dynamic, flexible, spatially diffuse population based network activity characterised by synchronisation amongst different neuronal groups. This synchronisation can be captured as oscillations in population based measures such as the LFP and deconstructed using mathematical techniques like Fourier analysis or wavelet convolution to uncover frequency specific components.

Oscillations in the beta frequency range, centred around 20 Hz, were discovered 75 years ago and are ubiquitous throughout the cortical – basal ganglia circuitry in Parkinson's disease (PD) (Jasper and Andrews 1938). A wealth of experimental data demonstrate selective beta modulation in response to movement and treatment with levodopa at multiple levels of the motor circuit and yet the function of beta activity remains elusive (Brittain & Brown 2013). Indeed, the mapping of a single cohesive, conceptually simple, function to beta may be an over-simplification given the multi-frequency

responses found in many circumstances and the complexities encountered in ascribing psychological concepts directly onto brain functions (Bennett & Hacker 2003). Nevertheless, a coherent conceptual understanding of beta and oscillations more generally is emerging both in health and disease and relates to a role in controlling information flow and encoding space across networks.

7.2.1 Physiological role of beta

EEGs and LFPs mainly represent the temporal-spatial summation of post synaptic potentials from the local neuronal population surrounding an electrode (Buzsáki et al. 2012). Beta oscillations therefore are the product of synchronisation across neurons and correspondingly, beta power indexes the strength of that synchronisation, the density and spatial extent of the involved neuronal pool and its constancy over time. Cortical beta power is robustly modulated by movements in healthy subjects and suppression is found to correlate with the degree to which warning cues are predictive of upcoming action (Doyle, Yarrow, and Brown 2005). Following movement, beta power rebounds to a higher than previous level and can also be augmented by tonic position holding and by stopping a pre-planned movement in a go/no-go task (van Wijk et al. 2012). As such, it has previously been conceptualised as an idling rhythm or, alternatively, as a promoter of the status quo (Engel & Fries 2010; Gilbertson et al. 2005). Periods of elevated beta are associated with slowing of spontaneous movement and increased corrective responses to postural perturbation suggesting that beta actively stabilises the current motor set (Gilbertson et al. 2005).

7.2.2 Pathological role of beta in Parkinson's disease

DBS treatment affords the opportunity to study subcortical beta activity in PD, either intra-operatively when single neuronal discharges can be picked up with microelectrodes, or post-operatively as

presented in this thesis. The former has confirmed that beta activity in the LFP is time locked to the bursting of neurons (Levy 2002). The latter recordings have turned out to be remarkably robust even over periods of years (Giannicola et al. 2012), and reliably find an increase in beta power in patients withdrawn from dopaminergic medication (Little & Brown 2012). Acutely, beta power is suppressed by levodopa and DBS in proportion to clinical improvement (Little & Brown 2012; Kühn, Kupsch, et al. 2006; Eusebio et al. 2011). The relationship between absolute beta levels and concurrent clinical state is less clear but a number of normalised metrics of beta have shown strong correlations with rigidity and bradykinesia at rest such as temporal variability of beta amplitude discussed in chapter 4 (Little, Pogosyan, et al. 2012; Chen et al. 2010). The spatial extent of subcortical beta activity coupling has also been correlated with clinical state (Pogosyan et al. 2010). These functional correlates are broadly in keeping with the posited role of beta in the healthy state, as an exaggerated promoter of the motor status quo which might reasonably be expected to manifest as an increase in postural activity (rigidity) at the expense of new movements (bradykinesia).

The suppression of beta activity by levodopa has led to the proposal that beta might serve to index net dopamine levels at the sites of cortical input to the basal ganglia (Jenkinson & Brown 2011). As such, beta would be intimately related to dopamine modulation by internal and external cues both before (and even in the absence of) movement and when movement is triggered. Those changes arising before (or in the absence of) movement have been considered as a marker of the likelihood that a new action will need to be performed (Jenkinson & Brown 2011).

In sum, beta activity is likely controlled by the level of dopaminergic activity in response to internal and external cues and serves to modulate the stability of the current motor state. However, the work so far presented is essentially correlative and as such cannot definitively show that beta has a mechanistic

role, and is not simply epiphenomenal (Leblois et al. 2006). In order to clarify this critical issue, we must consider attempts that have been made to directly manipulate beta activity and its behavioural consequences.

7.2.3 Manipulation of beta activity

Beta can be potentially enhanced by using a rhythmic electrical stimulus to entrain and boost the underlying physiological signal. At the cortical level this can be performed non – invasively using transcranial alternating current stimulation (TACS). Studies have demonstrated that beta frequency TACS slows movement and markedly reduces the force of errors of commission during no-go trials in healthy subjects (Pogosyan et al. 2009; Joundi et al. 2012). These data are complimented by sub-cortical stimulation studies in PD patients in which DBS pulses are delivered at low frequency within the beta range. These have previously shown only a small (but statistically significant) deterioration in bradykinesia in the low frequency stimulation condition (Table 7.1)(Timmermann & Florin 2011). It was in this context that the study in chapter 3 of this thesis was carried out in subjects ON medication, to prevent ceiling effects (Little, Joundi, et al. 2012). The finding of increased rigidity of 24% across low frequency conditions was therefore significant both in extending the causal role of beta to another symptom of PD, namely rigidity and also, in showing a greater effect size than had previously been found. This greater effect size is significant in its magnitude as it suggests that beta may play a substantial causal role in the pathophysiology of PD but also, in finding this larger effect ON medication, suggests that the effect of low frequency stimulation and potentially beta oscillations more generally, depends on the current state of functional population in question with regard to its baseline optimal level of synchronisation. This is in keeping with previous work that suggests that high

frequency stimulation can have a differential effect on motor function depending on the baseline motor output without stimulation at the time of testing (Chen, Brücke, et al. 2006; Ray et al. 2009).

Group	**No. of Patients**	**Task** (off/on medication)	**Effective frequency (Hz)**	**Effect size**
(Timmermann et al. 2004)	7	UPDRS akinesia (off)	10	10 % increase motor UPDRS
(Fogelson, Kühn, et al. 2005)	10	Finger tapping (off)	20	6% slowing
(Chen et al. 2007)	22	Finger tapping (off)	20	8% slowing
(Eusebio et al. 2008)	18	Finger tapping (off)	5 & 20	12% slowing
(Chen et al. 2011)	16	Grip force (off)	20	15% slowing of force development
(Little, Joundi, et al. 2012)	12	Rigidity (on)	5,10 & 20	24% increase in rigidity
(Chen et al. 2013)	15	Grip / elbow flexion speed (off)	20	Variable – dependent on baseline speed

Table 7.1. Table summarising studies that have attempted to demonstrate a causal role for low frequency oscillations on bradykinesia in PD. Adapted with permission (Little & Brown 2012).

Thus those subjects with poor pre-testing motor function tend to get better with high frequency stimulation; whereas those with good pre-testing function can deteriorate. This result is mirrored for stimulation at low frequencies by an elegant study which rather than use a dichotomy between good and bad baseline responders, created a continuous distribution across all subjects which generated an inverted U shaped response function (Chen et al. 2013). This result is particularly striking for the fact that it further challenges the concept that individual frequency bands are strictly associated with

specific motor outputs or states. The effect therefore of augmenting a particular frequency band will depend on its current relative position on its own synchronisation curve and could lead to an increase or decreased motor output as seen in this study with 20Hz stimulation.

Studies such as ours (aDBS, chapter 5) and that previously described in primates, that seek to selectively down-regulate beta oscillations through closed loop DBS are also beginning to argue in favour of a major mechanistic role for beta activity, at least in mediating motor impairment in PD (Little et al. 2013; Rosin et al. 2011). In using low frequency oscillations as a biomarker, these closed loop studies provide powerful insight into the functional role of beta. These two studies suggest that pathological levels of synchronisation can be quantitatively and mechanistically important in mediating motor impairment in the Parkinsonian state. But how can this come about, given that oscillatory synchronisation is often proposed to be physiologically advantageous? The answer may lie in the degree of synchronisation, and whether this is appropriate for the task in hand. Broadly, we can consider the physiological roles of neuronal synchronisation in two ways (Hanslmayr et al. 2012). First, it entails the temporal alignment of excitatory post synaptic potentials (EPSPs) leading to more efficient summation on target neurons and thus an increased likelihood of downstream firing. Providing that such synchronisation is spatially discriminating it will provide an efficient mechanism for increasing information flow. Such small scale ensembles involve limited spatial summation and are hence associated with low amplitude mesoscopic (LFP) and macroscopic (EEG) oscillatory activities which are generally detected in the gamma frequency range. If synchronisation is less spatially discriminative and pervades across large populations of neurons, it can act to limit the number of independent processing channels and as such potentially reduce information encoding capacity. Such large scale oscillatory synchronisation is associated with greater spatial summation and high amplitude mesoscopic and macroscopic oscillatory activities, and is generally seen at lower frequencies, including those in the

beta range. The decrease in information coding space, indexed by a reduction in entropy, can be advantageous in certain situations, for example when attempting to constrain a repertoire of actions, many of which could be sub-optimal (Brittain & Brown 2013). These two complimentary actions of oscillatory synchrony may serve to control the balance between information flow and encoding space, and thereby the performance of the overall system, which assumes an inverted U shape (Fig. 7.1).

Why does increased synchrony in the beta range, with its high power and extensive spatial distribution not lead to a motor output, even if that output merely consisted of meaningless repetitive movements as predicted by the low information content shown in this model? Another factor that must be incorporated into this scheme as more advanced models are created and tested is the differential effect of oscillation frequency on encoding space and temporal summation of EPSPs. As spatial synchrony increases (and therefore frequency of oscillations decrease), encoding space will decrease as small individual functional populations are subsumed into the bigger beta population. However, this shift to a lower frequency of oscillation will also affect the precision of temporal summation of EPSPs and hence information transmission. High frequency oscillations have a rapid rate of change and thus neurons with a high phase difference between them and the surrounding population may only be very slightly temporally misaligned in time, so that temporal facilitation is still possible. The phase difference between the current phase of the neuron and the population to which it is connected results in a strong synchronised input at a time just before or after the neuron in question fires. The synchronised input will move the EPSP towards threshold and increase the probability of the neuron firing in line with the population to which it is connected. This in effect pulls the neurons into phase with the population. The effect is stronger at higher frequencies given the higher rate of repetition intrinsic to the shorter cycle length and also the lower temporal difference between a misaligned neuron and the parent population. This effect will also be self-reinforcing as more neurons are

recruited to the current dominant functional population. This will "pull" the misaligned neuron back into sync very rapidly and ensure that the entire local population stays well synchronised for efficient downstream information transfer. In contrast, although neurons may be phase locked at lower frequencies, any jitter translates into a significant temporal offset so that temporal facilitation is absent or attenuated. Thus the push and pull back into synchronisation will be less. Overall, this means that although different frequencies of firing may have the same relative distribution of firing around the mean in terms of phase (rad), the absolute distribution will vary significantly (ms). It is the absolute distribution of neuronal firing which is important to information transmission through temporal summation. Therefore at low frequencies, although very large numbers of neurons over a distributed network are statistically synchronised with each other, the temporal precision with which this occurs is low (in absolute terms) and thus does not cause sufficient temporal summation of EPSPs to result in downstream firing and hence motor output. Paradoxically, a smaller group of neurons oscillating at a higher frequency will be more strongly temporally aligned in absolute terms, as well as having a higher firing rate. Together, these factors mean that statistically, temporal summation of sufficient EPSPs to reach threshold for firing on downstream neurons are much more likely to occur at higher frequencies.

Therefore, simultaneous arrival of action potentials at downstream neurons can occur through tight temporal alignment of a relatively small upstream population or alternatively through a larger population of less temporally precise upstream neurons. Meaningless motor output could occur if a stage of dopamine depletion in PD was reached when the spatial population of neurons involved was sufficiently large to statistically result in sufficient temporal summation to trigger information transmission despite the less focused temporal alignment. This could be a mechanism in the late development of tremor in some patients with PD.

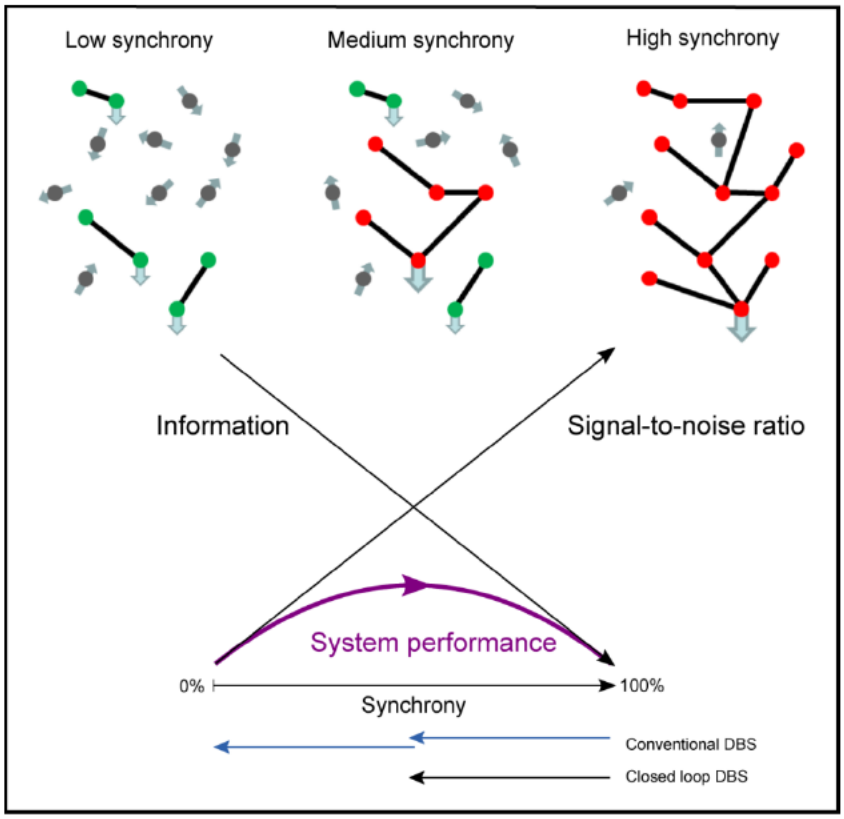

Figure 7.1 Idealised relationship between system performance and neural synchrony. As sub-populations of neurons become correlated, the signal-to-noise ratio or power of that cluster relative to the population increases. At the same time the amount of information that can be transmitted by the ensemble / system decreases. The result is an inverted U-shape to system performance as synchronisation increases. Gamma band interactions between neurons (green dots linked by thick black lines) operate to the left of the ensemble performance curve, as dictated by their low power, weakly and locally synchronised nature. Increases in synchronisation in these activities improve ensemble performance and the ability to react to changing circumstances. Beta (and alpha) band interactions tend to operate to the right of the ensemble performance curve in keeping with their higher power, more extensively synchronised nature (red dots linked by thick black lines). Further increases in synchronisation in the beta band diminish ensemble performance and the ability to react to changing circumstances. In interpreting the effects of DBS it should be recalled that the nature of synchrony is dynamic, changing with internal and external cues. Conventional DBS suppresses or over-rides synchrony regardless of whether it is starting from a pathological extreme to the right of the system performance curve, or if it is momentarily more physiological and lying towards the peak of system performance (bottom blue arrows). Thus conventional DBS can be paradoxically deleterious, if the underlying system spends most of its time with synchronization optimally balanced. In closed loop DBS stimulation only occurs when system performance is compromised by pathologically exaggerated synchronization in the beta band (bottom black arrow). Note that here 'synchronisation' denotes both the strength of coupling, and the density and spatial extent of the involved neuronal pool. Adapted with permission (Brittain & Brown 2013).

In the relative absence of dopamine as seen in PD, the spatial extent and density of beta synchrony is inappropriately increased (Pogosyan et al. 2010; Zaidel et al. 2010) and its reactivity diminished as shown in chapter 4 (Little, Pogosyan, et al. 2012), leading to a reduction in information coding space, an increasing drop in system performance and impaired motor processing. Dopaminergic therapy helps reverse this and closed loop DBS, by focusing stimulation at the time of bursts of beta activity of increased amplitude, preferentially suppresses (either directly or through driving networks at higher frequency) periods of particularly extensive beta synchrony, leaving undisturbed other periods in which the balance between information flow and encoding space, here termed system performance, is more optimal. Continuous high frequency DBS is less discriminating, so that some of the benefits of suppressing spatially extensive beta synchronisation may be off-set by, at other times, driving less marked degrees of synchronization down so that system performance is compromised (movement to the far left, as shown schematically by one of the blue arrows at the bottom of Fig. 7.1). Given the progressive nature of Parkinson's disease, different motor sub-circuits may deviate from the optimal synchronisation point by different degrees. As such, shifting the dynamic operating point towards the left side of the curve may be beneficial to one motor function (limb movement) whilst be deleterious to another (speech) within the same patient.

Our study correlating beta variability with parkinsonian state (chapter 4) adds a further dimension to this concept of dynamic synchronisation shifting. The notions introduced thus far have considered the broad concept of synchronisation as a measure of coupling and density and spatial extent of an involved neuronal pool. The specific degree of coupling and spatial extent of synchronisations at any given moment results in a certain position along the operating curve shown in Fig 7.1. Our result, demonstrating the importance of temporal variability of beta in PD and its modulation by dopamine,

extends this concept along a new axis - time. The optimal point of the dynamic operating curve will be different for different tasks and in different contexts and thus average dopamine also appears to control the flexibility of shifting of this operating point over time, again in a non – linear manner. Not only do subjects with PD exist on the right hand side of the curve on average, but as the disease progresses their position becomes ever more fixed and so their ability to appropriately move up and down the curve diminishes. The position on the right hand side therefore could cause the akinesia that is fundamental to PD by substantially reducing encoding space. However, as the disease progresses not only does the average position on the curve move to the right, but the variability of that position also reduces as reflected in the reduced CV of beta amplitude. This may in part reflect the deterioration of the ratio of tonic to phase dopamine that would result as dopamine neurons reduce in number (reduced phasic drive) whilst levodopa administration increases (increased tonic drive) (Jenkinson & Brown 2011). This may also therefore explain the reduced set-shifting capacities that have long been described in PD (Brown & Marsden 1988). Hence it may be that by developing models that consider the temporal variability of synchronisation in addition to the absolute levels of coupling (i.e. include a temporal as well as spatial domain), that more aspects of PD could be explained using this conceptual schema.

7.3 Adaptive DBS – clinical implementation

Our proof of principle study in subjects with PD demonstrates that aDBS is possible using a simple beta amplitude biomarker in the post-operative period. This achieved its primary objective of reducing time on stimulation and therefore, if clinically implemented, having the possible advantage of extending battery life and thereby saving on costs and recurrent operations. The study also demonstrated improved clinical performance despite this reduced stimulation time compared with conventional continuous stimulation. This provides further evidence for the emerging concept that

synchronisation sub-serves both physiological and pathological roles and that aDBS could be superior to cDBS by more selectively modulating the dynamic network synchronisation profile towards its optimal point.

The translation of this system into the clinical domain will take significant further technical and theoretical work. Our study in the acute post – operative period depended on specialised amplifiers and stimulators designed specifically for the task. Therefore a first technical hurdle is to miniaturise the equipment into a form that could be implanted into patients. Fortuitously, significant advances have been achieved in this domain already and an implantable device that theoretically could achieve the kind of algorithmic control described in our study has already been tested in animals (Afshar et al. 2012). Results in subjects with PD are eagerly anticipated.

7.3.1 Bilateral adaptive deep brain stimulation

Our system, using a simple control algorithm of beta amplitude threshold crossing triggering unilateral stimulation could therefore be potentially realised in an implantable system in the relatively near future. However, even with the simple solution, as adopted by us in our study, substantial questions remain. The first question is how to implement such a system bilaterally. To answer this, one first must know the degree of interdependence of amplitude fluctuations across the two sides. This thesis addresses this question in the study on bilateral coherence between the two STNs (chapter 6). We found that although there was statistically significant beta amplitude co-modulation across the two sides in the majority of patients, the absolute levels were relatively low and therefore would not be sufficient to drive unilateral sensing and bilateral triggering / stimulation. This is important as it implies that separate systems would be required for the two sides which may prove technically more challenging. Accepting the need for bilateral sensing and triggering, next one must consider how the

two sides will interact under aDBS conditions. Given that the stimulation is monopolar, might stimulation on one side leak into the recordings on the opposite, particular if a common reference is utilised? If this were the case and was found to have components in the band of interest, it could inappropriately trigger stimulation on the opposite side in the absence of a true physiological increase in beta. Bilateral implementation therefore will require further exploration.

7.3.2 Chronic stimulation and trigger thresholds

Practical constraints inherent in testing frail post-operative patients with externalised equipment limited us to short periods of stimulation only (<10 minutes per condition). How this system would respond under naturalised chronically implanted conditions is unknown. It should be noted that great care was used in setting of the trigger threshold level in order to achieve an appropriate reduction in time of stimulation, avoid self-triggering and maintain a clinical effect. Small changes in threshold level could result in substantial changes in the triggering dynamics of the system as a whole with slight reductions causing self-triggering of stimulation and yet modest increases resulting in the stimulator being turned off for much of the time. The stability of the optimal trigger threshold over longer periods of time remains to be determined. Subtle changes in impedance could lead to relatively dramatic changes in the behaviour of the system if a fixed trigger is utilised and it is envisaged that some form of automated trigger threshold adjustment will be required in order to keep the system at its optimal point.

Importantly, patient specific factors such as motor activity status and medication level will also have an effect on the behaviour and patterning of the stimulation system as a whole. In order to simplify our testing, we performed the aDBS experiments off medication and at rest (apart from movements required during UPDRS testing). How the system would perform under more naturalised conditions

of fluctuating medication levels and physiological movement induced beta fluctuations is currently unknown and needs investigating. Beta levels will on average be reduced during ON periods when medication has been taken and therefore this would cause triggering to be reduced if a fixed threshold were utilised. This could be appropriate in that aDBS would then act to smooth out motor variability induced by drug fluctuations and effectively target end of dose OFF periods. However, we also know that DBS and levodopa can have a small but significant additive effect in some subjects with PD and if DBS is switched off to too great an extent, this additive effect could be lost (Williams et al. 2010; Schuepbach et al. 2013). Beta will also appropriately fluctuate in response to internal and external cues and therefore using beta as a biomarker is complicated by this interaction with normal physiological motor programming. Beta desynchronisation precedes voluntary movement and DBS may assist this desynchronisation by generally supressing beta but then appropriately switch itself off at the moment of movement initiation as beta amplitude levels fall. It is hoped that by improving the specificity of DBS to periods of high beta as occurs in aDBS, that normal physiological motor programming will be less interrupted and patients will experience improved motor outcome. It is possible to envisage an alternate scenario however, in which withdrawal of DBS right at the moment prior to movement leads to a beta rebound and hence freezing or movement failure. The improvements seen in our study do not support this but the situation may change if more complex/naturalistic movements are initiated or different thresholds or timing constants employed in the algorithm. Sleep is another area where beta changes would be expected which would interact with an aDBS system in clinical practice. Beta appears to drop during slow wave sleep (which would result in DBS mainly switching off) and return to normal or even greater levels during REM behaviour which would switch the aDBS on (Urrestarazu et al. 2009). The effects that a control system such as ours would have on the complex dynamics of sleep therefore needs further exploration.

One potential solution would be to have the system automatically adjust the trigger threshold in order to maintain a fixed ratio of stimulation over time (e.g. ~45% of total). The time course of this adjustment would then be important. If too rapid, the threshold may simply adjust according to current medication state and therefore aDBS would no longer be sensitive to levodopa fluctuations which might prevent it from achieving its full benefit (e.g. stimulation fixed at 45% in both the ON and OFF medication state). If adjustments were too slow, it would likely not keep up with slower changes related to impedance changes and possible infradian fluctuations that may exist (Cheung et al. 2013). A compromise will have to be sought and an intermediate automated adjustment on the scale of hours to days is envisaged to be most effective on current evidence. Therefore, a system that looks at the total proportion of stimulation over the previous 24hrs and incrementally adjusts the threshold to return that proportion towards a set point (e.g. 45%) would appear to strike a balance between maintaining adaptability in the face of relatively rapid fluctuations caused by physiological state and medication but also retain stability in terms of longer term changes in beta. More complex solutions can also be envisaged in which multiple time windows are used to control the threshold. This would be appropriate if it were found that ultradian beta fluctuations occur throughout the day independently from medication. Recordings so far have generally been of short duration and longer term recordings would be very helpful in establishing beta stability over time. If diurnal fluctuations are significant the system could be set to automatically adjust the threshold during the day to take account of those diurnal changes after a period of appropriate algorithmic training. Alternatively a biomarker of motor state such as an accelerometer could be used to determine the current level of motor activity and adjust the threshold accordingly. Patients currently control some of their settings using a personal programmer and this could also be extended to allow them to make changes to their aDBS threshold within physician agreed limits.

Beta amplitude smoothing also affects the temporal resolution of the control system and its response to noise. Again, this was explored heuristically and set at 400ms in our study. This smoothing filtered out some of the intermittent electrical spike artefacts that were occasionally present in our setup but also captured the sub-second bursting of beta oscillations. The smoothing will however have resulted in a small delay in the onset of stimulation being triggered by a beta burst and as such, although short beta bursts will still trigger the appropriate ON and OFF of stimulation, this will be slightly temporally offset from the beta burst itself. Shorter duration of smoothing, if technically viable, would allow the stimulation profile to better match the temporal beta burst profile and may therefore be more effective. Similarly, a refractory period post-stimulation burst was implemented in some patients if there was significant off stimulation artefacts causing self-triggering. If implemented, this was set at between 500 – 750 ms which did prevent self-triggering but further reduced responsiveness to rapid fluctuations in beta amplitude.

7.3.3 aDBS - Parameter optimisation

Our aDBS study also required a number of other heuristic adjustments to stimulation parameters in order to achieve successful responsive stimulation. Initially we found that very rapid changes in stimulation amplitude resulted in significant, treatment limiting intermittent paraesthesia. This was somewhat improved by introducing a ramping period, which at 250ms, was sufficient to enable aDBS. This ramping period was therefore held constant across all the subjects. Longer ramping times may reduce paraesthesia but at the cost of temporal resolution of the system and therefore a compromise must be struck. An important further study will be therefore to look at how ramping times affect paraesthesia induction. This relationship may well be complex and relate to both ramping speed and stimulation voltage. Understanding this relationship better may allow aDBS to occur at higher, more

therapeutic, voltages but retain beneficial temporal resolution that can respond to beta bursts. An alternative approach could be to amplitude modulate stimulation rather than switch it on and off. This may reduce paraesthesia but again at the cost of always stimulating, to a degree, irrespective of beta. The ensemble performance profile discussed above may be difficult to optimise under such conditions as stimulation would inevitably interfere with networks at the left hand side of the curve (although less so due to reduced voltage at that time). Compromises will need to be struck therefore between different parameters and building a conceptual framework within which to understand these decisions will be important to optimising aDBS. Another area as yet unexplored is the effect of pulse shape on both clinical effect but also side effect inducement. Our symmetrically biphasic stimulation pulse shape was chosen for simplicity but may not be the optimal pulse shape for aDBS.

This discussion highlights the increased complexity involved in parameter adjustment with aDBS. Current, conventional, stimulation has simply three parameters, namely pulse width, frequency and voltage (plus contact choice). Despite this restricted parameter space, clinical DBS programming is already complex and labour intensive. Enlarging this parameter space across multiple new dimensions, as would be required in the clinical implementation of aDBS, could make the programming correspondingly more complex. If rational guiding principles for such parameter selection are not found, then this dimensional multiplication could cause the clinical setting of stimulation parameters to become nearly intractable as potential parameter space exponentially expands. A better understanding of the relationship between stimulation parameters, clinical outcome and side effects is required to guide rational programming. Alternatively, a different approach will need to be developed in which parameter space is automatically searched using algorithms that can efficiently explore the whole potential space available (Feng, Greenwald, et al. 2007). This will become a greater issue as the

complexity of aDBS increases with more biomarkers and more advanced control algorithms being implemented.

7.4 Future of Adaptive DBS

This thesis has explored biomarkers of PD, the pathological role of one such biomarker (beta) and the implementation of aDBS in PD. As discussed above, there is still much work to be done before this can be successfully translated into a clinical treatment for patients at large. Even in the relatively simple form in which we trialled aDBS, truly implementing this in a clinical population will be complex.

Successful proof of principle of aDBS in both primates and now humans does however potentially open up a significant new field of exciting translational research with a great range of possibilities. This work presented here has only just begun to explore this. We used beta amplitude as our biomarker as it is the best validated and simplest to compute. Recently though there has been a great advancement in the degree and complexity of biomarkers shown to correlate with clinical state, one of which, namely temporal variability of beta amplitude is presented in this thesis (Little, Pogosyan, et al. 2012; Pogosyan et al. 2010; López-Azcárate et al. 2010; Ozkurt et al. 2011; Tan, Pogosyan, Anzak, Foltynie, et al. 2013; Anzak et al. 2012). Whether these new biomarkers could be implemented in aDBS remains to be explored and it may be that combining different biomarkers together gives the best account of current clinical state and therefore the most effective aDBS (Ozkurt et al. 2011).

Our study treats beta simply as a biomarker, tracking its amplitude to control stimulation. Gratifyingly, this biomarker approach appears successful. Beta may be more than a simple biomarker however and may actually be important in the pathophysiology of PD as explored in chapter 3. If that were the case, selectivity of stimulation may be improved further over the aDBS setup that we have

designed thus far which only tracks beta amplitude and uses this to deliver ramped conventional stimulation. It may be possible to design a stimulation regime that interacts only with the pathological oscillations themselves, leaving the others intact. Phase specific stimulation that tracks the phase of beta oscillations and delivers pulses at a critical point during the cycle could reduce total stimulation further and increase specificity by disruption of beta oscillations in isolation (Rosin et al. 2011). Tracking beta phase in real time, uncontaminated by artefacts and designing a control system with the precision to deliver pulses at specific points in the oscillatory cycle will likely be challenging. If achievable it has the potential to deliver clinical benefit through increased specificity and inform the debate on the pathological role of beta in PD.

The last two decades have seen a decisive shift in our understanding of PD which started with early models invoking imbalance between the direct and indirect pathways, predicated on a rate based coding scheme. This has now developed to include an appreciation of the importance of patterning of neuronal firing which at a population level can be picked up with metrics such as spectral changes in the LFP. It appears from our aDBS study that tracking the degree of neuronal synchronisation (beta amplitude) and delivering stimulation at points of excessive stimulation can be beneficial in the reorientation the population dynamics back to a more optimal position. Might it be that other movement disorders that involve the basal ganglia may similarly benefit from an adaptive DBS approach?

Conventional DBS is already also established in essential tremor and dystonia. There is an extensive literature showing that essential tremor is associated with a specific spectral profile at the cortical and subcortical levels suggesting that it too could be considered a disorder of synchronisation (Raethjen & Deuschl 2012). Essential tremor may therefore be amenable to an adaptive DBS approach. A recent

study has shown that the effect of DBS can be dependent on the phase difference between the pulses delivered and the phase of the tremor cycle, causing either tremor suppression or amplification using a low frequency stimulation paradigm (Cagnan et al. 2013). If these effects could be validated using a central rather than peripheral signal then aDBS for essential tremor may also prove successful. Dystonia initially seems a less promising candidate than PD or essential tremor for an aDBS approach as it is a disease that fluctuates only very slowly and therefore, theoretically at least, should not benefit particularly from a therapy that attempts to tailor stimulation according to disease fluctuations. However, DBS in dystonia is also associated with motoric side effects, presumably through interference with normal motor processing (Berman et al. 2009; Schrader et al. 2011). Additionally, dystonia has also been found to have an association with excessive power in a low frequency bands (Silberstein et al. 2003; Liu et al. 2008). It may be therefore that specificity could be improved by targeting these low frequency oscillations directly, possibly improving clinical outcome and reducing side effects.

There are number of other conditions for which cDBS are being trialled including headache, depression, OCD, Tourette's and Lewy body dementia. It is possible that these different conditions will also reveal specific characteristic spectral profiles that could be used as biomarkers in an aDBS setup but this remains to be shown. It is hoped that aDBS will realise significant clinical benefit to patients across a wide range of conditions, but also that, through encouraging further exploration of the aberrant network dynamics that appear to be fundamental to these conditions, lead to a greater understanding of their pathophysiology.

7.5 Conclusion

This thesis has explored the neurophysiological biomarkers of PD and identified a biomarker that correlates with symptoms at rest and in response to treatment, namely temporal variability of beta amplitude in the STN. It presents data on a study into the pathophysiological role of beta through its augmentation with low frequency stimulation in chronically implanted PD patients. It then demonstrates that beta amplitude can be successfully used in an adaptive stimulation setup and that this can reduce the time on stimulation and improve clinical motor state relative to conventional stimulation. Anticipating the transition to clinical implementation, finally it examines the subcortical beta network and its implementation for bilateral aDBS.

This provides proof of principle that aDBS can be beneficial in human subjects. A number of further areas of research are required before the benefits of aDBS can be fully realised in the clinical settings:

1. Miniaturisation of a device for human implantation
2. Improved understanding of biomarkers of PD (within subjects)
3. Testing of bilateral aDBS
4. Prolonged stimulation
5. Drug and movement effects on aDBS system
6. Relationship between ramping, pulse shape and side effects

References

Abosch, A. et al., 2012. Long-term recordings of local field potentials from implanted deep brain stimulation electrodes. *Neurosurgery*, 71(4), pp.804–14.

Afshar, P. et al., 2012. A translational platform for prototyping closed-loop neuromodulation systems. *Frontiers in neural circuits*, 6, p.117.

Ahmed, I. et al., 2011. Glutamate NMDA receptor dysregulation in Parkinson's disease with dyskinesias. *Brain*, 134, pp.979–86.

Albin, R.L., Young, A.B. & Penney, J.B., 1989. The functional anatomy of basal ganglia disorders. *Trends in neurosciences*, 12(10), pp.366–75.

Alegre, M. et al., 2003. Movement-related changes in cortical oscillatory activity in ballistic, sustained and negative movements. *Experimental brain research*, 148(1), pp.17–25.

Alexander, G.E., DeLong, M.R. & Strick, P.L., 1986. Parallel organization of functionally segregated circuits linking basal ganglia and cortex. *Annual review of neuroscience*, 9, pp.357–81.

Allen, D. et al., 2007. On the use of low-cost computer peripherals for the assessment of motor dysfunction in Parkinson's disease—quantification of bradykinesia using target tracking tasks. *Neural Systems and Rehabilitation Engineering*, 15(2), pp.286–294.

Alonso-Frech, F. et al., 2006. Slow oscillatory activity and levodopa-induced dyskinesias in Parkinson's disease. *Brain*, 129, pp.1748–1757.

Amirnovin, R. et al., 2004. Visually guided movements suppress subthalamic oscillations in Parkinson's disease patients. *The Journal of Neuroscience*, 24(50), pp.11302–6.

Andersen, R., Musallam, S. & Pesaran, B., 2004. Selecting the signals for a brain-machine interface. *Current opinion in neurobiology*, 14(6), pp.720–726.

Anderson, V.C. et al., 2005. Pallidal vs subthalamic nucleus deep brain stimulation in Parkinson disease. *Archives of neurology*, 62(4), pp.554–60.

Androulidakis, A.G., Brücke, C., et al., 2008. Amplitude modulation of oscillatory activity in the subthalamic nucleus during movement. *The European journal of neuroscience*, 27(5), pp.1277–1284.

Androulidakis, A.G. et al., 2006. Corrective movements in response to displacements in visual feedback are more effective during periods of 13-35 Hz oscillatory synchrony in the human corticospinal system. *The European journal of neuroscience*, 24(11), pp.3299–304.

Androulidakis, A.G., Mazzone, P., et al., 2008. Oscillatory activity in the pedunculopontine area of patients with Parkinson's disease. *Experimental neurology*, 211(1), pp.59–66.

Anzak, A. et al., 2012. Subthalamic nucleus activity optimizes maximal effort motor responses in Parkinson's disease. *Brain*, 135, pp.2766–78.

Ardouin, C. et al., 1999. Bilateral subthalamic or pallidal stimulation for Parkinson's disease affects neither memory nor executive functions: a consecutive series of 62 patients. *Annals of neurology*, 46(2), pp.217–23.

Ballard, P.A., Tetrud, J.W. & Langston, J.W., 1985. Permanent human parkinsonism due to 1-methyl-4-phenyl-1,2,3,6-tetrahydropyridine (MPTP): seven cases. *Neurology*, 35(7), pp.949–56.

Bar-Gad, I. et al., 2003. Functional correlations between neighboring neurons in the primate globus pallidus are weak or nonexistent. *The Journal of neuroscience*, 23(10), pp.4012–6.

Barone, P., 2010. Neurotransmission in Parkinson's disease: beyond dopamine. *European journal of neurology*, 17(3), pp.364–76.

Bassett, D.S. & Gazzaniga, M.S., 2011. Understanding complexity in the human brain. *Trends in Cognitive Sciences*, 15(5), pp.200–209.

Basso, M.A., Israel, Z. & Bergman, H., 2008. Pathophysiology of the basal ganglia and movement disorders: From animal models to human clinical applications. *Neuroscience & Biobehavioral Reviews*, 32(3), pp.367–377.

Benabid, A.L. et al., 1987. Combined (thalamotomy and stimulation) stereotactic surgery of the VIM thalamic nucleus for bilateral Parkinson disease. *Applied neurophysiology*, 50(1-6), pp.344–6.

Benabid, A.L. et al., 2009. Deep brain stimulation of the subthalamic nucleus for the treatment of Parkinson's disease. *Lancet neurology*, 8(1), pp.67–81.

Bennett, M. & Hacker, P., 2003. *Philosophical Foundations of Neuroscience*, Blackwell, Oxford.

Bergman, H. et al., 1994. The primate subthalamic nucleus. II. Neuronal activity in the MPTP model of parkinsonism. *Journal of neurophysiology*, 72(2), pp.507–20.

Berman, B.D. et al., 2009. Induction of bradykinesia with pallidal deep brain stimulation in patients with cranial-cervical dystonia. *Stereotactic and functional neurosurgery*, 87(1), pp.37–44.

Bin-Mahfoodh, M. et al., 2003. Longevity of batteries in internal pulse generators used for deep brain stimulation. *Stereotactic and functional neurosurgery*, 80, pp.56–60.

Blahak, C. et al., 2011. Battery lifetime in pallidal deep brain stimulation for dystonia. *European journal of neurology*, 18(6), pp.872–5.

Blahak, C. et al., 2009. Rapid response of parkinsonian tremor to STN-DBS changes: direct modulation of oscillatory basal ganglia activity? *Movement disorders*, 24(8), pp.1221–5.

Braak, H. et al., 2003. Staging of brain pathology related to sporadic Parkinson's disease. *Neurobiology of Aging*, 24(2), pp.197–211.

Brittain, J.-S. & Brown, P., 2013. Oscillations and the basal ganglia: Motor control and beyond. *NeuroImage*, (Epub ahead of print).

Brittain, J.S., Probert-Smith, P. & Aziz, T.Z., 2010. Demand driven deep brain stimulation: regimes and autoregressive hidden Markov implementation. *IEEE Engineering in Medicine and Biology Society*, 2010, pp.158–61.

Bronte-Stewart, H.M. et al., 2009. The STN beta-band profile in Parkinson's disease is stationary and shows prolonged attenuation after deep brain stimulation. *Experimental neurology*, 215(1), pp.20–28.

Brown, P., 2007. Abnormal oscillatory synchronisation in the motor system leads to impaired movement. *Current opinion in neurobiology*, 17(6), pp.656–64.

Brown, P. et al., 2001. Dopamine dependency of oscillations between subthalamic nucleus and pallidum in Parkinson's disease. *The Journal of neuroscience*, 21(3), pp.1033–1038.

Brown, P., 2003. Oscillatory nature of human basal ganglia activity: relationship to the pathophysiology of Parkinson's disease. *Movement disorders*, 18(4), pp.357–363.

Brown, P. & Williams, D., 2005. Basal ganglia local field potential activity: character and functional significance in the human. *Clinical neurophysiology*, 116(11), pp.2510–2519.

Brown, R.G. & Marsden, C.D., 1988. An investigation of the phenomenon of "set" in Parkinson's disease. *Movement disorders*, 3(2), pp.152–61.

Brun, Y. et al., 2012. Does unilateral basal ganglia activity functionally influence the contralateral side? What we can learn from STN stimulation in patients with Parkinson's disease. *Journal of neurophysiology*, 108(6), pp.1575–83.

Bruns, A., 2004. Fourier-, Hilbert- and wavelet-based signal analysis: are they really different approaches? *Journal of neuroscience methods*, 137(2), pp.321–32.

Buehlmann, A. & Deco, G., 2010. Optimal information transfer in the cortex through synchronization. *PLoS computational biology*, 6(9).

Burchiel, K.J. et al., 1999. Comparison of pallidal and subthalamic nucleus deep brain stimulation for advanced Parkinson's disease: results of a randomized, blinded pilot study. *Neurosurgery*, 45(6), pp.1375–82; discussion 1382–4.

Butson, C. & McIntyre, C., 2007. Differences among implanted pulse generator waveforms cause variations in the neural response to deep brain stimulation. *Clinical neurophysiology*, 118(8), pp.1889–1894.

Buzsáki, G., Anastassiou, C. a. & Koch, C., 2012. The origin of extracellular fields and currents — EEG, ECoG, LFP and spikes. *Nature Reviews Neuroscience*, 13(6), pp.407–420.

Cagnan, H. et al., 2013. Phase dependent modulation of tremor amplitude in essential tremor through thalamic stimulation. *Brain*, (Epub ahead of print).

Carpenter, M.B. et al., 1981. Connections of the subthalamic nucleus in the monkey. *Brain research*, 224(1), pp.1–29.

Carpenter, M.B. & Strominger, N.L., 1967. Efferent fibers of the subthalamic nucleus in the monkey. A comparison of the efferent projections of the subthalamic nucleus, substantia nigra and globus pallidus. *The American journal of anatomy*, 121(1), pp.41–72.

Cassidy, M. et al., 2002. Movement-related changes in synchronization in the human basal ganglia. *Brain*, 125, pp.1235–1246.

Castrioto, A. et al., 2011. Ten-year outcome of subthalamic stimulation in Parkinson disease: a blinded evaluation. *Archives of neurology*, 68(12), pp.1550–6.

Chaudhuri, K.R., Healy, D.G. & Schapira, A.H. V, 2006. Non-motor symptoms of Parkinson's disease: diagnosis and management. *Lancet neurology*, 5(3), pp.235–45.

Chen, C.C. et al., 2010. Complexity of subthalamic 13-35 Hz oscillatory activity directly correlates with clinical impairment in patients with Parkinson's disease. *Experimental neurology*, 224(1), pp.234–240.

Chen, C.C., Brücke, C., et al., 2006. Deep brain stimulation of the subthalamic nucleus: a two-edged sword. *Current biology*, 16(22), pp.952–953.

Chen, C.C. et al., 2007. Excessive synchronization of basal ganglia neurons at 20 Hz slows movement in Parkinson's disease. *Experimental neurology*, 205(1), pp.214–221.

Chen, C.C., Pogosyan, A., et al., 2006. Intra-operative recordings of local field potentials can help localize the subthalamic nucleus in Parkinson's disease surgery. *Experimental neurology*, 198(1), pp.214–21.

Chen, C.C. et al., 2011. Stimulation of the subthalamic region at 20Hz slows the development of grip force in Parkinson's disease. *Experimental neurology*, 231(1), pp.91–96.

Chen, C.C. et al., 2013. The impact of low-frequency stimulation of subthalamic region on self-generated isometric contraction in patients with Parkinson's disease. *Experimental Brain Research*, 227(1), pp.53–62.

Cheung, T. et al., 2013. Longitudinal Impedance Variability in Patients with Chronically Implanted DBS Devices. *Brain Stimulation*, 6(5), pp.746–751.

De Cock, V.C. et al., 2007. Restoration of normal motor control in Parkinson's disease during REM sleep. *Brain*, 130, pp.450–456.

Cooper, I., 1953. Ligation of the anterior choroidal artery for involuntary movements; parkinsonism. *The Psychiatric quarterly*, 27(2), pp.317–9.

Cotzias, G.C., Van Woert, M.H. & Schiffer, L.M., 1967. Aromatic amino acids and modification of parkinsonism. *The New England journal of medicine*, 276(7), pp.374–9.

Curran, E.A. & Stokes, M.J., 2003. Learning to control brain activity: a review of the production and control of EEG components for driving brain-computer interface (BCI) systems. *Brain and cognition*, 51(3), pp.326–336.

Curran-Everett, D., 2000. Multiple comparisons: philosophies and illustrations. *American journal of physiology. Regulatory, integrative and comparative physiology*, 279(1), pp.R1–8.

Dams, J. et al., 2013. Cost-effectiveness of deep brain stimulation in patients with Parkinson's disease. *Movement disorders*, 28(6), pp.763–71.

Daniele, A. et al., 2003. Cognitive and behavioural effects of chronic stimulation of the subthalamic nucleus in patients with Parkinson's disease. *Journal of neurology, neurosurgery, and psychiatry*, 74(2), pp.175–82.

DBS PD Study Group, 2001. Deep-brain stimulation of the subthalamic nucleus or the pars interna of the globus pallidus in Parkinson's disease. *The New England journal of medicine*, 345(13), pp.956–63.

Delorme, A. et al., 2011. EEGLAB, SIFT, NFT, BCILAB, and ERICA: new tools for advanced EEG processing. *Computational intelligence and neuroscience*, 2011, p.130714.

Deuschl, G. et al., 2006. A randomized trial of deep-brain stimulation for Parkinson's disease. *The New England journal of medicine*, 355(9), pp.896–908.

Deuschl, G. et al., 2011. Treatment of patients with essential tremor. *The Lancet Neurology*, 10(2), pp.148–161.

Devos, D. et al., 2006. Predominance of the contralateral movement-related activity in the subthalamo-cortical loop. *Clinical neurophysiology*, 117(10), pp.2315–2327.

Doyle, L., Kühn, A.A., et al., 2005. Levodopa-induced modulation of subthalamic beta oscillations during self-paced movements in patients with Parkinson's disease. *The European journal of neuroscience*, 21(5), pp.1403–1412.

Doyle, L., Yarrow, K. & Brown, P., 2005. Lateralization of event-related beta desynchronization in the EEG during pre-cued reaction time tasks. *Clinical neurophysiology*, 116(8), pp.1879–88.

Ebel, R.L., 1951. Estimation of the reliability of ratings. *Psychometrika*, 16(4), pp.407–424.

Endo, T. et al., 2009. A novel method for systematic analysis of rigidity in Parkinson's disease. *Movement Disorders*, 24(15), pp.2218–2224.

Engel, A.K. & Fries, P., 2010. Beta-band oscillations - signalling the status quo? *Current opinion in neurobiology*, 20(2), pp.156–65.

Eusebio, A. et al., 2011. Deep brain stimulation can suppress pathological synchronisation in parkinsonian patients. *Journal of neurology, neurosurgery, and psychiatry*, 82(5), pp.569–573.

Eusebio, A. et al., 2008. Effects of low-frequency stimulation of the subthalamic nucleus on movement in Parkinson's disease. *Experimental neurology*, 209(1), pp.125–130.

Eusebio, A., Cagnan, H. & Brown, P., 2012. Does suppression of oscillatory synchronisation mediate some of the therapeutic effects of DBS in patients with Parkinson's disease? *Frontiers in integrative neuroscience*, 6, p.47.

Fahn, S. & Elton, R., 1987. Unified Parkinson's Disease Rating Scale. In *Recent developments in Parkinson's disease*. Florham Park (NJ): Macmillan Health Care Information, pp. 153–163.

Feng, X., Shea-Brown, E., et al., 2007. Optimal deep brain stimulation of the subthalamic nucleus--a computational study. *Journal of computational neuroscience*, 23(3), pp.265–282.

Feng, X., Greenwald, B., et al., 2007. Toward closed-loop optimization of deep brain stimulation for Parkinson's disease: concepts and lessons from a computational model. *Journal of neural engineering*, 4(2), pp.14–21.

Fisher, R. et al., 2010. Electrical stimulation of the anterior nucleus of thalamus for treatment of refractory epilepsy. *Epilepsia*, 51(5), pp.899–908.

Foffani, G. et al., 2005. Movement-related frequency modulation of beta oscillatory activity in the human subthalamic nucleus. *The Journal of Physiology*, 568(2), pp.699–711.

Foffani, G. et al., 2006. Subthalamic oscillatory activities at beta or higher frequency do not change after high-frequency DBS in Parkinson's disease. *Brain research bulletin*, 69(2), pp.123–130.

Fogelson, N. et al., 2006. Different functional loops between cerebral cortex and the subthalmic area in Parkinson's disease. *Cerebral cortex*, 16(1), pp.64–75.

Fogelson, N., Kühn, A.A., et al., 2005. Frequency dependent effects of subthalamic nucleus stimulation in Parkinson's disease. *Neuroscience letters*, 382, pp.5–9.

Fogelson, N., Pogosyan, A., et al., 2005. Reciprocal interactions between oscillatory activities of different frequencies in the subthalamic region of patients with Parkinson's disease. *The European journal of neuroscience*, 22(1), pp.257–266.

Follett, K.A. et al., 2010. Pallidal versus subthalamic deep-brain stimulation for Parkinson's disease. *The New England journal of medicine*, 362(22), pp.2077–91.

Foltynie, T. et al., 2011. MRI-guided STN DBS in Parkinson's disease without microelectrode recording: efficacy and safety. *Journal of neurology, neurosurgery, and psychiatry*, 82(4), pp.358–63.

Foltynie, T. & Hariz, M., 2010. Surgical management of Parkinson's disease. *Expert review of neurotherapeutics*, 10(6), pp.903–14.

Ford, B. et al., 2004. Subthalamic nucleus stimulation in advanced Parkinson's disease: blinded assessments at one year follow up. *Journal of neurology, neurosurgery, and psychiatry*, 75(9), pp.1255–9.

Fries, P., 2005. A mechanism for cognitive dynamics: neuronal communication through neuronal coherence. *Trends in Cognitive Sciences*, 9(10), pp.474–480.

Friston, K.J., 2000. The labile brain. I. Neuronal transients and nonlinear coupling. *Philosophical transactions of the Royal Society of London. Series B, Biological sciences*, 355(1394), pp.215–36.

Funkiewiez, A. et al., 2004. Long term effects of bilateral subthalamic nucleus stimulation on cognitive function, mood, and behaviour in Parkinson's disease. *Journal of neurology, neurosurgery, and psychiatry*, 75(6), pp.834–9.

Giannicola, G. et al., 2012. Subthalamic local field potentials after seven-year deep brain stimulation in Parkinson's disease. *Experimental neurology*, 237(2), pp.312–7.

Giannicola, G. et al., 2013. The effects of levodopa and deep brain stimulation on subthalamic local field low-frequency oscillations in Parkinson's disease. *Neuro-Signals*, 21(1-2), pp.89–98.

Gibb, W.R.G. & Poewe, W.H., 1986. The centenary of Friedreich H. Lewy 1885–1950. *Neuropathology and Applied Neurobiology*, 12(3), pp.217–221.

Gilbertson, T. et al., 2005. Existing motor state is favored at the expense of new movement during 13-35 Hz oscillatory synchrony in the human corticospinal system. *The Journal of neuroscience*, 25(34), pp.7771–9.

Goldberg, J. a et al., 2004. Spike synchronization in the cortex/basal-ganglia networks of Parkinsonian primates reflects global dynamics of the local field potentials. *The Journal of neuroscience*, 24(26), pp.6003–10.

Halliday, D.M. et al., 1995. A framework for the analysis of mixed time series/point process data--theory and application to the study of physiological tremor, single motor unit discharges and electromyograms. *Progress in biophysics and molecular biology*, 64(2-3), pp.237–78.

Hammond, C., Bergman, H. & Brown, P., 2007. Pathological synchronization in Parkinson's disease: networks, models and treatments. *Trends in neurosciences*, 30(7), pp.357–364.

Hanslmayr, S., Staudigl, T. & Fellner, M.-C., 2012. Oscillatory power decreases and long-term memory: the information via desynchronization hypothesis. *Frontiers in human neuroscience*, 6, p.74.

Hariz, M., 2012. Twenty-five years of deep brain stimulation: celebrations and apprehensions. *Movement disorders*, 27(7), pp.930–3.

Hassler, R., 1938. Zur Pathologie der Paralysis agitans und des post-enzephalitschen Parkinsonismus. *J Psychol Neurol*, 48, pp.387–476.

Hassler, R., Riechert, T. & Mundinger, F., 1960. Physiological observations in stereotaxic operations in extrapyramidal motor disturbances. *Brain*, 83(2), pp.337–350.

Hauptmann, C., Popovych, O. & Tass, P., 2005. Multisite coordinated delayed feedback for an effective desynchronization of neuronal networks. *Stochastics & Dynamics*, 5(2), pp.307–319.

Hauptmann, C. & Tass, P.A., 2006. Therapeutic rewiring by means of desynchronizing brain stimulation. *Bio Systems*, 89(1-3), pp.173–81.

De Hemptinne, C. et al., 2013. Exaggerated phase-amplitude coupling in the primary motor cortex in Parkinson disease. *Proceedings of the National Academy of Sciences*, 110(12), pp.4780–5.

Hilker, R. et al., 2005. Disease progression continues in patients with advanced Parkinson's disease and effective subthalamic nucleus stimulation. *Journal of neurology, neurosurgery, and psychiatry*, 76(9), pp.1217–21.

Hirschmann, J. et al., 2011. Distinct oscillatory STN-cortical loops revealed by simultaneous MEG and local field potential recordings in patients with Parkinson's disease. *NeuroImage*, 55(3), pp.1159–68.

Hornykiewicz, O., 2010. A brief history of levodopa. *Journal of neurology*, 257, pp.S249–52.

Huebl, J. et al., 2011. Modulation of subthalamic alpha activity to emotional stimuli correlates with depressive symptoms in Parkinson's disease. *Movement disorders*, 26(3), pp.477–83.

Hughes, A.J. et al., 1992. Accuracy of clinical diagnosis of idiopathic Parkinson's disease: a clinico-pathological study of 100 cases. *Journal of neurology, neurosurgery, and psychiatry*, 55(3), pp.181–4.

Israel, Z. & Bergman, H., 2008. Pathophysiology of the basal ganglia and movement disorders: from animal models to human clinical applications. *Neuroscience and biobehavioral reviews*, 32(3), pp.367–77.

Jankovic, J., 2008. Parkinson's disease: clinical features and diagnosis. *Journal of neurology, neurosurgery, and psychiatry*, 79(4), pp.368–76.

Jasper HH. & Andrews, H., 1938. Electroencephalography. III. Normal differentiation of occipital and precentral regions in man. *Archives of Neurology And Psychiatry*, 39(1), p.96.

Jenkinson, N. & Brown, P., 2011. New insights into the relationship between dopamine, beta oscillations and motor function. *Trends in neurosciences*, 34(12), pp.611–618.

Jobbágy, A. et al., 2005. Analysis of finger-tapping movement. *Journal of neuroscience methods*, 141(1), pp.29–39.

Jobst, B.C. et al., 2010. Brain stimulation for the treatment of epilepsy. *Epilepsia*, 51, pp.88–92.

Joundi, R. a et al., 2012. Driving Oscillatory Activity in the Human Cortex Enhances Motor Performance. *Current Biology*, 22(5), pp.403–407.

Kahn, E. et al., 2012. Deep brain stimulation in early stage Parkinson's disease: operative experience from a prospective randomised clinical trial. *Journal of neurology, neurosurgery, and psychiatry*, 83(2), pp.164–70.

Kawaguchi, Y., 1997. Neostriatal cell subtypes and their functional roles. *Neuroscience research*, 27(1), pp.1–8.

Kemp, J.M. & Powell, T.P., 1971. The connexions of the striatum and globus pallidus: synthesis and speculation. *Philosophical transactions of the Royal Society of London. Series B, Biological sciences*, 262(845), pp.441–57.

Kilpatrick, M. et al., 2010. Intracerebral microdialysis during deep brain stimulation surgery. *Journal of neuroscience methods*, 190(1), pp.106–111.

Kim, J.-W. et al., 2011. Quantification of bradykinesia during clinical finger taps using a gyrosensor in patients with Parkinson's disease. *Medical & biological engineering & computing*, 49(3), pp.365–371.

Kleiner-Fisman, G. et al., 2006. Subthalamic nucleus deep brain stimulation: summary and meta-analysis of outcomes. *Movement disorders*, 21, pp.S290–304.

Krack, P. et al., 2003. Five-year follow-up of bilateral stimulation of the subthalamic nucleus in advanced Parkinson's disease. *The New England journal of medicine*, 349(20), pp.1925–34.

Krack, P. et al., 1998. Subthalamic nucleus or internal pallidal stimulation in young onset Parkinson's disease. *Brain*, 121, pp.451–7.

Kühn, A.A. et al., 2004. Event-related beta desynchronization in human subthalamic nucleus correlates with motor performance. *Brain*, 127, pp.735–746.

Kühn, A.A. et al., 2008. High-frequency stimulation of the subthalamic nucleus suppresses oscillatory beta activity in patients with Parkinson's disease in parallel with improvement in motor performance. *The Journal of Neuroscience*, 28(24), pp.6165–6173.

Kühn, A.A., Doyle, L., et al., 2006. Modulation of beta oscillations in the subthalamic area during motor imagery in Parkinson's disease. *Brain*, 129, pp.695–706.

Kühn, A.A. et al., 2009. Pathological synchronisation in the subthalamic nucleus of patients with Parkinson's disease relates to both bradykinesia and rigidity. *Experimental neurology*, 215(2), pp.380–387.

Kühn, A.A., Kupsch, A., et al., 2006. Reduction in subthalamic 8-35 Hz oscillatory activity correlates with clinical improvement in Parkinson's disease. *The European journal of neuroscience*, 23(7), pp.1956–1960.

Kühn, A.A. et al., 2005. The relationship between local field potential and neuronal discharge in the subthalamic nucleus of patients with Parkinson's disease. *Experimental neurology*, 194(1), pp.212–220.

Kumar, R. et al., 1998. Double-blind evaluation of subthalamic nucleus deep brain stimulation in advanced Parkinson's disease. *Neurology*, 51(3), pp.850–5.

Lachaux, J. et al., 1999. Measuring phase synchrony in brain signals. *Human brain mapping*, 8(4), pp.194–208.

Lalo, E. et al., 2007. Phasic increases in cortical beta activity are associated with alterations in sensory processing in the human. *Experimental Brain Research*, 177(1), pp.137–45.

Lau, L. de & Breteler, M., 2006. Epidemiology of Parkinson's disease. *The Lancet Neurology*, 13, pp.2–9.

Leblois, A. et al., 2006. Competition between feedback loops underlies normal and pathological dynamics in the basal ganglia. *The Journal of Neuroscience*, 26(13), pp.3567–83.

Lees, A.J., 2010. The bare essentials: Parkinson's disease. *Practical neurology*, 10(4), pp.240–6.

Lees, A.J., 2009. The Parkinson chimera. *Neurology*, 72(7), pp.S2–11.

Lees, A.J., Hardy, J. & Revesz, T., 2009. Parkinson's disease. *The Lancet*, 373(9680), pp.2055–66.

Lesage, S. & Brice, A., 2009. Parkinson's disease: from monogenic forms to genetic susceptibility factors. *Human molecular genetics*, 18, pp.R48–59.

Levin, J. et al., 2009. Objective measurement of muscle rigidity in Parkinsonian patients treated with subthalamic stimulation. *Movement disorders*, 24(1), pp.57–63.

Levy, R., 2002. Dependence of subthalamic nucleus oscillations on movement and dopamine in Parkinson's disease. *Brain*, 125(6), pp.1196–1209.

Levy, R. et al., 2000. High-frequency synchronization of neuronal activity in the subthalamic nucleus of parkinsonian patients with limb tremor. *The Journal of Neuroscience*, 20(20), pp.7766–7775.

Limousin, P. et al., 1995. Effect of parkinsonian signs and symptoms of bilateral subthalamic nucleus stimulation. *Lancet*, 345(8942), pp.91–5.

Limousin, P. et al., 1998. Electrical stimulation of the subthalamic nucleus in advanced Parkinson's disease. *The New England journal of medicine*, 339(16), pp.1105–11.

Limousin, P. et al., 1999. Multicentre European study of thalamic stimulation in parkinsonian and essential tremor. *Journal of neurology, neurosurgery, and psychiatry*, 66(3), pp.289–96.

Little, S., Joundi, R., et al., 2012. A torque-based method demonstrates increased rigidity in Parkinson's disease during low-frequency stimulation. *Experimental Brain Research*, 219(4), pp.499–506.

Little, S. et al., 2013. Adaptive deep brain stimulation in advanced Parkinson disease. *Annals of neurology*, 74(3), pp.449–57.

Little, S., Pogosyan, A., et al., 2012. Beta band stability over time correlates with Parkinsonian rigidity and bradykinesia. *Experimental neurology*, 236(2), pp.383–8.

Little, S. & Brown, P., 2012. What brain signals are suitable for feedback control of deep brain stimulation in Parkinson's disease? *Annals of the New York Academy of Sciences*, 1265(1), pp.9–24.

Litvak, V. et al., 2012. Movement-related changes in local and long-range synchronization in Parkinson's disease revealed by simultaneous magnetoencephalography and intracranial recordings. *The Journal of Neuroscience*, 32(31), pp.10541–53.

Litvak, V. et al., 2011. Resting oscillatory cortico-subthalamic connectivity in patients with Parkinson's disease. *Brain*, 134(Pt 2), pp.359–374.

Liu, X. et al., 2008. The sensory and motor representation of synchronized oscillations in the globus pallidus in patients with primary dystonia. *Brain*, 131(Pt 6), pp.1562–73.

Loddenkemper, T. et al., 2001. Deep brain stimulation in epilepsy. *Journal of clinical neurophysiology*, 18(6), pp.514–32.

López-Azcárate, J. et al., 2010. Coupling between beta and high-frequency activity in the human subthalamic nucleus may be a pathophysiological mechanism in Parkinson's disease. *The Journal of Neuroscience*, 30(19), pp.6667–77.

Lopiano, L. et al., 2003. Temporal changes in movement time during the switch of the stimulators in Parkinson's disease patients treated by subthalamic nucleus stimulation. *European neurology*, 50(2), pp.94–9.

Magill, P.J. et al., 2004. Synchronous unit activity and local field potentials evoked in the subthalamic nucleus by cortical stimulation. *Journal of neurophysiology*, 92(2), pp.700–14.

Marceglia, S. et al., 2006. Dopamine-dependent non-linear correlation between subthalamic rhythms in Parkinson's disease. *The Journal of physiology*, 571, pp.579–591.

Marceglia, S. et al., 2007. Interaction between rhythms in the human basal ganglia: application of bispectral analysis to local field potentials. *Neural Systems and Rehabilitation Engineering, IEEE Transactions*, 15(4), pp.483–492.

Marreiros, A.C. et al., 2013. Basal ganglia–cortical interactions in Parkinsonian patients. *NeuroImage*, 66, pp.301–310.

Marsden, C.D. & Obeso, J.A., 1994. The functions of the basal ganglia and the paradox of stereotaxic surgery in Parkinson's disease. *Brain*, 117, pp.877–97.

Marsden, J.F. et al., 2001. Subthalamic nucleus, sensorimotor cortex and muscle interrelationships in Parkinson's disease. *Brain*, 124, pp.378–388.

Martinez-Martin, P. et al., 2011. The impact of non-motor symptoms on health-related quality of life of patients with Parkinson's disease. *Movement disorders*, 26(3), pp.399–406.

Meissner, W. et al., 2005. Deep brain stimulation in late stage Parkinson?s disease: a retrospective cost analysis in Germany. *Journal of Neurology*, 252(2), pp.218–223.

Meyers, R., 1940. Surgical proceedure for the postencephalitic tremor, with notes on the physiology of premotor fibres. *Arch Neurol Psychiatry*, pp.455–457.

Mink, J.W., 1996. The basal ganglia: focused selection and inhibition of competing motor programs. *Progress in neurobiology*, 50(4), pp.381–425.

Mitzdorf, U., 1985. Current source-density method and application in cat cerebral cortex: investigation of evoked potentials and EEG phenomena. *Physiological reviews*, 65(1), p.37.

Modolo, J. et al., 2011. Model-driven therapeutic treatment of neurological disorders : reshaping brain rhythms with neuromodulation Model-driven therapeutic treatment of neurological disorders : reshaping brain rhythms with neuromodulation. *Interface Focus*, (1), pp.61–74.

Moore, D.J. et al., 2005. Molecular pathophysiology of Parkinson's disease. *Annual review of neuroscience*, 28, pp.57–87.

Moran, A. et al., 2008. Subthalamic nucleus functional organization revealed by parkinsonian neuronal oscillations and synchrony. *Brain*, 131, pp.3395–409.

Morrell, M.J., 2011. Responsive cortical stimulation for the treatment of medically intractable partial epilepsy. *Neurology*, 77(13), pp.1295–304.

Morrison, C.E. et al., 2004. Neuropsychological functioning following bilateral subthalamic nucleus stimulation in Parkinson's disease. *Archives of clinical neuropsychology*, 19(2), pp.165–81.

Müller, V. et al., 2001. Investigation of brain dynamics in Parkinson's disease by methods derived from nonlinear dynamics. *Experimental brain research*, 137(1), pp.103–110.

Muthuswamy, J. & Thakor, N. V, 1998. Spectral analysis methods for neurological signals. *Journal of neuroscience methods*, 83(1), pp.1–14.

Nambu, A. et al., 1996. Dual somatotopical representations in the primate subthalamic nucleus: evidence for ordered but reversed body-map transformations from the primary motor cortex and the supplementary motor area. *The Journal of neuroscience*, 16(8), pp.2671–83.

Nambu, A., 2008. Seven problems on the basal ganglia. *Current opinion in neurobiology*, 18(6), pp.595–604.

Nambu, A., Tokuno, H. & Takada, M., 2002. Functional significance of the cortico-subthalamo-pallidal "hyperdirect" pathway. *Neuroscience research*, 43(2), pp.111–7.

National Collaborating Centre for Chronic Conditions, 2006. Parkinson's Disease: National clinical guideline for diagnosis and management in primary and secondary care. Appendix F.

NICE, 2005. *Deep brain stimulation for Parkinson ' s disease Interventional Procedure Guidance 19*,

Nyholm, D., 2012. Duodopa® treatment for advanced Parkinson's disease: a review of efficacy and safety. *Parkinsonism & related disorders*, 18(8), pp.916–29.

O'Gorman, R.L. et al., 2009. CT/MR image fusion in the postoperative assessment of electrodes implanted for deep brain stimulation. *Stereotactic and functional neurosurgery*, 87(4), pp.205–10.

Obeso, J.A. et al., 1989. Motor complications associated with chronic levodopa therapy in Parkinson's disease. *Neurology*, 39(11), pp.11–9.

Odekerken, V.J.J. et al., 2013. Subthalamic nucleus versus globus pallidus bilateral deep brain stimulation for advanced Parkinson's disease (NSTAPS study): a randomised controlled trial. *Lancet neurology*, 12(1), pp.37–44.

Okun, M.S. et al., 2009. Cognition and mood in Parkinson's disease in subthalamic nucleus versus globus pallidus interna deep brain stimulation: the COMPARE trial. *Annals of neurology*, 65(5), pp.586–95.

Olanow, C.W. et al., 2009. A double-blind, delayed-start trial of rasagiline in Parkinson's disease. *The New England journal of medicine*, 361(13), pp.1268–78.

Olanow, C.W. et al., 2004. Double-blind, placebo-controlled study of entacapone in levodopa-treated patients with stable Parkinson disease. *Archives of neurology*, 61(10), pp.1563–8.

Ozkurt, T.E. et al., 2011. High frequency oscillations in the subthalamic nucleus: A neurophysiological marker of the motor state in Parkinson's disease. *Experimental neurology*, 229(2), pp.324–331.

Pahwa, R. et al., 2006. Practice Parameter: treatment of Parkinson disease with motor fluctuations and dyskinesia (an evidence-based review): report of the Quality Standards Subcommittee of the American Academy of Neurology. *Neurology*, 66(7), pp.983–95.

Park, B.K. et al., 2011. Analysis of viscoelastic properties of wrist joint for quantification of parkinsonian rigidity. *IEEE transactions on neural systems and rehabilitation engineering*, 19(2), pp.167–76.

Parkinson, J., 1817. *An Essay on the Shaking Palsy*, London: Sherwood, Neely and Jones.

Parsons, T.D. et al., 2006. Cognitive sequelae of subthalamic nucleus deep brain stimulation in Parkinson's disease: a meta-analysis. *Lancet neurology*, 5(7), pp.578–88.

Patrick, S.K. et al., 2001. Quantification of the UPDRS Rigidity Scale. *IEEE transactions on neural systems and rehabilitation engineering*, 9(1), pp.31–41.

Pereda, E., Quiroga, R.Q. & Bhattacharya, J., 2005. Nonlinear multivariate analysis of neurophysiological signals. *Progress in Neurobiology*, 77(1-2), pp.1–37.

Pezard, L., 2001. Investigation of non-linear properties of multichannel EEG in the early stages of Parkinson's disease. *Clinical Neurophysiology*, 112(1), pp.38–45.

Pezzoli, G. & Cereda, E., 2013. Exposure to pesticides or solvents and risk of Parkinson disease. *Neurology*, 80(22), pp.2035–41.

Pogosyan, A. et al., 2009. Boosting cortical activity at Beta-band frequencies slows movement in humans. *Current Biology*, 19(19), pp.1637–41.

Pogosyan, A. et al., 2010. Parkinsonian impairment correlates with spatially extensive subthalamic oscillatory synchronization. *Neuroscience*, 171(1), pp.245–257.

Pollak, P. et al., 1993. Effects of the stimulation of the subthalamic nucleus in Parkinson disease. *Revue neurologique*, 149(3), pp.175–6.

Polymeropoulos, M.H. et al., 1997. Mutation in the alpha-synuclein gene identified in families with Parkinson's disease. *Science*, 276(5321), pp.2045–7.

Powell, D. et al., 2012. Amplitude and velocity dependency of rigidity measured at the wrist in Parkinson's disease. *Clinical neurophysiology*, 123(4), pp.764–73.

Priori, A. et al., 2002. Movement-related modulation of neural activity in human basal ganglia and its L-DOPA dependency: recordings from deep brain stimulation electrodes in patients with Parkinson's disease. *Neurological sciences*, 23(2), pp.S101–2.

Priori, A. et al., 2004. Rhythm-specific pharmacological modulation of subthalamic activity in Parkinson's disease. *Experimental neurology*, 189(2), pp.369–379.

Prochazka, A. et al., 1997. Measurement of rigidity in Parkinson's disease. *Movement disorders*, 12(1), pp.24–32.

Raethjen, J. & Deuschl, G., 2012. The oscillating central network of Essential tremor. *Clinical neurophysiology*, 123(1), pp.61–4.

Ramaker, C. et al., 2002. Systematic evaluation of rating scales for impairment and disability in Parkinson's disease. *Movement Disorders*, 17(5), pp.867–76.

Rascol, O. et al., 2000. A five-year study of the incidence of dyskinesia in patients with early Parkinson's disease who were treated with ropinirole or levodopa. 056 Study Group. *The New England journal of medicine*, 342(20), pp.1484–91.

Ray, N.J. et al., 2008. Local field potential beta activity in the subthalamic nucleus of patients with Parkinson's disease is associated with improvements in bradykinesia after dopamine and deep brain stimulation. *Experimental neurology*, 213(1), pp.108–113.

Ray, N.J. et al., 2009. The role of the subthalamic nucleus in response inhibition: Evidence from deep brain stimulation for Parkinson's disease. *Neuropsychologia*, 47(13), pp.2828–2834.

Reck, C. et al., 2009. Characterisation of tremor-associated local field potentials in the subthalamic nucleus in Parkinson's disease. *The European journal of neuroscience*, 29(3), pp.599–612.

Redgrave, P., 2007. Basal Ganglia. *Scholarpedia (2007)*, p.1825.

Rivlin-Etzion, M. et al., 2006. Basal ganglia oscillations and pathophysiology of movement disorders. *Current opinion in neurobiology*, 16(6), pp.629–637.

Rodriguez-Oroz, M.C. et al., 2005. Bilateral deep brain stimulation in Parkinson's disease: a multicentre study with 4 years follow-up. *Brain*, 128(10), pp.2240–9.

Rodriguez-Oroz, M.C. et al., 2011. Involvement of the subthalamic nucleus in impulse control disorders associated with Parkinson's disease. *Brain*, 134(Pt 1), pp.36–49.

Rodriguez-Oroz, M.C., Moro, E. & Krack, P., 2012. Long-term outcomes of surgical therapies for Parkinson's disease. *Movement Disorders*, 27(14), pp.1718–28.

Rosa, M. et al., 2011. Subthalamic local field beta oscillations during ongoing deep brain stimulation in Parkinson's disease in hyperacute and chronic phases. *Neuro-Signals*, 19(3), pp.151–62.

Rosa, M. et al., 2010. Time dependent subthalamic local field potential changes after DBS surgery in Parkinson's disease. *Experimental neurology*, 222(2), pp.184–190.

Rosin, B. et al., 2011. Closed-loop deep brain stimulation is superior in ameliorating parkinsonism. *Neuron*, 72(2), pp.370–84.

Rossi, L. et al., 2007. An electronic device for artefact suppression in human local field potential recordings during deep brain stimulation. *Journal of neural engineering*, 4(2), pp.96–106.

Rossi, L. et al., 2008. Subthalamic local field potential oscillations during ongoing deep brain stimulation in Parkinson's disease. *Brain research bulletin*, 76(5), pp.512–521.

Saint-Cyr, J.A. et al., 2000. Neuropsychological consequences of chronic bilateral stimulation of the subthalamic nucleus in Parkinson's disease. *Brain*, 123, pp.2091–108.

Schiff, S.J., 2010. Towards model-based control of Parkinson's disease. *Philosophical transactions*, 368(1918), pp.2269–2308.

Schrader, C. et al., 2011. GPi-DBS may induce a hypokinetic gait disorder with freezing of gait in patients with dystonia. *Neurology*, 77(5), pp.483–8.

Schrag, A., 2000. Dyskinesias and motor fluctuations in Parkinson's disease: A community-based study. *Brain*, 123(11), pp.2297–2305.

Schuepbach, W.M.M. et al., 2013. Neurostimulation for Parkinson's disease with early motor complications. *The New England journal of medicine*, 368(7), pp.610–22.

Schüpbach, M. et al., 2006. Neurosurgery in Parkinson disease: a distressed mind in a repaired body? *Neurology*, 66(12), pp.1811–6.

Schwartz, A.B. et al., 2006. Brain-controlled interfaces: movement restoration with neural prosthetics. *Neuron*, 52(1), pp.205–220.

Shapiro, M.B. et al., 2007. Effects of STN DBS on Rigidity in Parkinson ' s Disease. *Rehabilitation*, 15(2), pp.173–181.

Shon, Y. et al., 2010. High frequency stimulation of the subthalamic nucleus evokes striatal dopamine release in a large animal model of human DBS neurosurgery. *Neuroscience letters*, 475(3), pp.136–140.

Siderowf, A. & Stern, M., 2002. A controlled trial of rasagiline in early Parkinson disease: the TEMPO Study. *Archives of neurology*, 59(12), pp.1937–43.

Siegfried, J. & Lippitz, B., 1994. Bilateral chronic electrostimulation of ventroposterolateral pallidum: a new therapeutic approach for alleviating all parkinsonian symptoms. *Neurosurgery*, 35(6), pp.1126–9.

Silberstein, P., Pogosyan, A., et al., 2005. Cortico-cortical coupling in Parkinson's disease and its modulation by therapy. *Brain*, 128(6), pp.1277–1291.

Silberstein, P., Oliviero, A., et al., 2005. Oscillatory pallidal local field potential activity inversely correlates with limb dyskinesias in Parkinson's disease. *Experimental neurology*, 194(2), pp.523–9.

Silberstein, P. et al., 2003. Patterning of globus pallidus local field potentials differs between Parkinson's disease and dystonia. *Brain*, 126(12), pp.2597–2608.

Singleton, A.B., Farrer, M.J. & Bonifati, V., 2013. The genetics of Parkinson's disease: progress and therapeutic implications. *Movement Disorders*, 28(1), pp.14–23.

Smeding, H.M.M. et al., 2006. Neuropsychological effects of bilateral STN stimulation in Parkinson disease: a controlled study. *Neurology*, 66(12), pp.1830–6.

De Solages, C. et al., 2010. Bilateral symmetry and coherence of subthalamic nuclei beta band activity in Parkinson's disease. *Experimental neurology*, 221(1), pp.260–266.

Speigel, E., 1952. Stereoencephalotomy (Thalamotomy and Related Procedures). Part I. Methods and Stereotaxic Atlas of the Human Brain. *JAMA*, 148, pp.446–451.

Spieles-Engemann, A.L. et al., 2010. Stimulation of the rat subthalamic nucleus is neuroprotective following significant nigral dopamine neuron loss. *Neurobiology of disease*, 39(1), pp.105–15.

Stam, C., 2005. Nonlinear dynamical analysis of EEG and MEG: review of an emerging field. *Clinical Neurophysiology*, 116(10), pp.2266–2301.

Stefani, A. et al., 2007. Bilateral deep brain stimulation of the pedunculopontine and subthalamic nuclei in severe Parkinson's disease. *Brain*, 130(Pt 6), pp.1596–607.

Stibe, C.M.H. et al., 1988. Subcutaneous apomorphine in parkinsonian on-off oscillations. *The Lancet*, 331, pp.403–406.

Stoffers, D. et al., 2008. Increased cortico-cortical functional connectivity in early-stage Parkinson's disease: an MEG study. *Neuroimage*, 41(2), pp.212–222.

Suchowersky, O. et al., 2006. Practice Parameter: neuroprotective strategies and alternative therapies for Parkinson disease (an evidence-based review): report of the Quality Standards Subcommittee of the American Academy of Neurology. *Neurology*, 66(7), pp.976–82.

Sutton, R. et al., 2007. History of electrical therapy for the heart. *European Heart Journal Supplements*, 9, pp.I3–I10.

Takada, M. et al., 1998. Corticostriatal input zones from the supplementary motor area overlap those from the contra- rather than ipsilateral primary motor cortex. *Brain Research*, 791(1-2), pp.335–340.

Tan, H., Pogosyan, A., Anzak, A., Ashkan, K., et al., 2013. Complementary roles of different oscillatory activities in the subthalamic nucleus in coding motor effort in Parkinsonism. *Experimental Neurology*, 248, pp.187–195.

Tan, H., Pogosyan, A., Anzak, A., Foltynie, T., et al., 2013. Frequency specific activity in subthalamic nucleus correlates with hand bradykinesia in Parkinson's disease. *Experimental neurology*, 240, pp.122–9.

Tanner, C.M., 1992. Epidemiology of Parkinson's disease. *Neurologic clinics*, 10(2), pp.317–29.

Tanner, C.M. et al., 1999. Parkinson disease in twins: an etiologic study. *JAMA*, 281(4), pp.341–6.

Tass, P. et al., 2010. The causal relationship between subcortical local field potential oscillations and Parkinsonian resting tremor. *Journal of neural engineering*, 7(1), p.16009.

Temperli, P. et al., 2003. How do parkinsonian signs return after discontinuation of subthalamic DBS? *Neurology*, 60(1), pp.78–81.

Tepper, J.M., Abercrombie, E.D. & Bolam, J.P., 2007. Basal ganglia macrocircuits. *Progress in brain research*, 160, pp.3–7.

Thevathasan, W. et al., 2012. Alpha oscillations in the pedunculopontine nucleus correlate with gait performance in parkinsonism. *Brain*, 135(Pt 1), pp.148–60.

Timmermann, L. et al., 2013. A new rechargeable device for deep brain stimulation: a prospective patient satisfaction survey. *European neurology*, 69(4), pp.193–9.

Timmermann, L. et al., 2004. Ten-Hertz stimulation of subthalamic nucleus deteriorates motor symptoms in Parkinson's disease. *Movement disorders*, 19(11), pp.1328–1333.

Timmermann, L. et al., 2003. The cerebral oscillatory network of parkinsonian resting tremor. *Brain*, 126(1), pp.199–212.

Timmermann, L. & Florin, E., 2011. Parkinson's disease and pathological oscillatory activity: Is the beta band the bad guy? - New lessons learned from low-frequency deep brain stimulation. *Experimental neurology*, pp.9–11.

Tolosa, E. et al., 1998. History of levodopa and dopamine agonists in Parkinson's disease treatment. *Neurology*, 50, pp.S2–S10.

Tomaszewski, K.J. & Holloway, R.G., 2001. Deep brain stimulation in the treatment of Parkinson's disease: A cost-effectiveness analysis. *Neurology*, 57(4), pp.663–671.

Twelves, D., Perkins, K.S.M. & Counsell, C., 2003. Systematic review of incidence studies of Parkinson's disease. *Movement Disorders*, 18(1), pp.19–31.

Urrestarazu, E. et al., 2009. Beta activity in the subthalamic nucleus during sleep in patients with Parkinson's disease. *Movement Disorders*, 24(2), pp.254–260.

Le Van Quyen, M. & Bragin, A., 2007. Analysis of dynamic brain oscillations: methodological advances. *Trends in neurosciences*, 30(7), pp.365–373.

Visser-Vandewalle, V. et al., 2005. Long-term effects of bilateral subthalamic nucleus stimulation in advanced Parkinson disease: a four year follow-up study. *Parkinsonism & related disorders*, 11(3), pp.157–65.

Vlaar, A. et al., 2011. The treatment of early Parkinson's disease: levodopa rehabilitated. *Practical neurology*, 11(3), pp.145–52.

Volkmann, J. et al., 2002. Introduction to the programming of deep brain stimulators. *Movement Disorders*, 17, pp.S181–7.

Volkmann, J., Daniels, C. & Witt, K., 2010. Neuropsychiatric effects of subthalamic neurostimulation in Parkinson disease. *Nature reviews. Neurology*, 6(9), pp.487–98.

Voon, V. et al., 2008. A multicentre study on suicide outcomes following subthalamic stimulation for Parkinson's disease. *Brain*, 131(10), pp.2720–8.

Wakabayashi, K. et al., 2007. The Lewy body in Parkinson's disease: molecules implicated in the formation and degradation of alpha-synuclein aggregates. *Neuropathology*, 27(5), pp.494–506.

Walker, H.C. et al., 2011. Activation of subthalamic neurons by contralateral subthalamic deep brain stimulation in Parkinson disease. *Journal of neurophysiology*, 105(3), pp.1112–21.

Wallace, B.A. et al., 2007. Survival of midbrain dopaminergic cells after lesion or deep brain stimulation of the subthalamic nucleus in MPTP-treated monkeys. *Brain*, 130(Pt 8), pp.2129–45.

Wang, S. et al., 2007. Revealing the dynamic causal interdependence between neural and muscular signals in Parkinsonian tremor. *Journal of the Franklin Institute*, 344(3-4), pp.180–195.

Weaver, F.M. et al., 2009. Bilateral deep brain stimulation vs best medical therapy for patients with advanced Parkinson disease: a randomized controlled trial. *JAMA*, 301(1), pp.63–73.

Weaver, F.M. et al., 2012. Randomized trial of deep brain stimulation for Parkinson disease: thirty-six-month outcomes. *Neurology*, 79(1), pp.55–65.

Weinberger, M. et al., 2006. Beta oscillatory activity in the subthalamic nucleus and its relation to dopaminergic response in Parkinson's disease. *Journal of neurophysiology*, 96(6), pp.3248–3256.

Weinberger, M., Hutchison, W.D., et al., 2009. Increased gamma oscillatory activity in the subthalamic nucleus during tremor in Parkinson's disease patients. *Journal of neurophysiology*, 101(2), pp.789–802.

Weinberger, M. et al., 2008. Pedunculopontine nucleus microelectrode recordings in movement disorder patients. *Experimental Brain Research*, 188(2), pp.165–174.

Weinberger, M., Hutchison, W.D. & Dostrovsky, J.O., 2009. Pathological subthalamic nucleus oscillations in PD: can they be the cause of bradykinesia and akinesia? *Experimental neurology*, 219(1), pp.58–61.

Whitmer, D. et al., 2012. High frequency deep brain stimulation attenuates subthalamic and cortical rhythms in Parkinson's disease. *Frontiers in human neuroscience*, 6, p.155.

Van Wijk, B.C.M., Beek, P.J. & Daffertshofer, A., 2012. Neural synchrony within the motor system: what have we learned so far? *Frontiers in Human Neuroscience*, 6, pp.1–15.

Williams, A. et al., 2010. Deep brain stimulation plus best medical therapy versus best medical therapy alone for advanced Parkinson's disease (PD SURG trial): a randomised, open-label trial. *Lancet neurology*, 9(6), pp.581–591.

Williams, D. et al., 2002. Dopamine-dependent changes in the functional connectivity between basal ganglia and cerebral cortex in humans. *Brain*, 125(7), pp.1558–1569.

Williams, D. et al., 2005. The relationship between oscillatory activity and motor reaction time in the parkinsonian subthalamic nucleus. *The European journal of neuroscience*, 21(1), pp.249–258.

Wingeier, B. et al., 2006. Intra-operative STN DBS attenuates the prominent beta rhythm in the STN in Parkinson's disease. *Experimental neurology*, 197(1), pp.244–251.

Wirdefeldt, K. et al., 2011. Epidemiology and etiology of Parkinson's disease: a review of the evidence. *European journal of epidemiology*, 26, pp.S1–58.

Witt, K. et al., 2008. Neuropsychological and psychiatric changes after deep brain stimulation for Parkinson's disease: a randomised, multicentre study. *Lancet neurology*, 7(7), pp.605–14.

Woods, S.P., Fields, J.A. & Tröster, A.I., 2002. Neuropsychological sequelae of subthalamic nucleus deep brain stimulation in Parkinson's disease: a critical review. *Neuropsychology review*, 12(2), pp.111–26.

Wooten, G.F., 2004. Are men at greater risk for Parkinson's disease than women? *Journal of Neurology, Neurosurgery & Psychiatry*, 75(4), pp.637–639.

Worth, P.F., 2013. When the going gets tough: how to select patients with Parkinson's disease for advanced therapies. *Practical neurology*, 13(3), pp.140–52.

Yoshida, F. et al., 2010. Value of subthalamic nucleus local field potentials recordings in predicting stimulation parameters for deep brain stimulation in Parkinson's disease. *Journal of Neurology,*, 81(8), pp.885–9.

Zaidel, A. et al., 2010. Subthalamic span of beta oscillations predicts deep brain stimulation efficacy for patients with Parkinson's disease. *Brain*, 133, pp.2007–2021.

Zetusky, W.J., Jankovic, J. & Pirozzolo, F.J., 1985. The heterogeneity of Parkinson's disease: Clinical and prognostic implications. *Neurology*, 35(4), pp.522–6.

Zhang, Z.-X. & Román, G.C., 1993. Worldwide Occurrence of Parkinson's Disease: An Updated Review. *Neuroepidemiology*, 12(4), pp.195–208.

UNIVERSITY OF Southampton
Institute of Sound and Vibration Research

Institute of Sound and Vibration Research
University Road, Highfield
Southampton SO17 1BJ, UK

[redacted]
Lecturer in Biomedical Engineering

Direct Line: [redacted]
E-mail: [redacted]

2011-07-20

Review report on Ethics – 11/SC/0100

To Whom It May Concern:

This is a review report on Ethics – 11/SC/0100 (DBS Stimulator & Safety features) based on my research experience and knowledge in Biomedical Engineering, especially Neural Engineering and Biomedical Signal Processing.

There are two essential concerns in designing a brain stimulator, i.e., safety and side effects of the electrical stimulation. These two concerns have been well addressed in the Ethics 11/SC/0100.

The safety of the customised stimulator has been assured by limiting the electrical voltage to 5 volt, current to 15 mA and charge density to 30uQ/cm2. These settings avoid the potential risks of over-stimulating at high amplitude and neural damage over long time stimulation. Other common safety protocols are applied in the stimulator and experiment arrangement as well, for instance, optical isolation, direct current block between stimulator and patient, and battery powering. The customised stimulator is carefully designed to avoid the side effects of electrical stimulation by delivering bipolar stimulation pulses, ramping at onset and offset and preventing direct current drifting. The stimulator has been intensively tested in several conditions including continuous stimulation over a few days. In summary, the customised stimulator meets the standard of EN 60601-1 and safe to use based on the design and testing.

Kind regards,

[redacted]